DISSECTION OF THE GENETIC BASIS UNDERLYING WAX BIOSYNTHESIS IN HEXAPLOID WHEAT USING BI-PARENTAL LINKAGE MAPPING AND GENOME-WIDE ASSOCIATION STUDY

A Dissertation

by

XIANGKUN GU

Submitted to the Office of Graduate and Professional Studies of
Texas A&M University
in partial fulfillment of the requirements for the degree of

DOCTOR OF PHILOSOPHY

Chair of Committee,	Dirk Hays
Committee Members,	Shuyu Liu
	Scott Finlayson
	Charles Johnson
	Hongbin Zhang
Intercollegiate Faculty Chair,	Dirk Hays

August 2017

Major Subject: Molecular and Environmental Plant Sciences

ABSTRACT

Epicuticular wax acts as a plant's first line of defense against environmental afflictions. Wax is known to be a factor in stress adaptation and also provides resistance to disease, drought, and heat due to its ability to reduce water loss, increase light reflectance, and reduce fungal infection. The introgression of major wax genes into cultivars and breeding lines will improve wheat breeding. In order to dissect the quantitative trait loci (QTLs) underlying wax biosynthesis, a bi-parental QTL mapping study has been conducted on a RIL population and a genome-wide association study (GWAS) has been carried out on a panel of synthetic-derived wheat lines. QTL analysis was performed using 8,440 single-nucleotide polymorphisms (SNPs) identified from a wheat 90K iSelect SNP array. A QTL on chromosome 2BS controlling wax-related traits was stably detected across different developmental stages. The QTL explained up to 18.6% epicuticular wax load (EWL) variation and 18.9% glaucousness variation in the population. The QTLs for head length and tiller number were co-localized with this wax QTL. The pleotropic QTL on 4B may be a developmental stage-specific region controlling wax biosynthesis in the early reproductive stages, as well as controlling plant height. A novel QTL for plant height on 3B was detected in this study, which provides clues for the dissection of the genetic basis underlying this trait. The association panel of 300 synthetic-derived wheat lines has been genotyped using ddRAD-seq and phenotyped in conditions with different combinations of environments and developmental stages. 137,856 SNPs were identified from ddRAD-seq for further analysis. Epicuticular wax

load was measured in the conditions: BD16FL, BI16FL, CH16TD, CS16FL, CS16TD, BD17FL, BI17FL, and CL17FL. Glaucousness was recorded in the conditions: BD16HD, BI16HD, BD16FL, BI16FL, CH16TD, BD17FL and PR17FL. About 200 significant marker-trait associations (MTA) have been identified, with most of the SNPs being associated with glaucousness. A majority of significant SNPs were mapped on the short arm of the chromosome 2D. A QTL associated with glaucousness on 2D can be consistently detected across all the non-optimal conditions we studied. This QTL identified in GWAS analysis flanked by *5293194_2ds_2515* and *5348611_2ds_1248* may contain the locus of *INHIBITOR OF WAX2* (*Iw2*), which is also located on the distal region of 2DS. The major QTLs for wax-related traits and significant marker trait associations identified in this study will lay a foundation for the clarification of the genetic basis underlying the regulation of spatiotemporal expression of wax.

ACKNOWLEDGEMENTS

I would like to extend a heartfelt thank you to my advisor, Dr. Dirk B. Hays, for his guidance and patience, as well as for providing me with this great opportunity to study at Texas A&M University.

I would like to express my deepest gratitude to my committee: Dr. Shuyu Liu, who contributed much help and guidance to my research. Dr. Scott Finlayson, for providing me with support and suggestions for my experiments. Dr. Charles Johnson, for providing services and resources for this research. Also to Dr. Hongbin Zhang for his suggestions and help throughout the research process.

I would like to thank Drs. Amir Ibrahim and Jackie Rudd for sharing their resources and valuable knowledge. I appreciate the help from Dr. Geraldine B. Opena for experimental design and Mr. Bryan Simmoneux for the filed experiments.

Thanks also go to my colleagues and my friends: Dr. Trevis Huggins, Dr. Shichen Wang, Fatima Camarillo Castillo, Yalin Li, Tyler Adams, Alfredo Delgado, Dr. Yuanyuan Chen and Yan Yang for their assistance and encouragements. Many thanks go to the faculty and staff in the Soil and Crop Sciences Department for making my time at Texas A&M University a great experience. Thanks for the financial support from Chinese Scholarship Council.

Finally, thanks to my family for their encouragement and understanding.

CONTRIBUTORS AND FUNDING SOURCES

Contributors

This work was supervised by a dissertation committee consisting of Professor Dirk Hays and Professors Scott Finlayson and Hongbin Zhang of the Department of Soil and Crop Sciences and Professor Shuyu Liu of the Texas A&M AgriLife Research and Extension Center at Amarillo and Director Charles Johnson of the Genomics and Bioinformatics, Texas A&M AgriLife Research.

The analyses depicted in Chapter 2 were conducted in part under the advisement of Professor Shuyu Liu of the Texas A&M AgriLife Research and Extension Center at Amarillo. The genotypic data analyzed for Chapter 3 was provided by Professor Shuyu Liu.

All other work conducted for the dissertation was completed by the student independently.

Funding Sources

Graduate study was supported by a scholarship from Chinese Scholarship Council and an assistantship from Texas A&M University. This study was in part funded by an Agriculture and Food Research Initiative Competitive Grant under Grant Number 2010 - 65114 - 20389 from the USDA National Institute of Food and Agriculture to Dirk Hays.

NOMENCLATURE

BB	Booting Begin
CT	Canopy Temperature
CTD	Canopy Temperature Depression
DAP	Days After Pollination
FT	Flowering Time
Glau	Glaucousness
GWAS	Genome-Wide Association Study
HL	Head Length
LB	Late Booting
NGS	Next Generation Sequencing
PH	Plant Height
QTL	Quantitative Trait Loci
T	Temperature
TE	Tiller Emergence
TN	Tiller Number

TABLE OF CONTENTS

Page

LIST OF FIGURES

Page

LIST OF TABLES

Page

CHAPTER I

INTRODUCTION AND LITERATURE REVIEW

1.1 Executive summary

Wheat is one of the most important staple crops, providing various nutrients such as protein, vitamins and minerals for human health. Wheat is the major source of protein for more than half of the world's population (FAO 2016), but wheat-growing areas are subject to abiotic and biotic stress, especially climate change and environmental variations (Porter and Semenov 2005). Global warming and water shortage have become a considerable challenge in meeting the needs for crop yield increases (Lobell et al. 2013). Models predict that global wheat production will decrease by 5.5% of 1980 production when climate change is taken into account (Lobell et al. 2011). Wheat production is sensitive to heat and drought stress during certain vital developmental stages like anthesis, fertilization and grain filling (Gooding et al. 2003; Barnabas et al. 2008; Craufurd et al. 2013). For instance, it has been reported that heat and drought stress during the booting stage reduces grain number and grain weight (Alghabari et al. 2014). Therefore, it is imperative to breed new wheat cultivars adapted to climate change and environmental variations. Epicuticular wax (EW) is the outermost layer of plants that serves as a connection and buffer between plant material and the environment. It has multiple functions in plant defense against numerous stresses such as drought, heat and disease. It has been reported that EW can reduce non-stomata water loss (Kunst and

Samuels 2003; Zhang et al. 2013) and cuticle permeability (Zhang et al. 2013). Thus, EW contributes to a plant's adaptation to drought-stressed environment.

"Glaucousness" is defined as the visible substance that covers the leaf, and is often light bluish-white in color and is an affect of EW composition. Both EW and glaucousness can reflect visible and infrared wavelengths (Shepherd and Griffiths 2006) and protect plants against excess radiation (Reicosky and Hanover 1978). Surface topography and the amount of wax strongly influence the reflection of radiation (Cossani and Reynolds, 2012). The EW and/or glaucousness has a positive correlation with lower canopy temperatures (Richard et al. 1986; Bennett et al. 2012). Glaucousness was also positively correlated with wheat yield particularly in water-stressed environments (Richard et al. 1983). These effects indicate an important contribution of wax to wheat heat stress adaptation. In view of the vital importance and multiple functionality of wax, deciphering the mechanism of wax involvement in plant adaptation to stress and dissecting the major genes related to wax would provide valuable insights for wheat stress tolerance breeding.

Wax is a complex mixture composed of various components including very-long-chain fatty acids (VLCFA), esters, alcohols, aldehydes and ketones (Kunst and Samuels 2009). Our understanding of wax biosynthesis is mainly from *Arabidopsis* and many key elements involved in complex wax biosynthesis pathways have been identified, such as ECERIFERUM 4 (CER4) (Rowland et al. 2006), CER6 (Millar et al. 1999; Fiebig et al. 2000; Hooker et al. 2002), KCS1 (Todd et al. 1999), CER10 (Zheng et al. 2005), WSD1 (Li et al. 2008), ABCG12/CER5 (Pighin et al. 2004) and

ABCG11/WBC11 (Bird et al. 2007; Panikashvili et al. 2007). To date, few wax genes have been characterized in wheat. Given the vital importance of epicuticular wax, it is important to clarify the wax metabolism pathway, characterize the key genes involved in wax biosynthesis, and determine the correlation between wax and stress adaptation.

In wheat, few studies have been conducted relating to the identification and characterization of genes regulating the formation of wax. It has been established that there are two sets of genes controlling the glaucousnenss phenotype: *W1* and *W2* are wax production genes promoting the formation of glaucousness phenotype, while *Iw1* and *Iw2* are wax inhibitors, showing a glossy phenotype in plants that possess them. Wax production genes are dominant to wax inhibitor genes. In Zhang's study (Zhang et al. 2013), they used six near-isogenic lines (NILs) to characterize the effect of *W1, W2, Iw1* and *Iw2* and their interactions. It has been shown that the depletion of both wax production genes and the presence of either wax inhibitor genes can cause the non-glaucousness phenotype. By phenotyping a series of mutant lines, it has been shown that *W1* and *W2* are functionally redundant and that the presence of one wax inhibitor gene can cause the non-glaucousness phenotype. This is because the lines *W1W2, W1w2,* and *w1W2* showed glaucousness but *w1w2, Iw1iw2* and *iw1Iw2* showed non-glaucousness. Biochemical analysis on the wax compositions of glaucous lines and non-glaucous lines indicated that the expression of β-diketones was greatly reduced in *w1w2* and were completely depleted in *Iw1iw2* and *iw1Iw2* lines. This indicated that wax compositions determine the glaucousness phenotype, while β-diketones were required for the formation of glaucousness (Barber and Netting 1968).

Comparative fine mapping has been conducted on the localization of wax genes. The *Iw1* locus was mapped on wheat chromosome 2BS, flanked by the *BE498358* and *CA499581* EST markers, whose collinear region is on *Brachypodium* 5S, the sorghum 6S chromosome and rice 4S. *Iw2* was mapped on wheat chromosome 2DS, flanked by the *CJ886319* and *CJ519831* EST markers (Saintenac et al. 2013b). Another glaucousness inhibitor gene *Iw3* specific to the wheat glume was located on chromosome 1BS (Dubcovsky et al. 1997) and recently a high-resolution mapping located the *Iw3* gene on 1BS within a 0.135-cM interval, flanked with marker *XWL3096* and marker *Xpsp3000* (Wang et al. 2014b). The wax production gene *W1* is closely linked with *Iw1*, with the genetic distance 2cM on chromosome 2BS (Tsunewaki 1966; Mohammed 2016). A recent study has fine mapped the *W1* gene between markers *XWGGC*3197 and *XWGGC*2484 within a genetic interval of 0.93 cM (Lu et al. 2017). The other set of wax-related genes *W2* and *Iw2* are located on 2DS. However, they are not tightly linked. *W2* is located on the distal end of 2DS while *Iw2* is mapped near the centromere (Tsunewaki and Ebana 1999). As *Iw3* is specific to the determination of glume glaucousness, *Ws* has been characterized to the formation of the spike glaucousness phenotype. These two loci are not located on the same chromosome. *Iw3* is located on 1BS (Dubcovsky et al. 1997) and *Ws* is located on 1AS (Gadaleta et al. 2009). All of these genes are related to β-diketone biosynthesis. However, few studies have been conducted to dissect the genes involved in β-diketone synthesis pathways and to decipher the effects of β-diketone on glaucousness formation and stress tolerance.

In sorghum, it has been reported that a *cer-cqu* gene cluster regulates the expressions of genes involved in β-diketone biosynthesis. Schneider et al (2016) has characterized the important function of *cer-cqu* in a pathway producing β-diketone and hydroxy-β-diketones, as well as esterified alkan-2-ols. *cer-c* encodes a type III chalcone synthase-like synthase (Austin and Noel 2002), *cer-q* is a lipase/carboxyl transferase and *cer-u* encodes a cytochrome P450 enzyme (Maccaferri et al. 2016). In wheat, comparative analysis suggests that the probability that the homologs of wax production genes *W1*, *W2* and *W3* are barley *cer-cqu* genes (IWGSC 2014). And the syntenic region of *W1* on barley is the same region in which the *cer-cqu* gene cluster is located, which provides some support that wax production genes in wheat are corresponding to the *cer-cqu* cluster in barley (Adamski et al. 2013; Schneider et al. 2016).

1.2 Review of relevant literature

As an important source of human food and livestock feed, wheat provides 20% of calories consumed worldwide and nearly 40-50% of all calories in some developing areas like North Africa and West and Central Asia. According to the Wheat Initiative, by the year 2050 the world population will increase to 9 billion, which means that wheat production should increase by 60% and the annual wheat yield increase should reach at least 1.6 % from the current level of less than 1 % (FAO 2009). However, based on the latest data and projection from *Food Outlook* by FAO (FAO 2016), wheat production decreased slightly in 2016 when compared with that of 2015 as a result of a decrease in

planting area, although the general trend of wheat production has been an increase since 2007 (FAO 2016). It is imperative to increase wheat yields with fewer resources to meet increasing demand for wheat and ensure worldwide food security.

1.2.1 The importance of wax in plant adaptation to multiple environments

1.2.1.1 Wax and heat tolerance

Plants have evolved various mechanisms to adapt to heat-stress and drought environments. Under high-temperature conditions, plant transpiration will dissipate heat by emission of extra humidity and energy. Other morphological structures of plants such as leaf hairs, waxes on the plant surface and leaf angle play important roles in the reduction of plant temperature by decreasing energy absorption and increasing heat flux (Mondal 2011). Studies have shown that canopy temperature (CT) or canopy temperature depression (CTD) are correlated with increased yield in both heat and drought conditions (Reynolds et al. 1998; Pinto et al. 2010). Mondal (2011) found the co-localization of wax QTLs with yield-related QTL and heat tolerance QTLs, indicating that EW may be involved in the heat tolerance response for plant adaptation to heat stress.

Based on the modification of the conceptual model about the traits related to the main drivers of yield under drought from Reynolds et al. (2009), yield = LI × RUE × HI. LI is light interception; RUE is radiation use efficiency and HI is harvest index associated with partitioning of total assimilates. EW acts as a photo-protection barrier to

improve RUE when the assimilation capacity increases, thus making a contribution to yield (Cossani and Reynolds 2012). It is theorized that EW, including bluish-gray or bluish-white colored glaucousness can increase light reflection and reduce excess energy absorption, which decreases the temperature of canopies (Jenks et al. 1992; Shepherd and Griffiths 2006). It has been shown that surface topography substantially affects reflection, especially in the visible wavelengths, and wax is one of the important factors that determines surface morphology (Holmes and Keiller 2002; Lovelock and Robinson 2002). Holmes and Keiller (2002) found reflectivity at greater than 330nm was positively proportional to the amount of wax. The relationships between wax content and light reflection, canopy cooling and heat tolerance indicates that wax is one of the crucial traits that confer the plant's ability to adapt to a heat stress environment.

1.2.1.2 Wax and drought tolerance

Like heat stress, drought is also a constraining factor inhibiting plant growth and development. Under drought conditions phenological progression will be accelerated, which reduces the periods of normal stages, photosynthetic assimilation and yield (KiliÇ and YaĞbasanlar 2010). Water deficiency causes morphological, physiological and metabolic changes. Structurally, leaves roll and stomata close to reduce water evaporation and gas exchanges. Meanwhile, root growth will be enhanced and foliar growth rates will be depressed to ensure plant survival (Jaleel et al. 2008; Hund et al. 2009). At the molecular level, stress-related genes and proteins like osmoprotectants and signal transduction molecules are elevated to change the plant's metabolic ability to cope

with moisture deficiency (Shinozaki and Yamaguchi-Shinozaki 2007; Verbruggen and Hermans 2008; Urano et al. 2010). The expression and accumulation of secondary metabolites, including wax, also contributes to drought resistance (Seo and Park 2011). As a final barrier to the outside environment, the plant's hydrophobic cuticle layer, composed of cutin and wax, can control moisture permeability and reduce water evaporation, restricting plant dehydration (Jenks and Wood 2002). Many studies have shown that water loss rates decrease with increased wax deposition (Williams et al. 1999; Williams et al. 2000; Cameron et al. 2006). In a rice mutant, the plant was more susceptible to drought stress when the expression of total wax was reduced (Qin et al. 2011). Wax is a complex mixture composed of various lipids that can be assembled as a part of the cutin matrix, controlling water diffusion from cells to the outside (Riederer and Schreiber 1995; Kerstiens 1996a; Kosma and Jenks 2007). This allows a plant to conserve moisture and adapt to water-limited conditions (Grncarevic and Radler 1967), which is thought to have effects on maintaining yield in drought stressed environments. It has been shown that higher amounts of epicuticular wax has a positive correlation with drought tolerance in barley (Gonzalez and Ayerbe 2010) and sorghum (Jordan et al. 1984). Mohammed (2014) showed a correlation between high wax content and yield stability in wheat. In irrigation-limited conditions, leaf epicuticular wax most likely has an effect on drought stress tolerance, partially through cooling canopies and indirectly keeping yield relatively stable across different environments (Mondal 2011).

1.2.1.3 Mixed effects of wax on yield and other physiological traits

As mentioned above, wax plays various positive roles in plant adaptation to stressed environments. However, the association between wax, or glaucousness, and other physiological traits is largely environment-dependent. Wax exerts mixed effects on yield and water-use efficiency in different conditions and for different genetic backgrounds. Usually, in a water-limited environment, glaucousness may increase yield by improving water-use efficiency or transpiration (Chatterton et al. 1975; Monneveux et al. 2004; Jefferson et al. 2016). However, there was no significant difference in grain yield between glaucous lines and non-glaucous lines in dry conditions (Risk et al. 2013). In irrigated and rain-fed environments, glaucous lines produced higher grain yield than non-gloaucous lines (Febrero et al. 1998). The effect of wax on yield also depends on the timing of drought. Merah et al. noted that non-glauous lines had higher biomass than glaucous counterparts if drought stress occurred after the vegetative growth, which was in contrast to the early drought situation (Merah et al. 2000). This indicated that glaucousness had a negative effect on biomass production under relatively optimum conditions. Simmonds et al. (2008) conducted field trials under Mediterranean conditions in the UK and found a significant yield increase was associated with the *Vir* gene conferring a plants non-glaucous phenotype. Viridescent genotypes have longer growth periods with a greater number of days to full senescence, which is counter to previous studies (Richard, 1983; Monneveux et al. 2004). A series of near-isogenic lines were constructed based on the double haploid (DH) lines used by Simmonds (2008) to investigate the effect of the *Iw1* gene on yield, WUE, stomata conductance and canopy

temperature in different environments and different genetic backgrounds (Frizell-Armitage 2016). For this long-term, multi-location experiment, there was generally no significant effect of non-glaucousness conferred by *Iw1* on yield, WUE and canopy temperature. However, a significant yield increase associated with the *Iw1* was shown in the genetic background of Hereward and Alchemy. For the other 4 genetic background NILs pairs, the association between *Iw1* and yield increase is either none or negative, which indicated that the effect of *Iw1* depends on its interactions with other genes. Wax is a complicated quantitative trait whose function is largely dependent on environments and genetic background. Additionally, glaucousness is an expression of EW composition, which may be more important to stress adaptation.

1.2.2 The regulation of wax biosynthesis

Cuticular wax is a general name depicting complex mixtures of diversified hydrophobic molecules, including fatty acid of carbon lengths C24 or higher, and their derivatives like alkanes, aldehyde, alcohols and wax esters (Kosma and Rowland 2016). The expression and composition of wax vary widely between plant species, different cultivars in one species and even different developmental stages in one plant. A gene network controls the temporal and spatial expression and accumulation of wax, with lots of organelles involved in the process. Wax biosynthesis occurs predominantly in epidermal cells and starts in plastids (Li-Beisson et al. 2010). After plastidial de novo synthesis of C16 and C18 fatty acids, they are hydrolyzed by acyl-ACP thioesterases and

exported to the cytoplasm. Then under the catalysis of acyl-CoA synthetases (LACSs) located on the endoplasmic reticulum, fatty acyl CoAs, the active form of fatty acids, are produced for further elongation. It has been established that very long chain fatty acids (VLCFAs) are generated by the catalysis of fatty acid elongases (FAEs), a multi-enzyme complex located on the endoplasmic reticulum membrane. Four successive reactions including one condensation reaction, one dehydration reaction and two reduction reactions occur via FAEs to add one C2 unit per cycle. First, b-ketoacyl-CoA synthase (KCS) catalyzes the condensation between malonyl-CoA, with an acyl-CoA to form β-ketoacyl-CoA; then β-ketoacyl-CoA is reduced to β-hydroxyacyl-CoA by β-ketoacyl-CoA reductase (KCR). The product is then dehydrated to enoyl-CoA by a β-hydroxyacyl-CoA dehydratase (HCD). A C2 unit extended fatty acyl-CoA is generated by the final reduction of enoyl-CoA via enoyl-CoA reductase (ECR) (Bernard and Joubès 2013; Lee and Suh 2016). VLCFAs found in plants vary from C22 to C36, which might be related to the specificity of different types of multiple elongase complexes (Wettstein-Knowles 1982).

VLCFAs can subsequently diverge into two main pathways to produce derivatives of fatty acid. One is an alcohol-forming pathway generating primary alcohols and wax esters. In *Arabidopsis*, the CER4 enzyme, a fatty acyl-CoA reductase, plays a predominant role in this pathway. It can catalyze the formation of primary alcohols from fatty acyl-CoA, and the primary alcohols generated are the substrates for wax ester synthesis. WSD1, a bi-functional wax synthase/acyl-CoA:diacylglycerol acyltransferase (WS/DGAT) enzyme, catalyzes the esterification of primary alcohols with C16:0 acyl-

CoA (Stoveken et al. 2005; Lai et al. 2007). Alternatively, the VLCFAs can enter an alkane-forming pathway in which aldehydes, alkanes, secondary alcohols, and ketones are formed (Li-Beisson et al. 2010). In this pathway, a decarbonylase removes the carbonyl from fatty acid. Initially, very long chain fatty acyl-CoA is used as a precursor to be reduced to aldehyde intermediates by Acyl-CoA reductase (FAR), and then with the catalysis of CER1 enzyme, alkanes can be generated. A NADPH-cytochrome P450 reductase CYTB5s functions as a cofactor involved in the decarbonylation process (Reed et al. 1994; Qiu et al. 2012; Lee and Suh 2016). Alkanes are the substrates for the formation of secondary alcohols using the enzyme midchain alkane hydroxylase 1 (MAH1), which can be further oxidized to ketones (Lee and Suh 2016).

Wax biosynthesis pathways have been extensively characterized in *Arabidopsis*. But they are not well studied in other non-model plants. What's more, a crucial polyketide pathway related to β-diketone production doesn't exist in *Arabidopsis* compared to wheat and sorghum and other crops (Jackson 1971). In this pathway, type III polyketide synthases (PKSs), designated as pkKCS, will use the products from the FAS/FAE complex as precursors to catalyze 1-3 times the extension process, which results in the generation of different products. Two successive pkKCS extensions and the possible following decarboxylation can produce β-diketones that can be further hydroxylased to hydroxy-β-diketones (Wettstein-Knowles 2012). In barley, the *Cer-cqu* cluster is correlated with the synthesis of β-diketone, hydroxyl-β-diketone and esterified alkan-2-ol, among which β-diketone determines the glaucousness phenotype (Kosma and Rowland 2016). But still, the genes in this locus are elusive. In wheat, the *W1* and

W2 locus, which mapped to chromosome arms 2BS and 2DS, respectively (Tsunewaki and Ebana 1999; Zhang et al. 2015; Lu et al. 2017). The closest orthologs of *Cer- c*, *-q* and –u were assigned to the regions containing *W1* and *W2* locus, which are syntenic to barley 2HS (IWGSC, 2014)

After biosynthesis on the membrane of the ER, waxes are transported to the plasma membrane to form the cutin matrix and epicuticular wax. So far, ABCG12 encoded by *cer5* (Samuels et al. 2008), ABCG11 (Buschhaus and Jetter 2011) and the full-size ABC transporter, ABCG32 (Bessire et al. 2011) and lipid transfer proteins (LTPs) have been shown to correlate with wax transportation and deposition (Lee and Suh 2016). Both ABCG12 encoding a putative half ABC transporter and ABCG11 are located on the plasma membrane. It has been shown that LTPG1 and LTPG2 play a role in directly or indirectly transporting and depositing of cuticular waxes (Kissinger et al. 2005; Debono et al. 2009; Kim et al. 2012).

In response to developmental growth and environmental signals, plants have developed transcriptional and post-transcriptional regulation mechanisms to control the expression and deposition of wax. In *Arabidopsis*, three SHN proteins, SHN1, SHN2 and SHN3, belonging to the AP2/EREBP family of transcription factors, directly regulate cutin deposition and indirectly regulate epicuticular wax synthesis (Yazaki et al. 2004). In other species such as tomato (Al-Abdallat et al. 2014) and rice (Wang et al. 2012; Zhou et al. 2013), homologs of the SHN transcription factor have similar effects on wax biosynthesis and SHN1 is regulated by MYB106. In a drought environment, the increase of stress-inducible ABA triggers the up-regulation of the expression of MYB96

that can bind to the promoters of wax-related genes such as *KCS*, *CER3*, and *WSD1*. Up-regulation of these genes increases wax load and thus improves a plant's drought tolerance (Lee and Suh 2016). MYB16, along with MYB106, also affects the formation of cuticle and wax accumulation coordinately with WIN1/ SHN1 in *Arabidopsis*. Repression of the expression of MYB106 and MYB16 induced a reduction of epicuticular wax crystals and cutin nanoridges (Oshima et al. 2013). MYB31 is involved in the regulation of genes related to very long chain fatty acid elongation (Raffaele et al. 2008). MYB41 play roles in wax biosynthesis and cuticle function. The over-expression lines showed the up-regulation of a gene for a fatty acyl CoA reductase in the alcohol-forming pathway (Cominelli et al. 2008). Posttranscriptional regulators controlling the expression of wax-related genes are well known. For example, CER7 functions as a putative ribonuclease-degrading mRNA encoding a repressor of CER3/WAX2/YRE, thus regulating wax biosynthesis by controlling the expression of CER3/WAX2/YRE (Lee and Suh 2016). CER9, an E3 ubiquitin ligase gene, might negatively regulate wax biosynthesis in response to environmental stresses (Lu et al. 2012). Increased knowledge of wax biosynthesis pathways and regulation may shed light on the links between wax changes and stress tolerance. This in turn could result in breeding of cultivars with improved cutin and wax layers.

1.2.3 QTL analysis of wax-related genes

The wax biosynthesis pathways and the genes involved in them are well studied

in *Arabidopsis* mainly via reverse genetic methods (Kunst and Samuels 2003; Samuels et al. 2008; Borisjuk et al. 2014; Lee and Suh 2016). In other plant species, many genes haven't been cloned and functionally verified. QTL analysis using different mapping populations is the predominant method of locating the genomic regions controlling target traits, and provides bases for map-based cloning and candidate gene identification. Quantitative trait loci regulating wax biosynthesis have been mapped in different plant species such as rice [*Oryza sativa* L.] (Srinivasan et al. 2008), sorghum (Burow et al. 2008), maize [*Zea mays* L.] (Liu et al. 2012) and onion (Damon and Havey 2014). Gosney et al. extracted wax from *Eucalyptus globulus* and did component analysis of wax using GC-MS and mapped QTL associated with composition (Gosney et al. 2016). They found that many components have the same peak within the same genetic region on chromosomes. The most significant QTL for wax load is co-localized with QTL for β-diketones on chromosome 11, indicating that β-diketones are one of the major components of wax. Wax QTLs usually co-localize with other physiological or morphological traits, indicating the importance of wax biosynthesis in various metabolic pathways. In rice, QTL for epicuticular wax (EW) on chromosome 8 co-localized with drought tolerance QTLs related to root and shoot development in drought stressed environments. These pleiotropic QTLs or QTL clusters can be further dissected to identify the candidate genes and applied in MAS for breeding (Srinivasan et al. 2008).

In wheat, wax biosynthesis pathways haven't been well studied and the genes involved in the pathways are elusive. Several studies have been conducted on the clarification of wax related QTLs and putative genes. Mondal (2011) used a set of 121

recombinant inbred lines to map wax, glaucousness, canopy temperature (CT) and other physiological traits. The study identified stable EW QTLs across different environments located on chromosomes 1B and 5A. QTLs for leaf and spike temperature depression co-localized on chromosome 5A, indicating that wax is related to heat tolerance by mediating the decrease in the canopy temperature. In one a previous study involving a bi-parental population a glaucousness QTL on 5A was found to be associated with heat stress tolerance (Esten Mason et al. 2010). Bennett (2012) identified a novel QTL for flag leaf glaucousness on chromosome 3A that was stable across 6 environments and accounted for up to 52% of the genetic variance in a DH population. Various studies were conducted with the aim of identifying genes regulating wax or glaucousness biosynthesis in wheat, but several genes have been deciphered at the molecular level. Adamski (2013) pointed out that *Iw1* played a role in the inhibition of the formation of β-diketones related to the glaucousness phenotype.

Based on the previous studies, wax QTLs co-localize with various traits, including yield components, canopy temperature and stress tolerance, indicating that wax might be a part of a gene network affecting the expression of other genes and thus multiple traits. However, these QTLs were identified from the bi-parental populations and to date no studies mapping wax-related genes in a diverse set of germplasm have been reported. Association mapping is a widely used tool in plant genetic studies. Compared with bi-parental mapping, it can capture more recombinant events and has higher resolution to map traits of interest. In wheat, genome-wide association mapping identified significant regions related to yield (Breseghello and Sorrells 2006; Massman

et al. 2011; Tadesse et al. 2015) and diseases (Adhikari et al. 2011; Tadesse et al. 2014; Kertho et al. 2015; Jighly et al. 2015; Bajgain et al. 2016) and many QTLs with small effects can be characterized. However, the genes controlling the regulation of wax expression still remain unclear and the properties conferred by wax are still not clarified.

1.3 Research objectives and rational

In this study, we aim to map wax QTLs in a bi-parental mapping population and an association mapping population. The major wax QTLs across different populations and different environments are expected to be identified. These QTLs can be used for further dissection and identification of candidate genes underlying wax biosynthesis and regulation, which will play an important role in breeding of wheat cultivars with an improved layer of wax deposition and properties that can be well adapted to stressed environments.

The primary goals of this study are to define the correlation between wax load, glaucousness and other physiological traits at the reproductive stages, identify the QTLs related to wax biosynthesis combining phenotypic data with genotypic data in different environments, and finally find candidate genes through fine mapping and comparative genome analysis. As a prelude to this proposal, we have done the preliminary experiments in the greenhouse to investigate the primary components of EW in wheat as a result of heat stress. Wax-related QTLs and glaucousness QTLs were stably located on chromosome 2B in different stages. Previous studies showed that wax production gene

W1 is located on 2BS and is closely related to the synthesis of β-diketones, a determinant component for glaucousness formation (Zhang et al. 2013). The correlation between glaucousness and wax is not high, yet it has been shown that glaucousness is positively correlated with grain and biomass yield under water sufficient conditions (Johnson et al. 1983).

Based on the preliminary experiments and previous studies in our lab, we hypothesize that constitutive wax QTLs exist for the regulation of wax metabolism and early reproductive development wax biosynthesis pathways. QTLs that are activated during flower initiation are key to a plant's adaptation to abiotic stresses. Given the difficulty of visual and chemical assay to differentiate between varieties with diverse wax abundance and compositions, finding closely linked markers would prove vital to wheat breeding. Key aspects of EW formation are both genetic background and environment dependent. Many environments, such as drought, heat or disease, can trigger the increase in EW or glaucousness. In order to identify diagnostic markers that can be broadly applied for various environments, we need to characterize and verify the major QTLs under different environments using different mapping populations. This will allow us to define the key genomic regions in which wax candidate genes are located. We will test the hypothesis and identify markers for breeding using the following specific objectives:

Objective 1: Characterize the correlations between wax-related traits and other agronomic traits on a RIL population at different developmental stages. Determine the

genetic link between epicuticular wax production and glaucousness on different populations in different environments.

Objective 2: Develop a saturated genetic map using SNP array data. Characterize the QTLs regulating epicuticular wax load and other related traits at different developmental stages using RILs population.

Objective 3: Identify the significant marker-trait associations on an association panel in different environments and identify the diagnostic markers linked to wax-related traits.

This research will allow for the development of a saturated genetic map in wheat constructed with 90K SNP array data. Also, it will lead to the identification of wax-related QTLs using different mapping populations aimed at verifying major wax QTLs that are important in regulating wax biosynthesis. We expect to find the diagnostic markers closely linked to wax-related traits. This research will provide valuable insight into the identification of major wax biosynthesis pathways.

CHAPTER II

IDENTIFICATION OF THE QUANTITATIVE TRAIT LOCI (QTL) OF WAX-RELATED TRAITS IN THE BI-PARENTAL POPULATION

2.1 Introduction

Wheat is one of the most important crops, providing 20% of the daily protein and calories for 4.5 billion people in the world. It is predicted that by 2050 the needs of wheat production will increase 60% as the world population approaches 9 billion (The Wheat Initiative 2011), which requires that annual wheat production increase to at least 1.6%. However, the current annual yield increase is below 1%. Wheat-growing regions are subject to various biotic and abiotic stresses, which brings great challenges in terms of yield increase. Breeding wheat cultivars to be adaptive to environmental stresses and maintain yield stability can help relieve the pressure from world population increase and climate change. Wheat (*Triticum aestivum*) is one of the most widely-planted crops worldwide (FAO 2016).

Epicuticular wax is a major component of the cuticle covering the leaf surface, forming the barrier between the plant and the outer environments (Kerstiens 1996b). It has many functions contributing to the interaction between plants and biotic and abiotic environments, aiding plants in stress adaptation. It has been shown the cuticle can reduce non-stomatal water loss, which is beneficial for plant tolerance to drought and heat conditions (Kosma et al. 2009; Javelle et al. 2010; Yeats and Rose 2013). Wax can reflect and dissipate extra light, reducing received energy in plants and keeping plants

from the damages caused by UV radiation, thus further assisting in a plant's adaptation to the heat stress environment (Shepherd and Wynne Griffiths 2006). In addition, wax plays an important role in defense against various biotic stresses due to the participation of diversified cuticular compositions in the interaction between plants and bacteria, fungal pathogens and insects (Jenks et al. 1994; Eigenbrode and Espelie 1995; Eigenbrode et al. 2000). In certain environments, especially in drought-stressed conditions, there have been positive correlations between leaf wax and yield (Johnson et al. 1983), as well as between wax and canopy temperature depression, which likely provides plants with drought tolerance (Mondal 2011). However, the precise contribution of wax to yield and stress adaptation has not been determined. The effects of wax on plant growth and development are largely environment and genetic background-dependent (Johnson et al. 1983; Simmonds et al. 2008; Frizell-Armitage 2016). Environment-specific and genotype-specific studies are needed to dissect the genes involved in different wax biosynthesis pathways and to characterize the functions of wax on plant adaptation to various environments.

Epicuticular wax is a complex of various components including very-long-chain fatty acids (VLCFAs) and derivatives such as alkanes, alcohols, ketones, aldehydes and esters, as well as triterpenoids and flavonoids (Samuels et al. 2008; Javelle et al. 2010). Wax composition and its amount vary greatly among different species and even different cultivars within the same species. Wax composition and wax load change with the developmental stage (Jenks et al. 1995; PostBeittenmiller 1996; Wang et al. 2015b). In *Arabidopsis*, the fatty acids, alkanes and alcohols are the main components on the leaves

surface. Alcohols, alkanes, fatty acids and esters comprise the cuticular waxes. In wheat, the primary alcohols are the major components of cuticular waxes. The proportion of primary alcohols was decreasing with the developmental stages; meanwhile, the percentage of β-diketones, OH-β-diketones and alkanes fatty acids was increasing (Wang et al. 2015). Especially in glaucous wheat, β-diketones and OH-β-diketones are also viewed as major compositions in wheat wax (Bianchi and Figini 1986; Zhang et al. 2013; Adamski et al. 2013). It has been shown that β-diketones accounted for more than 60% of the wax load in glaucous NILs but were depleted in the glossy lines (Zhang et al. 2013). The loss of β-diketones was associated with a reduced glaucousness phenotype (Zhang et al. 2015).

There are three main wax biosynthesis pathways in wheat: the alcohol-forming pathway via acyl reduction process, the alkanes-forming pathway through decarbonylation reactions, and the type III polyketide pathway. VLCFA can be either converted into primary alcohols and esterified products or into secondary alcohols, alkanes and aldehydes (Dennis and Kolattukudy 1991; Vioque and Kolattukudy 1997; Rowland et al. 2006; Greer et al. 2007; Li et al. 2008; Bernard et al. 2012), which predominate in vegetative stages. In the reproductive stages, the β-diketone biosynthesis pathway is active, using C14 and C16 as precursors (Mikkelsen 1978). The three main pathways interact with each other; usually the depression of one pathway can activate the other pathways in the form of the compensation of different end products. It has been shown that the alcohol content decreased when β- and OH-β-diketones were synthesized

(Wang et al. 2015b). In the *Iw1* and *Iw2* NILs, the production of β-diketones decreased with the increase of primary alcohols and aldehydes (Zhang et al. 2013).

Considering the importance of epicuticular wax and its functions in biotic and abiotic stress tolerance, deciphering the mechanism of wax biosynthesis at important developmental stages and identifying wax-related genes can provide tools for breeding wheat cultivars with an improved amount and composition of wax, which may contribute to increased yield and stability under stressed conditions.

Quantitative trait locus (QTL) mapping provides a powerful tool for the dissection of the genetic basis underlying complex quantitative traits and candidate gene identification by the linkage of phenotypic variation with genetic variation. Conventionally, a few hundred markers may be used to map traits in a bi-parental population with a few hundred lines (Sonah et al. 2014). However, the genes controlling the traits are likely to be mapped to a large-interval genomic region with large numbers of candidate genes because of the low-resolution of the genetic maps constructed with low-density markers. Increasing the resolution of the linkage maps by using high-density genetic markers can greatly improve the efficiency of genetic dissection of complex traits. With the development of molecular biology, various molecular genetic markers have been developed, especially during the last four decades (Grover and Sharma 2016). The resolution of markers is increasing considerably with the advancement of molecular techniques, including nucleic acid hybridization, the polymerase chain reaction (PCR) and next generation sequencing (NGS). Single nucleotide polymorphism (SNP) markers have the highest abundance among molecular

markers, and have become the major type of marker widely used in genetic studies including linkage mapping, association mapping, evolutionary study, genomic selection and molecular breeding (Rafalski 2010; Kumar et al. 2012). With the rapid development of next generation sequencing technology, large-scale, high-throughput SNPs have been identified based on increasingly complete and available sequence information. Recently, a 90K SNP array with gene-associated SNPs densely covering the whole wheat genome has been developed. The development of this assay is based on RNA sequencing of 19 accessions of hexaploid and 18 accessions of tetraploid wheat and has been ordered using eight bi-parental doubled-haploid (DH) mapping populations. The sequence reads were mapped to reference transcripts that were assembled using RNA-seq data generated from several sequencing platforms. Most of the SNPs were Infinium II (one probe per SNP) assays and the others were Infinium I (two probes per SNP) (Wang et al. 2014). This assay has been used in the construction of high-density linkage maps for the identification of genetic regions conferring important agronomic and physiological traits in wheat (Gao et al. 2015; Wang et al. 2016; Zhai et al. 2016).

Some studies have clarified the correlation between wax and other traits in wheat, identified QTL related to wax biosynthesis, and fine mapped wax genes. In terms of the complexity of wax and the great variations with different environments and genotypes, wax is controlled by numerous loci, including several main-effect QTLs and many minor-effect QTLs. Bennett (2012) conducted a multi-year, multi-location experiment on a DH population to locate wax-related genes. A novel flag leaf glaucousness QTL with major effect was identified on chromosome 3A. This QTL, designated as *QW.aww-*

3A, was consistently detected in all the environments and accounted for up to 52% of the variation in the population. Another consistent QTL with a large effect was located on 2D. Meanwhile, some other small-effect QTLs specific to certain environments were mapped on chromosomes 1D, 4D, 5B, 2B, 3B, 3D and 7D (Bennett et al. 2012). A greenhouse study (Mondal et al. 2014) was conducted to map wax QTLs on an RIL population under heat-stressed environments for two years. Five different wax QTLs were detected on chromosome 1B, 3D, and 5A, explaining 9% to 12% of the phenotypic variation.

The co-localization of wax QTL and canopy temperature depression QTL indicated the importance of wax on heat stress tolerance, due to the fact that canopy temperature depression contributes to plant stress adaptation and maintaining yield under non-optimal environments (Pinto et al. 2008; Esten Mason et al. 2011). The correlation analysis indicated that there was a significantly positive relationship between wax and canopy temperature depression, although the association was low with $r = 0.14$. Huggins (2014) used a population of 180 RILs to identify QTL controlling important phenotypic traits including canopy temperature, wax and yield, as well as to characterize the effects of wax on wheat growth. A total of 44 QTLs were detected across nine environments, nine of which were related to epicuticular wax biosynthesis, located on the chromosome 1A, 1B, 2A, 2B, 3A, 3B, 4B, 6B, and 7A. On chromosome 2B and 3B, two yield-stability QTLs were detected that co-localized with epicuticular wax QTLs, and three yield-stability QTLs were co-localized with canopy temperature depression, which demonstrated that wax may have an effect on maintaining yield across multiple

environments. Mohammed (2014) identified a major epicuticular wax QTL located on 2B, which has pleiotropic effects on canopy temperature and yield components. Under heat stressed conditions, stable wax QTL were located on chromosome 5A and 1B, which co-localized with canopy temperature depression and yield components (Mondal 2011). The correlation between wax and yield has been studied, although there were no precise conclusions about the contribution of wax to yield. Under drought-stressed conditions, wax was reported to correlate with increased water use efficiency or transpiration and thus with yield increase (Chatterton et al. 1975; Monneveux et al. 2004; Jefferson et al. 2016). However, Risk pointed out that glaucous lines and non-glaucous lines produced the same amount of biomass in a dry environment (Risk et al. 2013). Even negative correlations between wax and yield in a Mediterranean environment have been characterized (Simmonds et al. 2008). Based on this information, it is likely that the contribution of wax to wheat growth and development and its correlation with other physiological traits is largely dependent upon environment and genetic background.

It has been well established that there are 2 sets of genes regulating glaucousness during reproductive stages: *W1*, *W2* and *Iw1*, *Iw2*. That is, wax production genes and wax inhibitor genes, respectively (Zhang et al. 2013). Wax production genes are usually closely linked to wax inhibitor genes. *W1* and *Iw1* are located on 2BS, and *W2* and *Iw2* are located on 2DS (Tsunewaki and Ebana 1999). Many studies have focused on the localization of the wax inhibitor genes via the construction of high-resolution genetic maps (Wu et al. 2013; Wang et al. 2014c). However, there is little in-depth information

about the location and function of wax production genes. Zhang et al. (2013) demonstrated that wax production genes regulate the biosynthesis of β-diketones, which play an important role in glaucousness formation during reproductive stages. However, it is still not fully understood which wax synthesis genes are involved in glaucousness formation and stress tolerance. Many aspects of wax biosynthesis and the mechanisms underlying the interactions between wax and other physiological traits are not well known. Dissection of the genes involved in the gene networks controlling the spatial and temporal expression of wax can lay a foundation for wheat breeding for wax.

The objectives of this study were to identify high-quality SNPs using the recent wheat 90K SNP iSelect assay screened on a RIL population derived from the cross between Halberd and Len, and to construct a saturated linkage map with the identified SNPs. The association between wax content, glaucousness visual score and other agronomic traits were characterized and QTL analysis was performed to identify QTL related to wax biosynthesis and other important traits. The SNPs closely linked to different agronomic and physiological traits on the RIL population were identified.

2.2 Materials and methods

2.2.1 Plant materials

A population of 180 RILs was derived from a cross between spring wheat Halberd and Len. Halberd is an Australian hexaploid wheat with heat and drought tolerance, rust resistance and boron resistance (Paull et al. 1992; Bariana et al. 2007)

developed at Roseworthy Agricultural College in 1969 (Paull et al. 1998). Len, a hard red spring wheat susceptible to drought and heat stress, was developed in North Dakota in 1979. Len has moderate leaf rust resistance conferred by the *Lr34* gene (Kolmer et al. 2011). Morphologically, Halberd has a thick layer of epicuticular wax platelets deposited on the flag leaf surface, based on SEM images of flag leaves collected at 10DAP (Mondal 2011). However, Len has less visible wax deposited on the leaf and stem and has a lower glaucousness score than Halberd. Both Halberd and Len have similar flowering times and maturity. To determine similarity in phenological traits and difference in wax content between the parents, a RIL population of 180 individuals was developed for mapping epicuticular wax-related traits. This RIL population was developed via single seed descent in the greenhouse until the F5 generation, and advanced in the field until the F8 generation. In this population, there is phenotypic variation for various traits like wax content, glaucousness and canopy temperature based on previous studies in our lab (Mondal 2011; Mohammed 2014). Flowering time differed little, which is beneficial for the elimination of the noise caused by the phenology differences.

2.2.2 Genotyping with 90K SNP iSelect array

The leaf samples from every individual in the Hal x Len RIL population and parents were collected from 2-week-old seedlings from the F8 generation. A modified CTAB method was used for genomic DNA extraction (Doyle, 1987; Cullings 1992;

Stein et al. 2001). Seedlings for every genotype were ground to a fine powder in mortar and pestle with liquid nitrogen. The powder was suspended in buffer solution made with 0.35 M sorbitol, 0.1 M TrisHCl and 5 mM EDTA. The suspended samples were then heated at 65 °C for one hour. A mixture of chloroform and isoamyl alcohol (24:1) was added to the solution. After spinning down, the supernatant was transferred into a fresh tube and the same volume of cold isopropanol was added to the aliquot. Gently inverting the tube fabout 10 times made the nucleic acids become visible. After discarding the supernatant, the DNA pellet was washed with 70% ethanol and the pellet dried in the tube. Finally, DNA quality and quantity was checked on a 0.8% agarose gel or by spectrophotometry.

Hybridization to high-density wheat 90K SNP iSelect arrays was performed on the DNA extracted from the RIL population (according to the manufacturer's protocol from Illumina) and analyzed at the USDA-ARS Biosciences research laboratory located in Fargo, North Dakota by Dr. Shiaoman Chao. GenomeStudio (GS) software (Illumina) was used for clustering and genotype calling for the array data. Manual curation was conducted after automatic clustering and analysis conducted with the default algorithm implemented in the software.

Manual correction and validation were performed on the polymorphic SNPs. The monomorphic SNP markers were ignored, which were shown as single clusters on the software (Figure 1d). The polymorphic markers can separate RIL lines into 2 or 3 distinct clusters (Figure 1 a-c). As the Figure 1 showed，one circle defines each cluster. When the data was curated, the circle boundary was adjusted and expanded to include as

many genotypes as possible. Meanwhile, all genotypes were confirmed to be within 0.2 Norm Theta for a single cluster. In order to differentiate clusters, we set 0.2 Norm Theta as the low threshold for the distance between clusters. SNPs with more than 4 clusters were marked as multisite variants (MSV) and excluded from the analysis (Figure 1e). SNPs with clusters close to the x-axis can be viewed as missing data (Figure 1f). Data was exported once the clusters had been manually curated. SNPs with more than 20% missing data and those with the ratio of the parents' genotypes outside of the range of 0.25 to 4 were removed from further analysis. After all the filtering steps, the polymorphic markers were grouped into 6 types (Table 1) based on the genotype calling of the parents and the number of clusters in the GS software. Finally, data was transferred into a format that can be used for the construction of linkage map and QTL analysis.

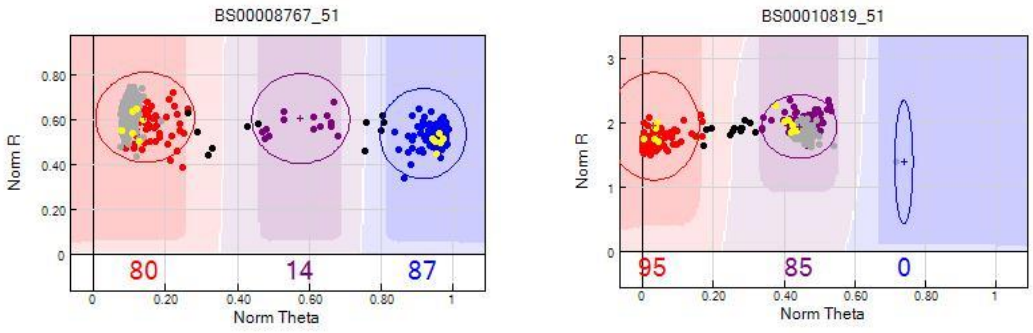

a b

Figure 1 Different types of SNPs displayed in the Genome Studio.

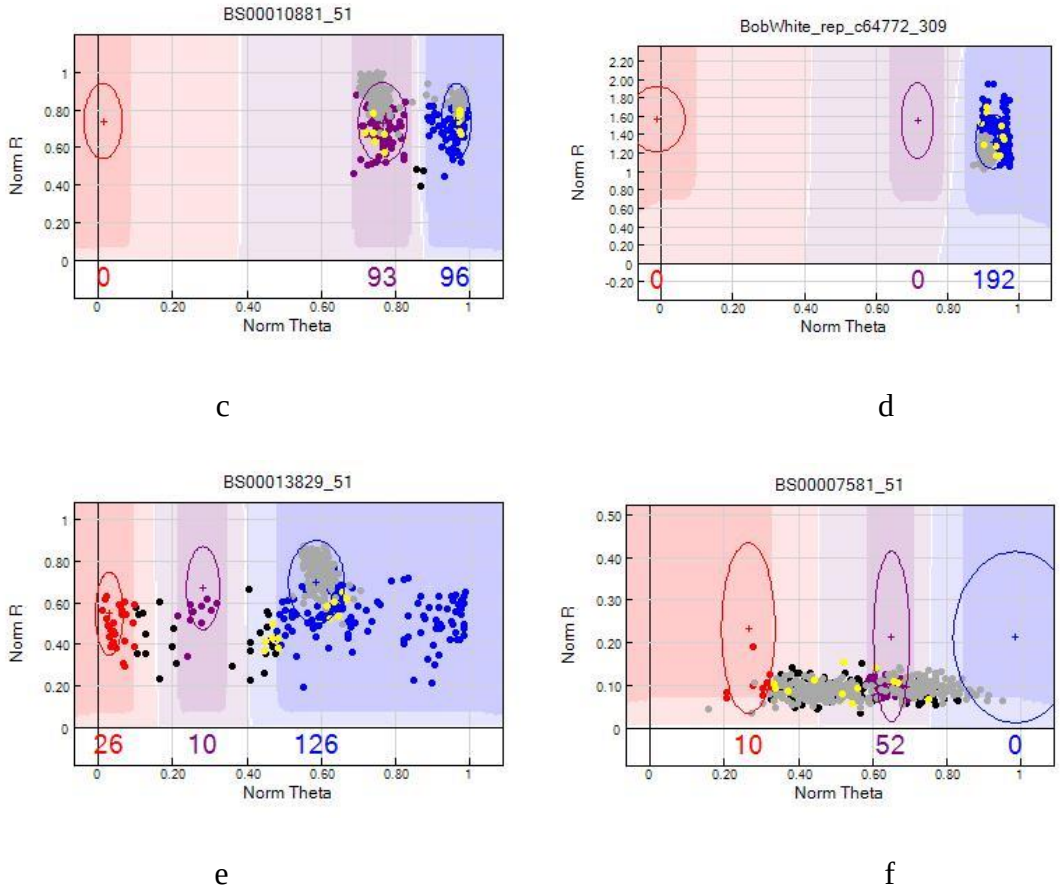

Figure 1 Continued

Table 1 Summary of the different types of polymorphic single nucleotide polymorphisms (SNPs) identified in Genome Studio.

Type	Halberd	Len	Heterozygote	NO.of SNPs	Percentage of mapped SNPs
I	AA	BB	AB	832	0.1
II	BB	AA	AB	848	0.11
III	AA	AB	_	1267	0.16
IV	AB	AA	_	1322	0.16
V	AB	BB	_	1887	0.23
VI	BB	AB	_	1892	0.24

2.2.3 Genetic map construction

The MSTmap program (Wu et al. 2007) was used to construct the linkage map with 8,440 SNPs identified from the 90K wheat SNP array data. This process was executed using R/ASMap package (Taylor and Bulter, 2014) in the R statistical environment (R Development Core Team, 2014). mstmap() function with the kosambi algorithm was used to construct an object containing linkage groups information. The function pullCross() was used to identify the markers with excessive segregation distortion and the threshold of p value in this function was set as 1e-10. The function genClones() and fixClones() were used for the identification of lines with high similarity (tol = 0.99) and the generation of consensus genotypes for each of the clonal groups, respectively. After profiling and visualization of the basic statistics including crossovers, double crossovers and missing values using the function statGen() and profileGen(), the lines with excessive crossovers and double crossovers were removed from further analysis. The cleaned dataset was then used for the linkage map construction.

A p-value = 1e-22 was used for the function of mstmap() to group markers. Based on the output, we removed groups with less than 9 SNPs. The wrongly assigned SNPs in each group were also removed. Here, 40K SNPs with known chromosome location mapped by Wang (2014d) were used as anchored markers, which helped define the chromosome locations of the grouped SNPs. In Wang's study (2014d), they used eight bi-parental populations to make a consensus map with 40,267 (thereafter, 40K) out of 91,829 (90K) SNPs. The wrongly assigned SNPs were defined as markers with known chromosome locations different from the majority of the known-location markers

in a linkage group. The anchored markers mapped on different chromosomes were kept as long as one of the chromosome locations was in consensus with the chromosome location of the majority of the SNPs in a linkage group. Linkage groups were named based on the chromosome location. The number of bins for each linkage group was recorded, which was used for the calculation of the average genetic distance on different chromosomes. That is, the total genetic distance for each linkage group or chromosome was divided by the number of bins for every group or chromosome and the overall average distance across the whole wheat genome, which is the overall genetic distance divided by the total number of bins.

2.2.4 Planting, growth conditions and experimental design

All the plants were grown in a greenhouse, in which the air temperature changed with the external environment. This provides a relatively optimal condition for growth with enough water and fertilizer. Plants were watered every other day and fertilized 3 times until maturity. Fungicide was applied to protect plants from powdery mildew disease at flowering stage. RIL lines including the parents were arranged according to a randomized complete block design (RCBD) with 2 biological replications. They were used for QTL analysis to map wax-related genes and other physiological traits. Here, we focused on 3 important reproductive stages: late booting, flowering and 5-10 DAP stage.

2.2.5 Trait evaluation

Sampling and physiological trait measurements usually occurred at 12:00 pm - 2:00 pm during the appropriate stage. Glaucousness was visually scored based on its distribution on abaxial flag leaf side at late booting, flowering and 5DAP stages. The time for glaucousness evaluation was 12:00 pm on a sunny day. The leaf was first divided into 8 even parts. This trait was scored from 0 to 8. 0 stands for non-glaucous, 4 stands for glaucousness covering the half of the leaf and 8 stands for glaucousness covering the whole leaf.

Canopy temperature (CT) was measured three times for three individuals in one pot using a handheld IR thermometer (Fluke 566 series, Everett, Washington, USA). The average CT was recorded for every individual. The air temperature was also recorded. Canopy temperature depression (CTD) was calculated as the difference between air temperature and the corresponding canopy temperature.

For every plant, the date was recorded in relation to phenology including late booting, heading and flowering date. Booting was recognized as being the day when the top of the head reached the top of the flag leaf sheath, heading was when the bottom of the head emerged from the leaf sheath and flowering was when the spikelets in middle of the spike flowered. The number of days from planting to the phenology date were recorded as the corresponding phenological time, which can be used for QTL analysis. In the greenhouse experiment, the maximum difference in flowering time in the RIL population was seven days. We used the flowering time as a covariate to adjust the data in order to minimize the phenological noise in the identification of target QTLs.

For every plant, we recorded the height of the part of plants above the soil. Other traits like tiller number, head length and awn were also recorded. Throughout this experiment, the measurements of the traits mentioned above were conducted at every stage for QTL analysis.

2.2.6 Wax extraction and quantification

After key physiological traits such as glaucousness, flowering date and canopy temperature were measured, flag leaf samples were collected. One individual plant in a pot was used for tissue sampling for wax extraction. Discs were collected from the flag leaf using punchers with a diameter of 0.65cm.

Wax extraction: After disc collection, the discs were air-dried and the wax content was measured according to published methods (Richardson et al. 2005). Two ml chloroform was added to the vials with discs at room temperature, making sure that all the discs were immersed into the solution. After 30 seconds, the epicuticular wax was dissolved. The extraction solution was moved to a new glass vial and the solution was air-dried. The resulting wax samples were stored in a 4°C refrigerator for further analysis.

Wax quantification: Colorimetric methods (Ebercon et al. 1977) were used for the quantification of wax content. The reaction reagent was made by dissolving $K_2Cr_2O_7$ in H_2SO_4 and distilled water. Three-hundred □l reaction reagent was added to each vial with dry wax samples and incubated in a water bath at 100° C for 30 minutes in order to

achieve oxidization. After cooling down, 700 ul ultra pure water was added to each vial. The solution was mixed and allowed to develop color for 1 hour. One hundred ul of each mixed solution was loaded into 96-well polystyrene plates (Greiner Bio-One) and analyzed on a spectrophotometer (PHERAstar plus, BMG LABTECH, Offenburg, Germany), which can detect the optical density of samples at 590nm. Wax content was quantified using the formula: X = (A-0.0189)/0.3328; A stands for absorbance, and X means wax content using mg/dm^2 units. The calculation formula was taken from a standard curve, which was developed according to the methods mentioned in Ebercon's study (Ebercon et al. 1977).

2.2.7 Data analysis

Pearson's correlation analysis was performed using SAS 9.4 (SAS Institute Inc. Cary, NC, USA) to characterize the correlation between important agronomic and physiological traits including glaucousness, canopy temperature, canopy temperature depression and epicuticular wax load at 3 different developmental stages.

Multiple QTL Mapping (MQM) analysis was performed using MapQTL 6.0 (Van Ooijen, 2011) by using all the SNP markers identified as cofactors. QTLs can be characterized by the combination of phenotypic data and the genetic linkage map constructed. The QTLs with LOD score more than 3.0 were declared as significant ones. MapChart 2.2 software (Voorrips 2002) was applied for the graphical presentation of the linkage groups and QTLs for each trait.

The peak SNPs identified from the QTL analysis were used to identify potential candidate genes. The 90K SNP sequence information can be downloaded from the T3/ Wheat website (https://triticeaetoolbox.org/wheat/view.php?table=markers&uid=92235). With the SNPs sequence, we can perform a blast search from NCBI (https://blast.ncbi.nlm.nih.gov/Blast.cgi?PROGRAM=blastn&PAGE_TYPE=BlastSearch&LINK_LOC=blasthome).

2.3 Results

2.3.1 Validation and manual correction of SNP calling from 90K iSelect SNP array

The 90K SNPs array was used for genotyping the RIL population. Based on the types of clusters of individuals, the polymorphic markers were used for linkage group construction. Figure 1 presents different types of SNP markers. Figure 1a shows the heterozygous markers. This kind of SNP can clearly group individuals into three clusters according to the description in Liu's study (Liu et al. 2015). Based on the clusters in which the parents reside, heterozygous markers were defined as type I or type II, as shown in Table 1. Other kinds of polymorphic markers are shown in Figure 1b and c. They can divide the RIL lines into two groups. Based on the genotype of parents, SNPs like Figure 1b were defined as type III or type IV markers and SNPs shown in Figure 1c were defined as type V or type VI markers, respectively. Only these six types of polymorphic markers that can differentiate the RIL lines can be used for linkage map construction. The monomorphic markers shown as only one cluster (Figure 1d) and the

multisite-variants-type (MSV) markers did not define clusters (Figure 1e and f) and were removed from further analysis. After manually removing the monomorphic markers, multisite-variant-type SNPs and those with extreme segregation ratios, 8,440 SNPs were finally identified for further analysis.

2.3.2 Linkage map construction

Genetic maps are broadly used for the detection of DNA region underlying the traits of interest, which provides the framework and baseline for the dissection of the genetic basis for important traits. There are various software programs for linkage map construction like JoinMap (Van Ooijen, 2006), Onemap (Margarido et al. 2007), R/qtl (Broman et al. 2003), GACD (available from www.isbreeding.net) and MSTmap (Wu et al. 2007). In this study, we followed the instructions in MSTmap to make linkage groups. First, the SNPs with a high segregation ratio and missing values should be removed from the analysis. Using the function pullCross() with parameter seg.thresh = 1e-10, 24 SNPs with high segregation ratios have been identified. The lines showing high similarity were grouped together and only one individual was kept for every group. In the Hal x Len population, HL49 and HL140, HL55 and HL120, HL62 and HL137, HL63 and HL144, HL64 and HL126, HL89 and HL95, HL136, HL165, HL169 shared high similarity, and lines HL49, HL62, HL63 and HL89 were kept to represent each similarity group for further analysis. Lines with excessive crossovers and double crossovers were eliminated from the study. The threshold for crossover and double

crossover was set at 280 and 40, respectively. At this step, the lines HL27, HL83 and HL141 showed extreme high crossovers and double crossovers, which were removed. In total, 164 lines and 8416 SNPs were used for further analysis. Using the function mstmap() in the package with the parameter p-value=1e-22, 78 linkage groups were constructed. Based on this framework, linkage groups with less than 9 SNPs were eliminated. According to the 40000 anchored markers with known chromosome locations, the linkage groups were named based on the chromosome location of the majority of the markers in a linkage group, thus the incorrectly assigned markers were removed from the analysis. Finally, 8048 SNPs were kept to construct 46 linkage groups, among which 2B, 4A, 4B, 4D, 5B, 5D and 6A have one linkage group, 1A, 1B, 3A, 5A, 6B, 6D and 7D have 2 linkage groups, 1D, 2A, 3B, 3D and 7A have 3 linkage groups, 7B has 4 linkage groups and 2D has 6 linkage groups (Table 2). Among the mapped 8048 SNPs, the number of different types of makers is 832, 848, 1267, 1322, 1887 and 1892, respectively (Table 1).

About 95.4% of the identified polymorphic SNPs were mapped on the linkage map covering all the wheat chromosomes. The overall genetic distance is 2471.71 centi morgon (cM) and the average distance is 0.31 cM per SNP and 1.39 cM per bin, which indicated the high density of this genetic map. However, the distribution of SNPs was uneven across different chromosomes. The genetic distance of every chromosome ranged from 7.44 cM to 199.50 cM (Table 3). More than 50% of the SNPs were mapped on the B genome and about 39.3% of the SNPs were distributed on genome A. Compared with A and B subgenome, the D genome had the lowest number of SNPs,

which accounted for 7.9% of the total mapped markers. This result is in consensus with previous studies (Wang et al. 2014d; Liu et al. 2015). Compared with the other 2 subgenomes, the D genome has the lowest diversity. However, the average genetic distance on the D genome is greater than that of the A genome and B genome. Among the 46 linkage groups, 2B is the largest linkage group with 1,044 SNPs, with a genetic distance up to 172.21 cM. Almost all the A and B chromosomes have more than 200 SNPs mapped, and the genetic distance is more than 100 cM, which is generally larger than the groups for D genome (Table 3, Figure 2). For the D subgenome, more than 200 SNPs were mapped on each of the 1D and 2D chromosomes, but less than 100 SNPs were mapped on the other D chromosomes. Chromosome 4D has the lowest number of SNPs, with only 9 SNPs mapped. The genetic distance for every D chromosome was less than 100 cM. The average genetic distances for all the chromosomes except for 4D and 6D were less than 1cM per SNP (Figure 2). Thus, the summary data indicated the high resolution of this linkage map.

Table 2 Summary of the distribution of SNPs mapped on 46 linkage groups.

Chromosome	NO. of bins	NO. of SNPs	Genetic distance (cM)	Average distance (cM/SNP)	Average distance (cM/bin)	Max distance (cM)
1A1	116.00	672.00	129.54	0.19	1.12	7.69
1A2	3.00	11.00	2.48	0.23	0.83	2.13
2A1	30.00	71.00	35.20	0.50	1.17	5.06
2A2	88.00	332.00	132.71	0.40	1.51	10.59
2A3	26.00	71.00	55.09	0.78	2.12	10.43
3A1	14.00	132.00	10.66	0.08	0.76	4.71
3A2	3.00	16.00	1.85	0.12	0.62	1.50
4A	30.00	91.00	57.16	0.63	1.91	9.87
5A1	36.00	81.00	71.92	0.89	2.00	10.71
5A2	4.00	14.00	9.00	0.64	2.25	3.98
6A	139.00	1044.00	172.21	0.16	1.24	8.14
7A1	7.00	80.00	3.69	0.05	0.53	1.13
7A2	13.00	21.00	16.84	0.80	1.30	6.71
7A3	4.00	18.00	1.03	0.06	0.26	0.35
1B1	4.00	99.00	5.21	0.05	1.30	3.76
1B2	11.00	17.00	30.80	1.81	2.80	10.61
2B	5.00	15.00	3.98	0.27	0.80	1.83
3B1	98.00	398.00	160.77	0.40	1.64	9.07
3B2	13.00	33.00	20.02	0.61	1.54	4.93
3B3	108.00	543.00	95.29	0.18	0.88	7.69
4B	9.00	62.00	11.07	0.18	1.23	5.53
5B	29.00	60.00	36.66	0.61	1.26	8.26
6B1	4.00	23.00	5.78	0.25	1.45	3.58
6B2	8.00	31.00	14.10	0.45	1.76	11.61
7B1	8.00	20.00	4.71	0.24	0.59	1.01
7B2	135.00	483.00	161.53	0.33	1.20	9.33
7B3	73.00	216.00	134.78	0.62	1.85	10.23
7B4	7.00	9.00	15.16	1.68	2.17	4.78
1D1	79.00	266.00	119.47	0.45	1.51	10.92
1D2	17.00	50.00	55.92	1.12	3.29	11.45
1D3	144.00	892.00	199.50	0.22	1.39	12.90
2D1	5.00	12.00	7.44	0.62	1.49	4.98
2D2	111.00	455.00	132.56	0.29	1.19	8.41
2D3	79.00	463.00	105.06	0.23	1.33	9.54

Table 2 Continued

Chromosome	NO. of bins	NO. of SNPs	Genetic distance (cM)	Average distance (cM/SNP)	Average distance (cM/bin)	Max distance (cM)
2D4	18.00	52.00	26.93	0.52	1.50	3.85
2D5	9.00	10.00	28.10	2.81	3.12	9.54
2D6	4.00	10.00	14.24	1.42	3.56	9.83
3D1	103.00	394.00	131.71	0.33	1.28	8.07
3D2	25.00	102.00	26.48	0.26	1.06	11.15
3D3	32.00	115.00	33.81	0.29	1.06	6.49
4D	57.00	317.00	72.60	0.23	1.27	6.88
5D	32.00	136.00	48.54	0.36	1.52	5.84
6D1	11.00	23.00	18.50	0.80	1.68	9.49
6D2	12.00	35.00	24.77	0.71	2.06	9.75
7D1	3.00	16.00	0.69	0.04	0.23	0.34
7D2	11.00	37.00	26.18	0.71	2.38	6.01

Table 3 Summary of the distribution of SNPs mapped on different chromosomes.

Chromosome	NO. of bins	NO. of SNPs	Genetic distance (cM)	Average distance (cM/SNP)	Average distance (cM/bin)	Max distance (cM)
1A	119	683	132.02	0.19	1.11	7.69
2A	70	186	138.08	0.74	1.97	10.71
3A	111	431	180.79	0.42	1.63	9.07
4A	135	483	161.53	0.33	1.20	9.33
5A	96	316	175.38	0.56	1.83	11.45
6A	111	455	132.56	0.29	1.19	8.41
7A	160	611	192.00	0.31	1.20	11.15
A subgenome	802	3165	1112.35	0.35	1.39	11.45
1B	118	403	167.91	0.42	1.42	10.59
2B	139	1044	172.21	0.16	1.24	8.14
3B	146	665	143.02	0.22	0.98	8.26
4B	73	216	134.78	0.62	1.85	10.23
5B	144	892	199.50	0.22	1.39	12.90
6B	97	515	131.99	0.26	1.36	9.54
7B	112	511	164.40	0.32	1.47	9.75
B subgenome	829	4246	1113.81	0.26	1.34	12.90
1D	43	219	67.59	0.31	1.57	10.43
2D	44	250	61.55	0.25	1.40	10.61

Table 3 Continued

Chromosome	NO. of bins	NO. of SNPs	Genetic distance (cM)	Average distance (cM/SNP)	Average distance (cM/bin)	Max distance (cM)
3D	20	74	24.60	0.33	1.23	11.61
4D	7	9	15.16	1.68	2.17	4.78
5D	5	12	7.44	0.62	1.49	4.98
6D	13	20	42.34	2.12	3.26	9.83
7D	14	53	26.87	0.51	1.92	6.01
D subgenome	146	637	245.56	0.39	1.68	11.61
Overall	1777	8048	2471.71	0.31	1.39	12.90

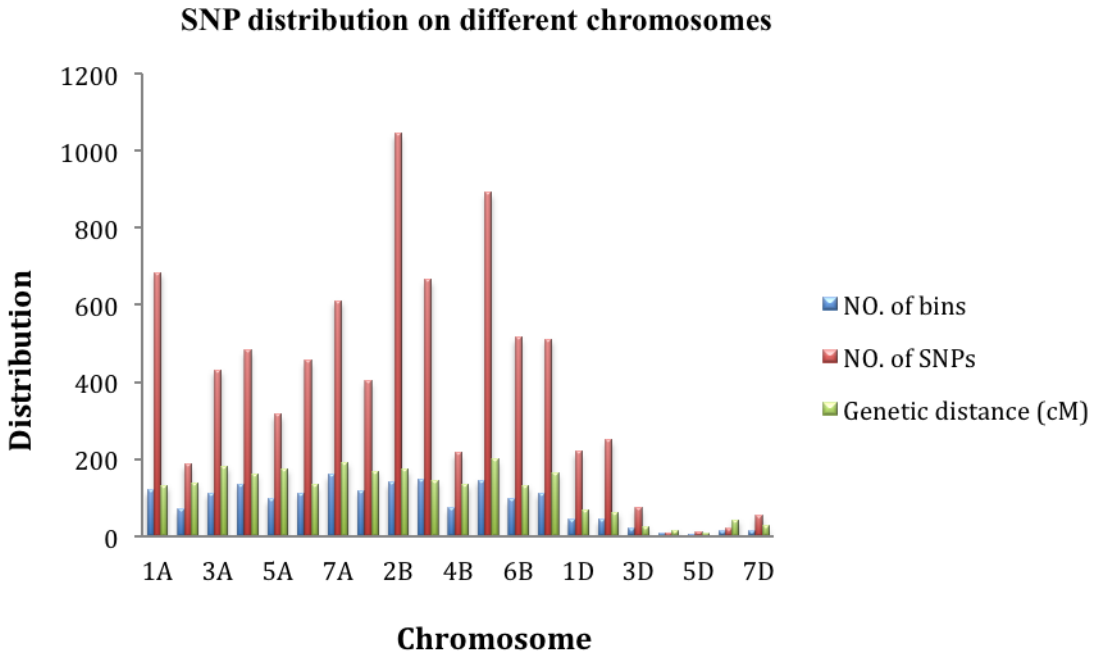

a

Figure 2 SNP distribution and genetic coverage on different chromosomes. (a) The number of SNPs and total genetic distances on different chromosomes. (b) The average genetic distance covered by SNPs on different chromosomes.

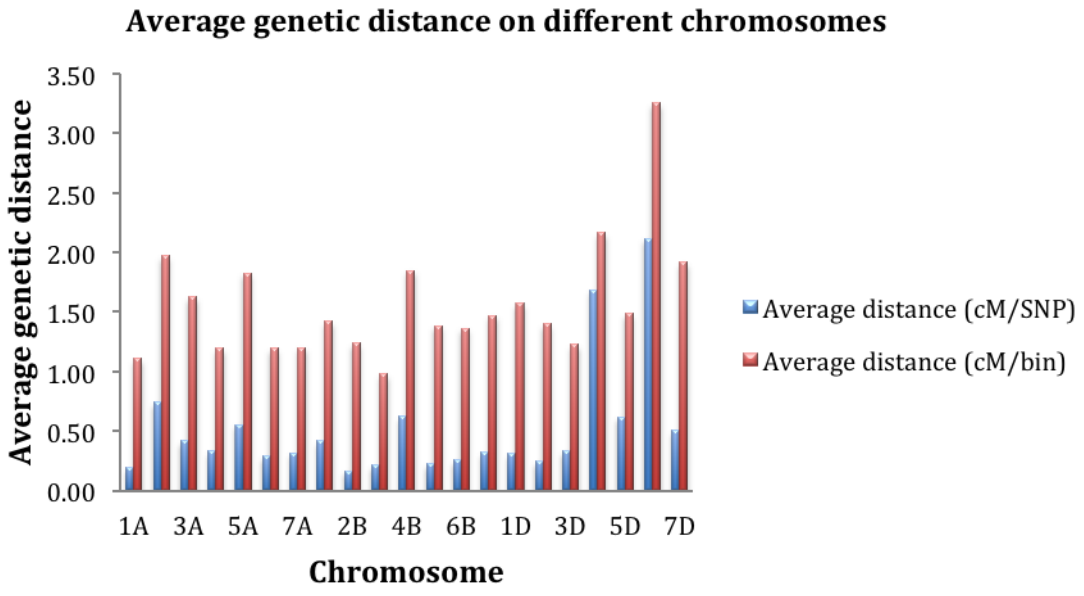

b

Figure 2 Continued

2.3.3 Agronomic data

In the greenhouse, wax load varied at different stages, ranging from 0.45-2.26 mg/dm^2 (Table 4). On average, wax was expressed more at later developmental stages than earlier stages. The air temperature in the greenhouse ranged from 18 - 35°C and the range of the canopy temperature was 16.9 - 30.8°C. The canopy temperature was generally lower than the air temperature. Based on the Table 4, we can see that wax accumulated with the development of plants and reached its highest value at the 5DAP stage. The population was grown in a greenhouse with the temperature fluctuating based on the outer air temperature. The temperature in the greenhouse and the canopy

temperature increased with the developmental stages of the plants. However, the glaucousness score was highest at the flowering stage. Canopy temperature depression (CTD) decreased with the phenological stages, which may be related to the changes in leaf area. A chi-square test was conducted to test the segregation of the awn and awnless trait. It was shown that the segregation ratio deviated significantly from 1:1, which meant there was more than one loci controlling awn development. Awn development was therefore viewed as a quantitative trait.

Table 4 Combined physiological, agronomic and phenological traits means and range for the RIL population grown in the greenhouse at different growth stages.

Traits	Unit	Late booting stage			Flowering stage			5DAP		
		Mean	Minimum	Maximum	Mean	Minimum	Maximum	Mean	Minimum	Maximum
EWL	mg/dm2	1.25	0.45	2.26	1.34	0.78	2.35	1.39	0.63	2.46
CT	°C	24.72	16.90	30.80	25.25	18.70	32.60	25.60	18.10	32.50
T	°C	27.40	18.00	35.50	27.89	18.00	35.00	27.65	21.50	33.00
CTD	°C	2.63	-1.90	8.00	2.20	-0.80	6.30	1.86	-1.40	27.00
Glau		5.08	0.00	8.00	6.26	0.00	8.00	6.20	0.00	8.00
PH	cm	31.63	22.50	41.88	31.17	20.88	40.88	30.53	2.00	42.38
HL	inch	3.84	3.13	4.88	3.60	2.75	4.50	3.89	2.88	27.50
BB	days	98.32	80.50	114.00	93.79	79.50	102.00	92.75	81.00	101.00
LB	days	100.82	85.00	112.50	100.82	85.00	112.50	99.90	87.50	112.00
TE	days	NA	NA	NA	103.28	88.50	116.00	102.98	91.50	113.00
FT	days	NA	NA	NA	105.68	93.00	116.00	104.81	94.00	114.00
5DAP	days	NA	NA	NA	NA	NA	NA	109.02	3.00	119.00

Table 4 Continued

Traits	Unit	Late booting stage			Flowering stage			5DAP		
		Mean	Minimum	Maximum	Mean	Minimum	Maximum	Mean	Minimum	Maximum
TN		3.73	2.00	5.00	3.36	2.00	5.00	3.65	1.00	5.00
Awn		0.57	0.00	1.00	0.58	0.00	1.00	0.57	0.00	1.00

Key: Epicuticular wax load (EWL), canopy temperature (CT), temperature (T), canopy temperature depression (CTD), Glaucousness (Glau), plant height (PH), head length (HL), phenological traits including booting begin (BB), late booting (LB), tiller emergence (TE), flowering time (FT), 5 days after pollination (5DAP), tiller number per plant (TN) and awn and awnless (Awn) at late booting, flowering and 5-10 DAP stage.

2.3.4 The correlations among different physiological traits

Pearson's correlation analysis was performed for important physiological traits at 3 different developmental stages using SAS (SAS v9.4, SAS institute Inc. Cary, NC, USA) to investigate the associations between different traits. Epicuticular wax load has a highly significant correlation with glaucousness, head length and phenology-related traits. These significant correlations stably existed at all 3 stages. Epicuticular wax load was positively correlated with glaucousness. However, the correlation between wax and glaucousness was not high, and the correlation coefficients were 0.58, 0.49 and 0.47 at late booting, flowering and 5 DAP stage, respectively. EWL has a significant positive association with phenological traits, especially with flowering time, and the coefficient can reach up to 0.56 at flowering stage. There were significantly negative correlations between wax and canopy temperature depression at later reproductive stages. However, the correlation was not high ($r = -0.16$, $r = -0.19$ at flowering and 5DAP stage, respectively, $P \leq 0.001$) (Table 5). There was no correlation between EWL and canopy temperature in this study, which is contrary to the previous field experiments in our lab (Huggins 2014). As a component of leaf epicuticular wax, glaucousness has significantly positive correlations with EWL and phenological traits at all three stages. Like EWL, glaucousness negatively correlated with CTD, and this significant correlation consistently existed at later reproductive stages. Positive correlation between plant height and EWL and the significantly positive correlation between glaucousness and head length existed in the early development stages.

Table 5 Pearson's correlation coefficients of epicuticular wax and other agronomic traits for Hal x Len population at different stages in the greenhouse.

Late booting stage												
Trait	EWL	CT	T	CTD	Glau	PH	HL	BB	LB	TN		
CT	0.04ns											
T	-0.01ns	0.84***										
CTD	-0.12ns	0.15ns	0.62***									
Glau	0.58***	0.03ns	-0.03ns	-0.1ns								
PH	0.36***	-0.1ns	-0.19*	-0.31***	0.2*							
HL	0.31***	0.05ns	-0.08ns	-0.2*	0.25**	0.27***						
BB	0.51***	-0.02ns	-0.13ns	-0.23**	0.6***	0.22**	0.39***					
LB	0.52***	-0.03ns	-0.16*	-0.27***	0.58***	0.26***	0.38***	0.78***				
TN	0.05ns	0.05ns	0ns	-0.11ns	0ns	0ns	0.02ns	0.01ns	0.05ns			
Awn	-0.02ns	0.08ns	0.06ns	0.02ns	0.07ns	-0.09ns	-0.01ns	0.17*	0.15ns	0.1ns		
Flowering stage												
Trait	EWL	CT	T	CTD	Glau	PH	HL	BB	LB	TE	FT	TN
CT	0.08ns											
T	-0.09ns	0.77***										
CTD	-0.16*	0.08ns	0.57***									
Glau	0.49***	0.1ns	-0.14ns	-0.17*								
PH	0.19*	-0.1ns	-0.13ns	-0.09ns	0.06ns							
HL	0.34***	-0.05ns	-0.11ns	-0.03ns	0.2**	0.14ns						
BB	0.49***	-0.16ns	-0.45***	-0.3**	0.48***	0.28**	0.34***					
LB	0.6***	0.02ns	-0.27***	-0.33***	0.64***	0.12ns	0.4***	0.96***				

Table 5 Continued

Flowering stage													
Trait	EWL	CT	T	CTD	Glau	PH	HL	BB	LB	TE	FT	TN	
TE	0.54***	-0.02ns	-0.29***	-0.31***	0.62***	0.09ns	0.45***	0.93***	0.98***				
FT	0.56***	0.01ns	-0.31***	-0.35***	0.63***	0.03ns	0.41***	0.92***	0.97***	0.97***			
TN	0.07ns	-0.04ns	0.03ns	0.04ns	-0.06ns	-0.18*	0.05ns	-0.07ns	-0.08ns	-0.02ns	-0.04ns		
Awn	0.08ns	-0.03ns	-0.1ns	-0.11ns	0.03ns	-0.08ns	-0.08ns	0.17ns	0.18*	0.17*	0.2**	0.14ns	
5 DAP stage													
Trait	EWL	CT	T	CTD	Glau	PH	HL	BB	LB	TE	FT	DAP5	TN
CT	0.03ns												
T	0.08ns	0.83***											
CTD	-0.19*	-0.12ns	-0.02ns										
Glau	0.47***	-0.09ns	-0.13ns	-0.26***									
PH	0.14ns	0.14ns	0.13ns	-0.48***	0.08ns								
HL	0.22**	-0.01ns	-0.1ns	0.84***	-0.12ns	-0.41***							
BB	0.57***	0.27**	0.11ns	-0.33***	0.19*	0.29**	0.29**						
LB	0.67***	-0.09ns	-0.09ns	-0.28***	0.41***	0.16*	-0.07ns	0.9***					
TE	0.66***	-0.06ns	-0.08ns	-0.25**	0.42***	0.11ns	-0.02ns	0.85***	0.95***				
FT	0.64***	-0.08ns	-0.1ns	-0.21**	0.4***	0.08ns	0ns	0.83***	0.96***	0.95***			
DAP5	0.31***	-0.06ns	-0.1ns	-0.17*	0.21**	0.16*	-0.01ns	0.19*	0.45***	0.45***	0.42***		
TN	0.10ns	-0.02ns	0.01ns	0.05ns	0.14ns	0.04ns	-0.01ns	0ns	-0.05ns	-0.05ns	-0.1ns	0.25**	
Awn	0.2*	0.03ns	0.04ns	-0.11ns	0.14ns	-0.09ns	0ns	0.11ns	0.23**	0.24**	0.27***	0.25**	0.01ns

*, **, *** significant at p≤ 0.05, 0.01 and 0.001 respectively.

Key: epicuticular wax load (EWL), canopy temperature (CT), temperature (T), canopy temperature depression (CTD), glaucousness (Glau), plant height (PH), head length (HL), phenological traits including booting begin (BB), late booting (LB), tiller emergence (TE), flowering time (FT), 5 days after pollination (5DAP), tiller number per plant (TN) and awn/awnless (Awn)

2.3.5 QTL analysis

From the Hal x Len population, a total of 176 lines were genotyped, while 8,048 polymorphic SNPs identified from genome studio defined 46 linkage groups covering all the wheat chromosomes. To eliminate the effect of flowering time on the detection of the QTLs for other agronomic traits, we used flowering time as a covariate to adjust every trait. By combining genotypic data and the phenotypic data, QTL analysis and visualization were conducted using the software MapQTL 6.0 (Van Ooijen, 2011) and Mapchart 2.2 (Voorrips RER, 2002).

A total of 30 QTLs were identified from different developmental stages of the Hal x Len population for different traits, including epicuticular wax load (EWL), glaucousness (Glau), canopy temperature (CT), plant height (PH), head length (HL) and phenology-related traits (PT). Eight QTLs linked to wax including wax epicuticular load and glaucousness visual score were detected, distributing across the chromosomes 1A, 2B, 4B and 7B. Three QTLs, 3 QTLs and 2 QTLs were detected at late booting stage, flowering stage and 5DAP stage, respectively. Generally, wax-related QTLs can be frequently detected on 2B chromosome, including one EWL QTL for each late booting stage and 5DAP stage and one glaucousness QTL for each late booting stage and flowering stage. However, the co-localization of EWL and glaucousness can only be detected at the early reproductive stage - late booting stage. This genomic locus can explain up to 18.6% of EWL variation in the population and up to 18.9% of glaucousness variation across different RIL lines. The EWL variation explained by this

QTL decreased from the early reproductive stage to the late developmental stage, but the glaucousness variation explained increased from the late booting stage to the flowering stage. Many other agronomic traits including tiller number and head length and phenological traits were also located on the same 2B genomic region, which indicated that this locus may have pleiotropic effects on multiple traits or that a gene cluster controlling multiple traits was located on 2B. Stage-specific QTLs linked to EWL have been detected on 4B at the late booting stage and flowering stage and 1A at the 5DAP stage. EWL QTL on 4B accounted for up to 10.9 % EWL variation in the population. The LOD score associated with wax QTLs ranged from 3.24 to 7.68 (Table 6). However, no glaucousness QTL could be found at the 5DAP stage.

In terms of wax-related traits, Len contributed the favorable alleles for all the wax QTLs except for those located on 4B, which has been found co-localized with plant height with Halberd contributing the favorable alleles. In this study, three glaucousness QTLs have been identified and two out of three were detected at the flowering stage. They were located on chromosome 2B and 7B. The QTL on 2B explained the largest glaucousness variation (18.9%), and the total effects of glaucousness QTLs detected at the flowering stage accounted for 27.2% of the population variation.

Table 6 Summary of QTLs associated with different traits at late booting, flowering and 5DAP stages.

Trait	Stage	QTL	Position	Peak SNP	LOD	VE(%)	Additive	Favorable allele
EWL	Late booting	*Qewl.tam-2B*	31.972	IACX1098	7.2	18.6	-0.183252	Len
		Qewl.tam-4B	38.771	RAC875_rep_c105718_430	4.05	10.9	0.138351	Halberd
	Flower	*Qewl.tam-4B*	45.71	Excalibur_c56787_95	3.24	8.5	9.82E-02	Halberd
	5DAP	*Qewl.tam-2B*	31.972	IACX1098	4.19	11	-0.108035	Len
		Qewl.tam-1A1	24.939	Tdurum_contig43360_1381	3.46	9.2	-9.84E-02	Len
Glau	Late booting	*QGlau.tam-2B*	31.972	IACX1098	5.66	14.7	-0.842559	Len
	Flower	*QGlau.tam-2B*	31.972	IACX1098	7.68	18.9	-0.961908	Len
		QGlau.tam-7B4	7.11	wsnp_Ex_c46061_51675763	3.19	8.3	-0.644998	Len
PH	Late booting	*Qph.tam-4B*	38.771	Tdurum_contig42229_113	15.3	34.8	2.52889	Halberd
		Qph.tam-3B2	2.437	RAC875_c13256_1359	3.48	9.3	1.31834	Halberd
	Flower	*Qph.tam-4B*	45.71	Excalibur_c56787_95	15.77	34.8	2.76241	Halberd
		Qph.tam-3B2	2.437	Kukri_c39915_340	5.12	13	1.67201	Halberd
	5DAP	*Qph.tam-4B*	37.689	wsnp_Ku_c28756_38667953	9.69	23.5	2.38211	Halberd
HL	Late booting	*Qhl.tam-2B*	30.018	Kukri_c11318_591	4.98	13	-0.147722	Len
		Qhl.tam-6B1	31.729	Excalibur_c43557_540	4.47	11.7	-0.141815	Len
		Qhl.tam-7A2	19.221	BobWhite_c25527_109	3.16	8.4	-0.119057	Len
TN	Late booting	*Qtn.tam-2B*	129.832	Ex_c13213_2517	3.85	10.3	0.200261	Halberd
		Qtn.tam-2B	110.651	Excalibur_c57713_105	3.04	8.2	0.177884	Halberd
	Flower	*Qtn.tam-2B*	31.972	IACX1098	3.44	8.9	-0.205462	Len
		Qtn.tam-7A1	70.09	Kukri_s118416_65	3.23	8.4	-0.199824	Len
Awn	Late booting	*QAwn.tam-5A2*	38.338	BobWhite_c8266_227	13	30.9	-0.249467	Len
	Flower	*QAwn.tam-5A2*	38.338	BobWhite_c8266_227	24.72	48.8	-0.334117	Len
		QAwn.tam-1A1	97.726	Kukri_c35030_266	3.55	9.2	-0.141933	Len
CT	Flower	*Qct.tam-2B*	73.899	RAC875_rep_c70357_917	4.11	10.7	-0.831343	Len
PT	Flower	*Qlb.tam-3A1*	11.904	Tdurum_contig86206_149	5.39	13.7	-0.473968	Len
		Qlb.tam-3B1	28.729	BS00069274_51	3.02	7.9	0.357672	Halberd
		Qlb.tam-4B	32.63	Tdurum_contig64772_417	4.07	10.6	0.426525	Halberd
	5DAP	*Qbb.tam-2B*	18.462	Excalibur_c46590_290	3.89	14.3	-0.596832	Len
		Qlb.tam-2B	41.918	RAC875_c41476_217	4.19	11	-0.477686	Len
		Qte.tam-2B	31.972	IACX1098	4.83	13	-0.470723	Len

We also recorded other agronomic traits, including plant height, head length, tiller number, canopy temperature and awn presence. QTLs for plant height with a high LOD score at different stages were consistently detected within a genetic region on the short arm of chromosome 4B, with an interval of 8.53cM, which accounted for 34.8%, 34.8% and 23.5% of the phenotypic variance at the late booting, flowering and 5DAP stages, respectively (Table 6, Figure 3). A small-effect QTL on the short arm of 3B was identified at the late booting stage and flowering stage. It can explain 9.3% and 13% of phenotypic variation in the population at these two early reproductive stages, respectively.

Three QTLs for head length have been identified at the late booting stage and totally accounted for 33.1% of the variation in the population. No head length QTLs was identified at the other stages. The three QTLs were located on 2B, 6B and 7A, respectively. The QTL *Qhl.tam-2B* at the late booting stage with the highest LOD score was co-localized with the wax-related QTLs on 2B. As one of the important yield component traits, tiller number was also recorded across different developmental stages. Two QTLs associated with tiller number were detected for each late booting stage and flowering stage. The QTL with a peak position of 129.83cM identified at the late booting stage has the largest effect, with 10.3% of variation explained. Interestingly, Halberd contributed the favorable allele to the determination of tiller number at the late booting stage and Len contributed to the development of it at the flowering stage. The favorable allele for head length at the late booting stage was from Len. However, we cannot detect any QTLs for tiller number and head length at 5DAP.

In this study, we viewed the awn trait as a quantitative trait and recorded it dynamically across different developmental stages. The genes controlling awn at the late booting and flowering stages were consistently mapped in a genomic region on chromosome 5A, with the interval of 2.64cM flanked by the marker *tplb0049a09_2097* and *BS00068108_51*. The QTL *QAwn.tam-5A2* identified at the flowering stage, having a very high LOD score (24.72), can explain up to 48.8% of phenotypic variation in the population at the flowering stage. Len contributed the favorable allele for awn. A small-effect QTL associated with awn has been identified at the flowering stage, which was located on the genomic region with an interval of 13.18cM on chromosome 1A. QTLs associated with canopy temperature at the flowering stage and phenology-related traits at later reproductive developmental stages were detected with the LOD scores ranging from 3.02 to 5.39. Most of the QTLs were located on the chromosome 2B, with Len contributing the favorable alleles (Table 6).

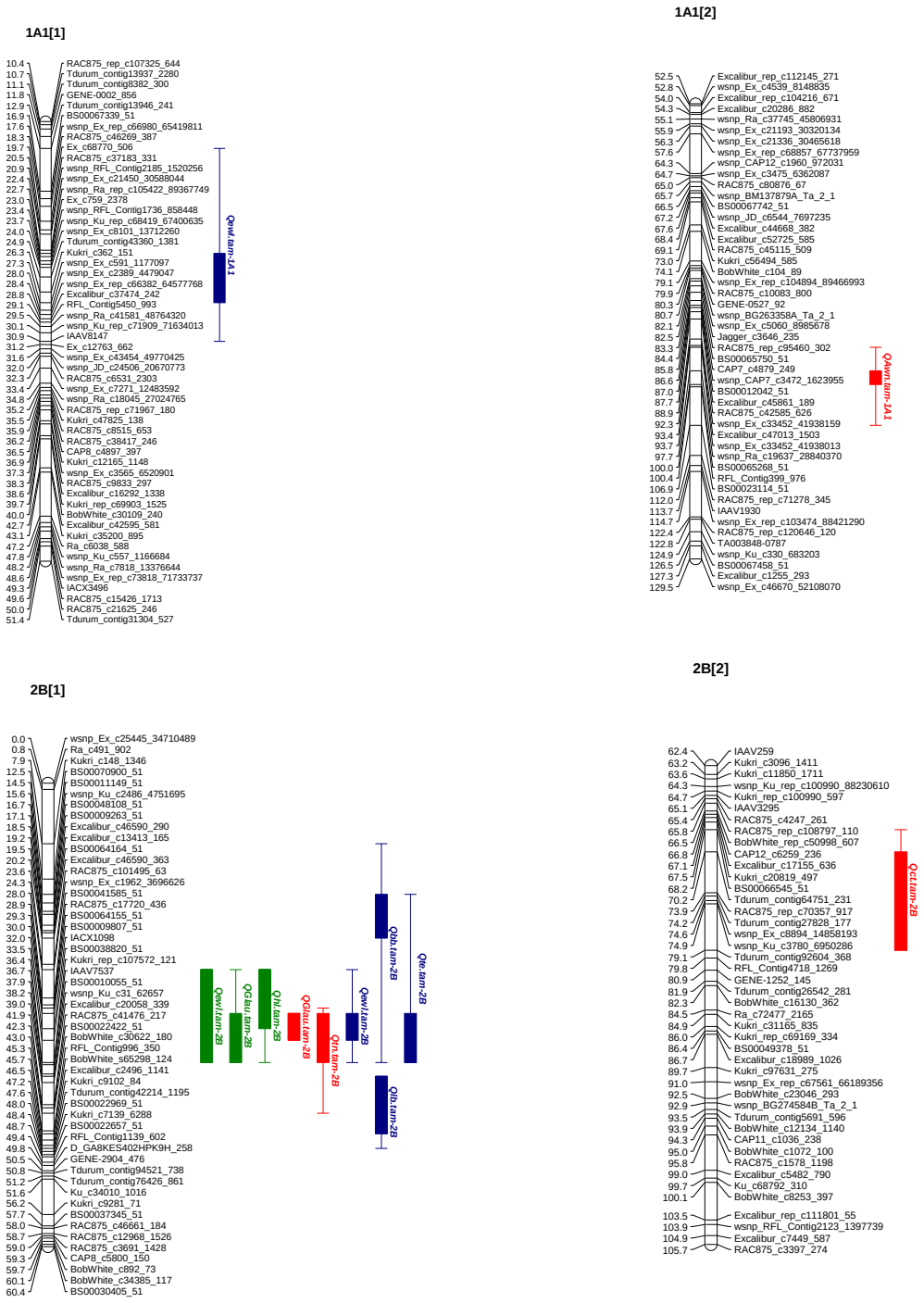

Figure 3 Linkage map and quantitative trait loci (QTL) for epicuticular wax load (EWL), glaucousness (Glau), plant height (PH), head length (HL), tiller number (TN), awn (Awn), canopy temperature (CT) and phenology-related traits. Key: Green, red and blue color stands for the QTLs detected at late booting, flower and 5DAP stage, respectively.

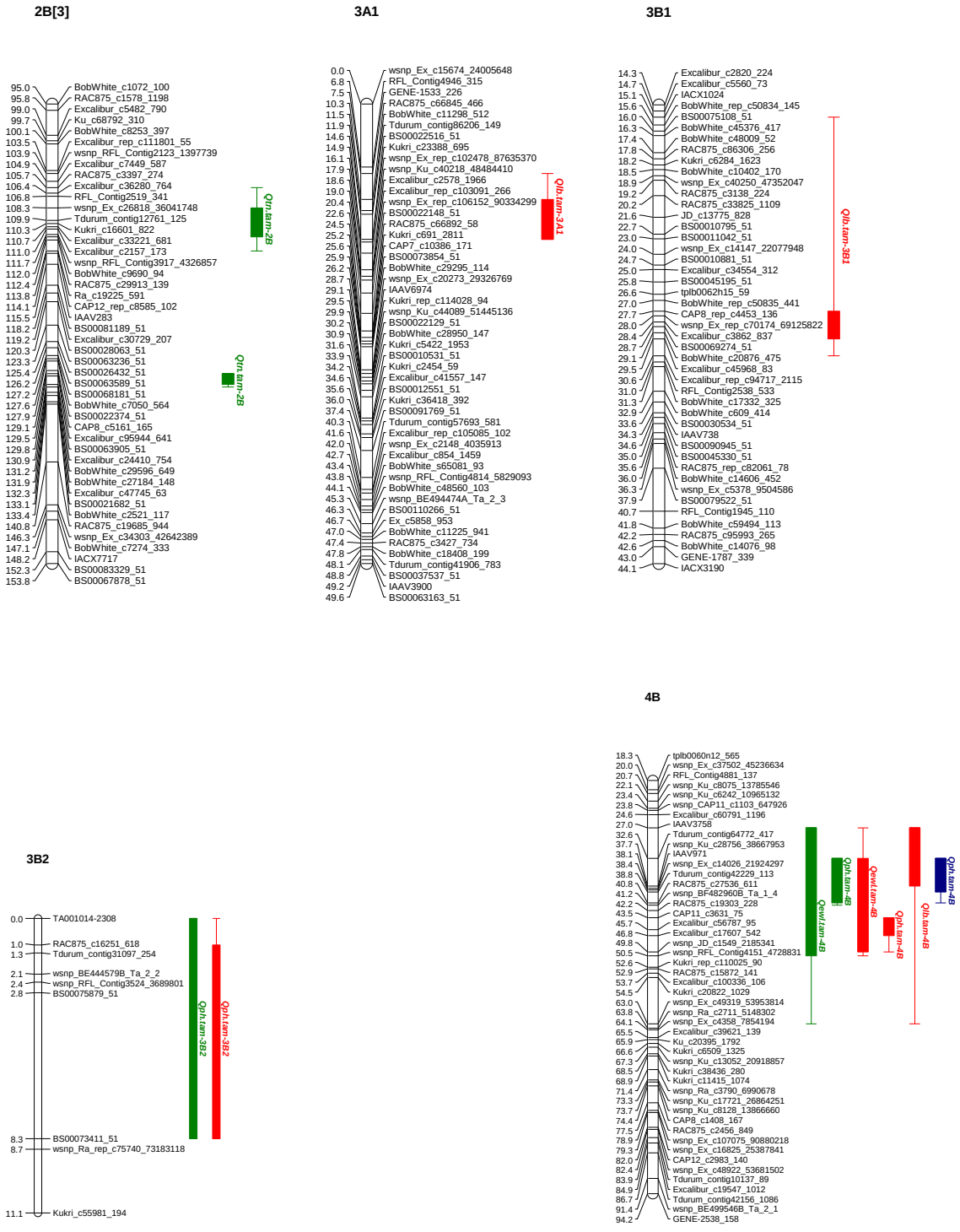

Figure 3 Continued

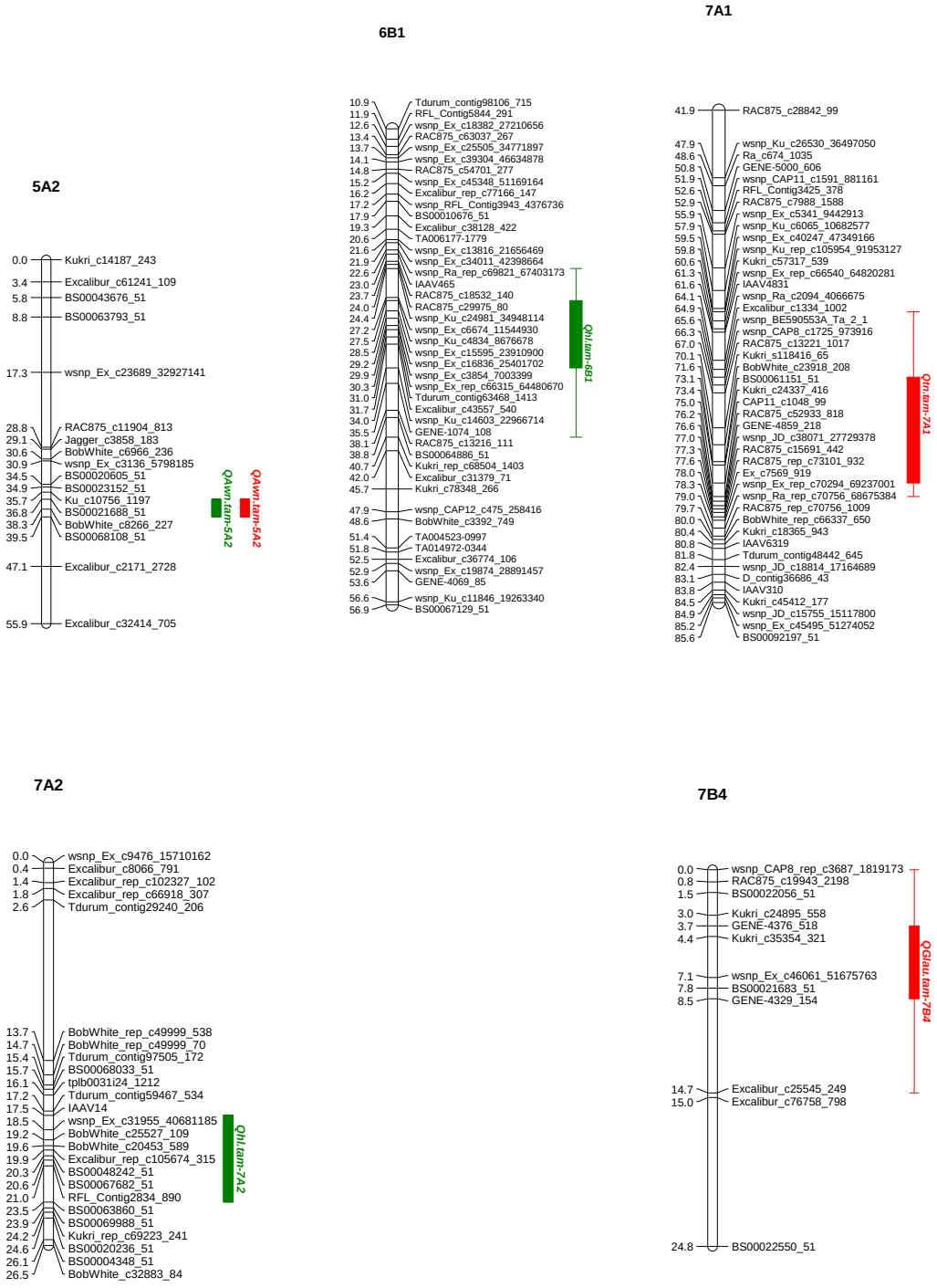

Figure 3 Continued

2.4 Discussion

2.4.1 SNP identification from wheat 90K iSelect SNP array data and linkage map construction

In this study, the Hal x Len RIL population in the 8th generation has been genotyped using the recent 90K SNP assay developed by Wang (Wang et al. 2014d), which provided a platform for the identification of high-density gene-associated SNP markers. A total of 8,440 polymorphic SNPs have been identified, among which 21% are heterozygous markers. With the algorithm function incorporated in R/ASMap package, we have constructed a high-resolution linkage map with the identified SNPs. In all, 8,048 out of 8,440 polymorphic SNPs have been mapped on the wheat genome, covering all the 21 wheat chromosomes. However, the mapped SNPs were not evenly distributed across different chromosomes. The B subgenome had the most mapped markers and D genome has the lowest amount of SNPs. Hexaploid wheat evolved from the hybridization of tetraploid wheat (*Triticum turdigum*, AABB) with a diploid wheat (*Aegilops tauschii*, DD). It has been confirmed that hexaploid wheat evolved 8,000 years ago, whereas, tetraploid wheat has existed for 400,000 years (Nesbitt and Samuel. 1996). From the perspective of evolution, the D genome was the latest event incorporating into hexaploid wheat genome, which may explain the low genetic diversity of D genome in hexaploid wheat. In a recent wheat consensus map constructed by Wang (Wang et al. 2014d), about 50% of SNPs were mapped on the B subgenome and only 14.7% of SNPs were mapped on the D subgenome. 2B has the most SNPs mapped. Zhai (Zhai et al.

2016) used the same 90K SNP array screened on a population of 191 F9 wheat RILs population. They also found that the B genome had the largest amount of SNPs and less than 1000 markers mapped on the D genome. The average genetic distance was 1.4 cM per locus. High-resolution linkage maps using the same assay have been constructed in the studies working on the identification of QTLs associated with yield components (Gao et al. 2015) and tiller number (Wang et al. 2016), and the average genetic distance was 1.95 cM per locus and 0.45 cM per SNP, respectively. The same 90K SNP array also was used for the linkage map construction on the RIL populations derived from the cross of CO960293-2 x TAM 111 and the cross of TAM 112 x TAM 111, the genetic distance was 0.27cM per SNP and 0.87 cM per SNP for each map (Liu et al, 2015). In our study, we constructed a linkage map with a total distance of 2471.71 cM and the average genetic distance of 1.39 cM per bin and 0.31 cM per SNP, which is in consensus with previous studies, indicating the high resolution of the genetic map constructed in this research.

2.4.2 Agronomic and physiological traits

In response to environmental stimulus, plants have developed various mechanisms to adapt to changing environments. One of the mechanisms is physiological change, including leaf rolling, increased transpiration, changes in the expression of secondary metabolism and the generation of various biochemicals. It has been shown that high temperature can trigger the expression of epicuticular wax on leaves. In

response to increasing temperature, EWL usually increases to fortify the generation of a hydrophobic barrier covering on the leaf surfaces for limiting water loss, which is beneficial for the plant's heat stress adaptation (Bird et al. 2007). In this study, air temperature in the greenhouse increased with the growth and development of the plants. In correspondence to changes in the air temperature, the general trend of canopy temperature is increasing. The expression of EW increased across the 3 different stages. This trend is similar to the changes of air temperature and canopy temperature, which indicated that the accumulation of EW might be in responding to increasing temperature.

Leaf area expansion may also account for the increase of epicuticular wax across the analyzed developmental stages. In Wang's study (Wang et al. 2015b), the continuous increase of wax content on the leaf surfaces matched leaf expansion and development. However, the change of the glaucousness score was different from epicuticular wax changes. The expansion of leaf area may account for the increase of glaucousness score from the late booting stage to the flowering stage, but the glaucousness score decreased a little from the flowering stage to the 5DAP stage. This alteration may be caused by the changes of epicuticular wax metabolism and wax constitution changes. As is known, wax is a hydrophobic layer consisting of various aliphatic compounds, including very-long-chain fatty acids (VLCFA), esters, alcohols, aldehydes and ketones (Kunst and Samuels 2009). There are many pathways involved in the epicuticular wax biosynthesis, and one to several pathways may predominate in a specific stage for a certain environment. It has been well established that the alcohol-forming pathway, the alkanes-forming pathway, or both of them are the predominant pathways in the vegetative stage,

with the main products being alcohols, alkanes and aldehydes (Cheesbrough and Kolattukudy 1984; Vioque and Kolattukudy 1997; Rowland et al. 2006; Greer et al. 2007; Li et al. 2008; Bernard et al. 2012; Bernard and Joubès 2013). In reproductive stages, the generation of alcohol decreases and the products from type III polyketide pathway increase (Wang et al. 2015b). β- and OH-β-diketones, which are mainly activated and synthesized in the reproductive stage (Tulloch 1973; Mikkelsen 1978), are the main components for glaucousness. A detailed composition analysis on wheat cuticular wax has characterized the changes of wax components with the development of plants. It has been demonstrated that at early stages of leaf development, the predominant composition is alcohols, which accounted for about 90% of the total wax amount. Although in later reproductive stages the major constituents were still alcohols, the proportion of alcohols in the total wax decreased. The amount of other important compositions like alkanes and β-diketone increased (Wang et al. 2015b), so the alteration of the metabolism pathways from vegetative growth to reproductive growth may account for the changes of the glaucousness visual score. The environmental changes can also partially explain the variation of EWL and the different expressions of EWL and glaucousness. Several studies (Baker 1974; Giese 1975; Kim et al. 2007) have shown that high temperature can cause changes in wax compositions. So the expression of EW and glaucousness depends on both internal and external factors. In this study, canopy temperature depression decreased with the growth stages. Although the negative association between EWL and canopy temperature has been identified in the studies of Richards (1986) and González and Ayerbe (2010), more EWL was associated with high

canopy temperature in this study, which indicated that the increase of EWL cannot compensate for the effects of increased temperature on maintaining cooler temperature.

2.4.3 The correlations among different physiological traits

Glaucousness is the visible light bluish-white wax on the wheat leaf surfaces and glumes. It has been reported that wax content was positively correlated with glaucousness (Koch et al. 2006; Shepherd and Griffiths 2006). In this study, the significantly positive correlations between EWL and glaucousness have been stably identified at different developmental stages. The coefficients of correlations were around 0.5. As a composition of epicuticular wax, glaucousness just accounts for part of the wax content. We cannot use glaucousness to represent the amounts of epicuticular wax. The constitution of wax dynamically changes with the growth and development of plants, which explained the changes of the correlation between wax and glaucousness at different stages.

EWL was positively correlated with head length at all the three stages and plant height at late booting and flowering stages. These positive correlations may indicate the relationship between wax and yield-contributing traits. In Merah's study (2000), glaucousness positively contributed to the increase of the plant biomass if the drought stress occurred at early vegetative growth stage. However, some studies reported that there were no significant correlations between wax and yield or yield components (Risk et al. 2013; Frizell-Armitage 2016). In our study, a negative correlation between EWL

and CTD has been identified and there was no correlation between EWL and CT, which were different from the field study (Huggins 2014). It may indicate that the effect of epicuticular wax on CTD depends on the environments. EWL was closely related to the phenological traits and many other physiological traits had significant associations with the phenological traits. Large amounts of traits are dynamically changing with the developmental phases, especially for some morphological traits such as leaf size, texture and shape. These changes are in corresponding to the developmental stages and also are in response to the environmental changes (Huijser and Schmid 2011; Wang et al. 2015b).

2.4.4 QTL analysis and bioinformatics analysis

Epicuticular wax is a complex trait regulated by many genes involved in multiple biosynthetic pathways, and its expression is largely dependent on the environments (Jenks et al., 1992; Sánchez et al., 2001; Kunst and Samuels, 2003; Broun et al., 2004). Epicuticular wax increased in response to heat and drought stress (Richards et al., 1986; Araus et al., 1991; Oliveira et al., 2003; Kim et al., 2007). Huggins (2014) used the same Hal x Len population to map EWL across different growth conditions. It has been shown that there were no significant associations between EWL and yield stability. The QTLs for EWL were mapped on 2A, 2B, 3A, 6B and 7A. Most of the wax QTLs was co-localized with QTLs for other yield-related traits. A total of three QTLs for EWL have been mapped on the long arm of chromosome 2B. In his study, the QTL on 7A

QWax.tam-7A.2 explained the largest genetic variation with R^2 = 12.1. A few studies also reported QTLs for wax-related traits located on chromosome 1D, 2B, 2D, 3A, 3B, 3D, 4A, 4D, 5A, 5B and 7D (Börner et al., 2002; Mason et al., 2010; Bennett et al., 2012).

In our study, the QTLs associated with EWL and glaucousness were located on chromosome 1A, 2B, 4B and 7B. The main-effect QTL for wax-related traits was the one identified on the short arm of 2B, with the peak marker *IACX1098*. Multiple small-effect QTLs were also detected on different chromosomes. Only at the early stage can we find the co-localization of EWL QTL and glaucousness QTL. Combining the results from pearson correlation analysis, the correlation between EWL and glaucousness was low, although the association was highly significant, indicating that glaucousness can account for part of the wax expression and that multiple genomic regions were involved in the regulation of wax biosynthesis. The main-effect QTL for wax-related traits on 2B was stably detected across all the three stages we studied. This region may play an important role in the regulation of wax biosynthesis at all times. It is known that a huge gene network controls wax metabolism and various pathways are involved in the wax synthesis and expression. If a QTL can be detected longitudinally across different developmental stages, it is either a constitutive element or a major regulator/signaling factor controlling multiple pathways.

We used the peak marker sequence to conduct a blast search. One of the best hits is the accession HM754654.1 with the function of phosphoinositide-specific phospholipase C in *Triticum aestivum*. Phosphoinositide-specific phospholipase C (PI-

PLCs) is an essential regulator involved in the regulation of multiple pathways related to development and stress response (Rupwate and Rajasekharan 2012; Zhang et al. 2014). With the activation by a certain concentration of calcium, PLCs can hydrolyzes phosphatidylinositol 4,5-bisphosphate (PIP2) to generate the secondary messengers inositol 1,4,5-trisphosphate (IP3) and 1,2-diacylglycerol (DAG), which can trigger a series of signaling cascades in the phosphoinositide signaling pathway (Berridge 1993; Rupwate and Rajasekharan 2012). Given the many PLC isoforms with different structure, tissue distribution and various patterns of the interaction between regulatory domains and receptors, this pathway is a highly regulated pathway by many developmental signals and environmental stimuli (Rhee 2001), which may partly explain the co-localization of multiple traits on 2B region with *IACX1098* as peak marker.

EWL QTL on 4B can be identified at late booting stage and flowering stage, which indicated this genomic region played an important role in the regulation of wax biosynthesis at relatively early reproductive stages. Above all, the QTLs for plant height across all three stages were co-localized with this developmental-stage dependent QTL for EWL on 4B. This genomic region either has pleiotropic effects on EWL and plant height or has gene clusters located within a maximum interval of 36.02 cM on 4B. Only the one EWL QTL *Qewl.tam-4B* identified at flowering stage shared the same peak marker with plant height QTL *Qph.tam-4B* at the same reproductive stage, which explained 8.5 % of EWL variation and 34.8% plant height variation in the population, respectively. The sequence of the peak marker *Excalibur_c56787_95* has the best hit of a putative zinc induced facilitator-like 1 (ZIF1) sequence. Within the plant, ZIF1 belongs

to a superfamily transporter. Its different isoforms played an important role in the polar transportation of auxin, the regulation of auxin-related process and stress response through the regulation of stomata closure (Remy et al. 2013). Based on the blast search and comparative analysis, most of the peak markers for wax QTLs are corresponding to putative regulators like pentatricopeptide repeat-containing protein (PPR), with transcriptional regulator SLK3 functioning in the transcriptional regulation. In view of the large percentage of phenotypic variation explained by the QTLs located on 2B and 4B and the co-localization of multiple traits on these two regions, they can be viewed as important candidate QTLs for further dissection.

Plant height has been extensively studied in wheat. The dwarfing genes that are widely adopted in the wheat breeding program are *Rht-B1* located on 4B and *Rht-D1 located on 4D*, both of which are GA-insensitive genes (Ellis et al, 2004; Börner et al, 2002; Cadalen et al, 1998; Huang et al, 2003; Ellis et al, 2005). In this study, we have identified a major-effect QTL strongly associated with plant height on the short arm of the 4B chromosome, which is in consensus with the chromosome position of the most common dwarf gene, *Rht-B1*, in wheat. From Gao et al. (2015), they already used the gene-specific markers of *Rht-B1* to verify the QTL *QPH.caas-4BS.2*, It has been shown that this QTL is *Rht-B1* flanked by markers *RAC875_c6749_954* and *BobWhite_c44691_648.* In our study, the plant height gene across different stages was located within the maximum interval flanked by *Tdurum_contig64772_417* and *wsnp_JD_c1549_2185341 (*or *RAC875_c12495_1391)*. Based on the consensus map constructed by Wang (2014d). We compared the results of these two QTLs. These two

regions had overlapped genetic regions on CSS consensus genetic map, indicating that the QTL for plant height on 4B identified in our study may contain the *Rht-B1*, and the association between this QTL and *Rht-B1* needs to be verified further in the future. Another class of *Rht* genes are GA-responsive, among which *Rht* 4, 5, 7, 8, 9, 12, 13 and 14 have been characterized in Ellis' study (Ellis et al. 2004). These genes have the function of reducing plant height without affecting early growth indicated that they played an important role in the regulation of plant height in the later development of plants. The consistent QTLs controlling plant height across different genetic backgrounds have been located on 1B, 2D, 4B, 5A, and 7A (Jantasuriyarat et al. 2004; Kumar et al. 2007; Cui et al. 2012; Xu et al. 2013; Gao et al. 2015; Zhai et al. 2016). A recent genome-wide linkage mapping study on plant height in wheat (Gao et al. 2015) reported plant height QTLs located on 2BL, 4AL, 4BS, 4DS, 5AS and 7AL. To our best knowledge, there are no reports on the identification of QTLs for plant height on chromosome 3B. Since the plant height QTL located on 3B identified in this study can only be detected at the late booting and flowering stages. It indicated that the QTL is probably a novel stage-specific QTL controlling plant height at the early reproductive developmental stages in hexaploid wheat.

In wheat, yield-contributing traits have been subjected to QTL analysis, one of which is head length. QTLs for head length have been mapped on 1B, 4A, 5A, 2B, 2D, 7A, 2A and 6B at late reproductive stages like the late grain-filling stage and harvest stages (Börner et al. 2002; Sourdille et al. 2003; Kumar et al. 2007; Gao et al. 2015; Li et al. 2016). To date, there are no studies published on the identification of head length

QTLs at early developmental stages. In this study, we recorded the head length of Hal x Len RIL population along three key reproductive stages. However, the QTLs for head length were only detected at the late booting stage. There were no QTLs associated with head length discovered at late reproductive stages, which is different from the previous studies. One of the head-length QTL was co-localized with EWL QTL and glaucousness QTL on chromosome 2B, and the Pearson correlation analysis showed a significantly positive association between EWL, glaucousness and head length, which indicated that wax may have an effect on yield-contributing traits.

As one of the important yield components, tillering capacity largely affects yield potential of cereal crops (Yan et al. 1998; Kuraparthy et al. 2007; Naruoka et al. 2011). It has been shown that free-tillering plants have a yield reduction as compared with the genotypes with limited tillering capacity (Richard 1988; Kebrom et al. 2012) due to young tillers consuming nutrients during vegetative stages, therefore not contributing to yield. In our study, we can identify the QTLs for tiller number and head length at early developmental stages. This is in contrast to the results in Wang's study with tillering QTLs identified across all the 4 stages (GS 37, 49, 60 and 85) they examined (Wang et al. 2016). This may indicate that the QTLs identified in our study determining the tiller number and head length can mainly function at the early reproductive developmental stages. In wheat, tillering QTL have been mapped on 1A, 1B, 2A, 2B, 2D, 3A, 3B, 4D, 5A, 5D, 6D, and 7A across different environments and genetic backgrounds (Law 1967; Kato et al. 2000; Li et al. 2002; Huang et al. 2003; Spielmeyer and Richard 2004; Kuraparthy et al. 2007; Cui et al. 2012; Wang et al. 2016). In our study, we mapped

QTLs for tiller number on chromosome 2B and 7A. The QTL *Qtn.tam-2B* identified at the flowering stage was co-localized with glaucousness QTL on 2B at the same stage.

The awn is a needle-like structure extended from the spikelet. From an evolutionary perspective, it has been demonstrated that the awn plays an important role in both protection against animals (Hua et al. 2015) and in seed dispersion (Sorensen 1986). The awn can contribute up to 40% of the photosynthetic assimilates in wheat grain (Peleg et al. 2010). During the domestication process of wheat, the awnless phenotype has been under selection for the convenience of harvest. The genetic basis underlying awn formation has been characterized and three dominant inhibitors of awn have been localized on wheat chromosome 4AS, 5AL and 6BL, which are known as Hooded (Hd), Tipped1 (B1) and Tipped2 (B2), respectively (Watkins AE and Ellerton S 1940; McIntosh et al. 1998; Sears 1954). The genotypes with these three recessive homologs are awned phenotype; otherwise, those with two dominant alleles are awnless (McIntosh et al, 1998). In our study, an awn QTL with very high LOD score was consistently identified on chromosome 5AL at the late booting and flowering stages, which is similar to Li et al (2016). In his study, the QTL for awn on 5A has been identified consistently across different environments, explaining up to 99.3% of the phenotypic variation. Torada (2006) also reported the common awn QTL previously. An eight-founder multiparent advanced generation inter-cross population (MAGIC) has been genotyped using the same 90K SNP array. The SNP *BobWhite_c8266_227* was highly significantly associated with awn/awnless. It has been shown that the 7.5 cM genetic region on 5AL with this peak marker contained B1 locus (Mackay et al. 2014).

In our study, a QTL with high LOD score (24.72) located on 5A has been identified. The peak marker was the same *BobWhite_c8266_227* with in a genetic interval of 2.64 cM. This QTL was highly probably containing B1 locus.

The blast search was conducted using the sequence of the peak marker-*BobWhite_c8266_227*. One of the best hits is the putative hexose carrier protein (HEX6-like protein) in *Ae tauschii*. It is well known that hexose carrier protein is a kind of membrane protein that transports various metabolites including carbohydrates, alcohols and acids (Silverman 1991) , which is in consensus with the role of awn in carbohydrates accumulation and mobilization in plants. A stage-specific awn QTL has been mapped on the long arm of 1A at the flowering stage, which can explain 9.2% of phenotypic variation in the population. Len contributed the favorable alleles for all the awn QTLs identified. However, we cannot detect any awn QTL at the 5DAP stage, which may demonstrate that developmental stage-dependent factors contribute to the formation and development of awn.

Canopy temperature has been widely studied in wheat due to its function in plant stress adaptation. It has been demonstrated that cooler canopy temperature is negatively associated with grain yield (Reynolds et al. 1994; Oliveira et al. 2003). In a drought environment, EWL has a positive correlation with yield (Huggins 2014), while the increase of EWL is also associated with reduced canopy temperature in wheat (Elham et al. 2012; Huggins 2014). However, in our study, we cannot find a significant association between canopy temperature and EWL and other yield contributing traits; QTLs for canopy temperature can only be detected at the flowering stage. Therefore, The effect of

canopy temperature on EWL and other traits in the population and their associations are possibly environment-dependent.

2.5 Conclusion

The agronomic and physiological traits and their associations observed in this study dynamically changed with the development of plants. Wax-related traits, including epicuticular wax load and glaucousness, are largely dependent on developmental stage and environments. The significant positive associations between EWL with head length can be stably detected across all the stages investigated. Also, the positive correlation between wax-related traits with plant height can be identified at late booting and flowering stages, which indicated that wax might have an effect on yield-contributing traits. Based on the association and QTL analyses, awn/awnless should be viewed as a quantitative trait, while the shape also changes dynamically with the developmental stages.

We have constructed a high-resolution genetic map for Hal x Len population with the total genetic distance of about 2471.71 cM and the average genetic distance of 1.39 cM per locus. Based on this framework, we mapped different agronomic and physiological traits on the wheat genome. The QTL located on chromosome 2B is an important QTL worthy of further dissection, since multiple traits co-localized in this genomic region. This can explain up to 18.6% EWL variation, 18.9% glaucousness variation, 8.9% tiller number variation and 13% head length variation. The co-

localization of these traits on 2B partially explained the significantly positive associations of wax-related traits and yield contributing traits across the most of the three developmental stages studied. The early reproductive development stage-specific QTL for EWL located on 4B may have pleiotropic effects on plant height, presenting the possibility that wax may have a role in affecting yield-contributing traits. A novel QTL associated with plant height have been identified on 3B, which provides clues for the dissection of the genetic basis underlying this trait.

Based on the blast search, most of the best hits for the peak markers for wax-related traits are major regulators that can be involved in multiple pathways, including hormone regulation pathways, signaling transduction pathways and transcriptional regulation, thus conferring the expression of traits both development and environment-dependent. It is necessary to conduct a co-expression network analysis to dissect the biological process controlling these traits in the future.

CHAPTER III

GENOME-WIDE ASSOCIATION MAPPING ANALYSIS OF WAX-RELATED TRAITS

3.1 Introduction

With the fast development of next-generation sequencing technology, abundant DNA or RNA-based markers are available for genetic studies, making the construction of high-resolution mapping covering the whole genome available. In addition, the development of sophisticated statistic algorithms improves the accuracy of the identification and characterization of targets.

Currently, genome-wide association mapping has been widely applied in many species for various traits due to the advantages over regular linkage mapping analysis. First, linkage mapping is used for mapping the traits on bi-parental populations, which is based on recombination between the two parents. However, the association panel used for association mapping is composed of a set of know/unknown genotypes, which has a more diversified source of recombination events (Gupta et al. 2014). It usually takes time for the construction of bi-parental populations. A RIL population needs at least 6 generations to develop. For association mapping, the currently available materials can be selected for the association panel, which eliminates the time used for the development of mapping a population. Second, association mapping has much finer mapping results than linkage mapping. Association mapping is also called “linkage disequilibrium (LD)”

mapping, which detects the correlation between markers and target traits, whereas linkage mapping is based on the crossovers between markers and target genes. Association mapping is more likely to identify the marker-trait associations across the whole genome with higher resolution. Genome-wide association studies (GWAS) are more powerful in detecting small effects for some traits than linkage mapping analysis (Risch and Merikangas 1996). However, there are still some disadvantages in the association studies. The key problem is the high type I error. The identified marker-trait associations (MTA) can be spurious because of population structure rather than the truly significant associations. And the imprecise characterization of the population relatedness will cause inflation of the statistics and falsely called relationships between markers and traits (Kang et al. 2010), which requires the development of sophisticated algorithms and powerful statistical tools to clarify the population structure and relatedness.

Currently, a Q+K model built by Yu (Yu et al. 2006) has been broadly used for association mapping, especially for diploid species. Here, K stands for relative kinship, which is based on the relationship of individuals in a family base. K can be viewed as a modified identity by decent (IBD) adjusted with the IBD between two random samples. Q stands for the population structure caused by geography, natural selection or artificial selection. It has been shown that this model can effectively detect multiple levels of relatedness among individuals with improved type I and type II error rates. The formula for the model is: $y = Xb + Sa + Qv + Zu + e$, where y is the vector of phenotypic observation, b is the vector of fixed effects other than SNP or population structure, and a, v, u and e are the vector for SNP effects (QTN), population effects, polygene

background effects and residual effects, respectively. Q stands for the population structure matrix; and X, S and Z means incidence matrices of y to b, a, and u, respectively. Based on the model, the markers with significant effects on the target traits can be identified.

Association mapping has been widely applied in plant genetic studies due to its power in the identification of genomic regions associated with complex traits. Historical recombination events can be explored in the selected population through genome-wide association mapping (Risch and Merikangas 1996; Nordborg and Tavaré 2002). Many examples are involved in the successful application of association mapping to identify the significant markers related to the traits of interest. Maize is an outcrossed species with great genetic variation and phenotypic diversity. A large artificial population called the maize Nested Association Mapping (NAM) population has been developed for the detection of natural variations by crossing 25 inbred lines with B73 reference line (McMullen et al. 2009). A total of 4,699 recombinant inbred lines (RILs) across 25 families are included in this population, capturing about 136,000 recombination events, therefore providing high power and resolution to identify the marker-trait associations. Wallace (Wallace et al. 2014) used NAM population to identify the function variations associated with various traits, including yield components, seed protein, starch, chlorophyll content, malate and fumarate. It has been shown that copy number variation and gene regulation are the source of functional variation rather than protein-coding sequences (Wallace et al. 2014). In Arabidopsis, a Multiparent Advanced Generation Inter-cross (MAGIC) population was developed by intermating the 19 accessions of *A.*

thaliana for 4 generations (Scarcelli et al. 2007). In the MAGIC population, great phenotypic variations related to the phenological traits were observed (Kover et al. 2009). Kover (2009) used a panel of 527 recombinant inbred lines (RILs) to dissect QTLs for the development-related traits using different statistical models. GWAS has also been widely used in rice since the development of next generation sequencing technology (Huang et al. 2010; Zhao et al. 2011; Huang et al. 2012; Wang et al. 2014a; Kumar et al. 2015; Wang et al. 2015a). A recent GWAS identified significant multiple loci, explaining up to 39.9% of phenotypic variation related to the morphological traits in certain environments. Novel loci and candidate genes have also been identified, laying a foundation for genetic dissection of traits of interest.

In wheat, association studies have been conducted to identify the genomic regions associated with the important physiological traits, as well as to characterize the natural allelic variation explaining the quantitative trait variations. Sukumaran (2015) carried out GWAS on a spring wheat panel of 287 elite lines. Multiple significant marker-trait associations (MTAs) have been identified for yield-related traits as well as other phonological traits. In addition, pleotropic loci have been found to be related to yield, thousands kernel weight, plant height and other physiological traits (Sukumaran et al. 2015). In Tadesse's study (2015), more than 3,000 diversity array technology (DArT) polymorphic markers were used to genotype a panel of winter facultative wheat lines. Through association mapping, the genetic structure within the population has been characterized and QTLs associated with grain yield and quality have been identified, which lays a foundation for marker-assisted selection (MAS). The application of

genome-wide association study in wheat has been reported for the identification of QTLs associated with yield (Crossa et al. 2007), quality (Breseghello and Sorrells 2006) and disease resistance, including foliar disease (Crossa et al. 2007; Tadesse et al. 2014; Jighly et al. 2015), nodorum blotch (Adhikari et al. 2011) and rust disease (Kertho et al. 2015; Bajgain et al. 2016).

In this study, we used a panel of 300 synthetic-derived wheat lines called AMPSY population to conduct a genome-wide association mapping for the identification of QTLs related to wax biosynthesis, which is the first time to identify the QTLs related to wax using GWAS in hexaploid wheat. Double digested RAD-seq (ddRAD-seq) technology has been used for the SNP identification in the association panel. A total of 137,856 polymorphic SNP markers have been called from the ddRAD-seq analysis. We aimed to clarify the wax variations in the association panel at different stages in different environments, identify significant marker-trait associations (MTA) by combining genotypic data with phenotypic data and find the diagnostic markers closely linked to wax, which will play an important role in the characterization of wax biosynthesis and its function in plant adaptation to the environment.

3.2 Materials and methods

3.2.1 Plant material and experimental design

Three-hundred genotypes of synthetic-derived wheat were selected as an association panel, which is called AMPSY population. This panel was mainly derived

from the cross between TAM111 and TAM112 with elite wheat cultivars. Both of TAM111 and TAM112 are hard red winter varieties developed by Texas A&M AgriLife Research, and are well adapted to the Southern Great Plains of the United States (Lazar et al., 2004; Rudd et al., 2014). It has been reported that TAM111 and TAM112 are drought-tolerance cultivars with different mechanisms of drought adaptation (Reddy et al. 2014; Battenfield et al. 2013; Xue et al. 2014). TAM112 has higher yield stability across low yield potential environments, while TAM111 performed better under optimum conditions (Battenfield et al. 2013; Reddy et al. 2014). TAM112 is a translocation line with 1AL.1RS rye fragments contributing to plant wheat curl mite resistance and greenbug resistance (Dhakal. 2014; Liu et al. 2014; Rudd et al. 2014; Reddy et al. 2013, Dhakal et al. 2017).

The association panel was planted in the field in November to December during the 2015-2016 and 2016-2017 seasons. Four growth environments in 2015-2016 have been selected for the association study: Bushland dry (BD), Bushland irrigated (BI), Chillicothe (CH) and College Station (CS). Four environments were selected in year 2016-2017: Bushland dry, Bushland irrigated, Prosper (PR) and Clovis (CL). In order to avoid the noise caused by disease stress and drought stress in the irrigated environments, optimal management techniques, including supplementary irrigation, optimum fertility and complete protection from disease and pests using insecticides and fungicides, were applied. For the other locations, the same fertilization and disease and pest control were used, but the fields were not watered artificially after planting. Two biological replications were used for the association panel per environment. Every genotype was

planted as a 0.5 x 3 meter plot arranged as an alpha lattice design, with the space between plots being 0.3m.

3.2.2 Leaf glaucousness score and epicuticular wax quantification

The leaf samples for wax quantification and the glaucousness score were recorded depending on the availability of the population and the experimental conditions. Generally, leaf samples were collected when the majority of the AMPSY population was at the important reproductive stages of flowering to 10DAP. The glaucousness score was collected during sunny days at the stages of heading to 10DAP. In the 2015-2016 year, we collected leaf samples for wax quantification in Bushland dry, Bushland irrigated and College Station at the flowering stage, and Chillecothe and College Station at the 10 DAP stage. The glaucousness score was recorded twice in Bushland dry and Bushland irrigated environments when the majority of the lines were at the heading and flowering stages, respectively, while in the Chillocothe environment glaucousness was recorded at the 10DAP stage. In the 2016-2017 year we collected the leaf samples in the Bushland dry and Bushland irrigated environments in Texas, and the Clovis samples in New Mexico at the flowering stage. Glaucousness score was recorded in the Bushland dry environment and Prosper, Texas at the same stage. Leaf glaucousness was scored based on the performance on the whole plot. The range of the score is from 1-3, With 1 representing non-glaucousness and the whole plot being almost fresh green, 3 representing the glaucousness covering the whole flag leaf with the whole plot white-

bluish incolor, and 2 representing visual glaucousness in a state between non-glaucousness and whole glaucousness. For every plot, 12 leaf discs from the flag leaves of three randomly selected individuals in the plot for wax quantification were collected using paper punchers with a diameter of 0.625 cm.

After disc collection, the discs were air-dried and the wax content was measured according to published methods (Richardson et al. 2005): 2 ml chloroform was added to the vials with discs at room temperature, making sure that all the discs were immersed in the solution. After 30 seconds, the epicuticular wax was dissolved in the chloroform with HPLC grade. Then, the extraction solution was moved to a new glass vial and the solution was air-dried. The resulting wax samples were stored in a 4 °C refrigerator for further analysis.

Colorimetric methods (Ebercon et al. 1977) were used for the quantification of wax content. A reaction reagent was made by dissolving $K_2Cr_2O_7$ in H_2SO_4 and distilled water. Three-hundred ul reaction reagent was added in each vial with dry wax samples, with wax reacting with acidic $K_2Cr_2O_7$ in a water bath at 100° C for 30 minutes in order to achieve oxidization. After cooling down, 700 ul ultra pure distilled deionized water was added to each vial. The solution was then mixed and allowed to develop color for 1 hour. 100 ul of each mixed solution was loaded to 96-well polystyrene plates (Greiner Bio-One) and analyzed on a spectrophotometer (PHERAstar plus, BMG LABTECH, Offenburg, Germany), which can detect the optical density of samples at the wavelength 590 nm. By doing this, absorbance data was generated for every sample. Wax content was quantified and calculated through the formula: $X = (A-0.0189)/0.3328$, with A

representing absorbance and X representing wax content using mg/dm2 units. The calculation formula was taken from a standard curve, which was developed according to the methods mentioned in Ebercon's study (Ebercon et al. 1977).

3.2.3 Genotyping using double digested RAD-seq

The 300 lines in the association panel called AMPSY population have been sequenced using ddRAD-seq with Illumina HiSeq 2500 platform (2×125 bp paired-end) at the Genomics and Bioinformatics Center, Texas A&M Agrilife Research at College Station. Six main steps were involved in the generation of raw reads (Saintenac et al. 2013a): (1) Genomic DNA preparation: the modified CTAB method was used to extract DNA from the lines and Nanodrop was used for the DNA quality check. The DNA samples with A260/A280 ratio of 1.7-2.0 can be used for the following sequencing procedure. (2) Restriction enzyme digestion: Two different kinds of restriction enzymes (PstI and MseI) were used to cut the genomic DNA into pieces. (3) Adaptor ligation: Y-adaptors were ligated to the ends of DNA fragments, which ensured that only the fragments with the adaptor combinations can be amplified in PCR. (4) Size selection: (ddRAD-seq or indirect selection by using PCR). (5) Barcoding: Barcodes were built into the adaptors for multiplexing different samples, which can reduce the sequencing cost and time. In this experiment, we used combinatorial barcodes; one being an in-line barcode and the other an Illumina index. (6) Next-generation sequencing: Illumina Hiseq 2500 was used for the production of raw paired-end reads.

Once the raw data was obtained, post-sequencing analyses were conducted using various bioinformatics tools. A custom Perl pipeline was developed to analyze the genotypic data. The analysis procedure and parameter settings were conducted according to the description in Wang et al. (2014d) with slight modification. First, the raw reads were trimmed and quality-filtered via QC toolkit v2.3 (Patel and Jain 2012). The reads with more than 80% of the bases having a Phred score ≥15 were used for further analysis. A three-step iterative mapping strategy was used for the ungapped alignment of the quality-filtered reads to the CSS assemblies using Bowtie2. A more stringent mapping strategy was used on the reads that had not been mapped. A gapped mapping process preceded for the identification of insertion/deletion (indel) polymorphisms. The aligned reads with low mapping quality (MAQ < 5) were removed from the analysis. Variant calling was performed using GATK. The SNPs with the allele separation of 1:1 in the progenies were filtered for further analysis. The SNPs with more than 20% of missing data were removed.

3.2.4 Statistical analysis and association mapping

The correlation coefficient analysis was conducted in R environment to discover the association between epicuticular wax load and glaucousness score for those environments with both wax and glaucousness data. METAR was executed in R for best linear unbiased prediction analysis (BLUPs) of the phenotypic data to get the adjusted means for every physiological trait, which were then used for the association mapping

study. Association mapping was performed on the software TASSEL version 5.0 by combining the SNP data identified from ddRAD-seq and the phenotypic data on the AMPSY population. In this analysis, Mixed Linear Model (MLM), a Q+K model (Yu et al. 2006) incorporating both information related to population structure and the familial relatedness, was used for the identification of markers significantly linked to the traits. Both Q and K information was calculated in TASSEL 5.0. Q is the population structure matrix determined from principal component analysis, while K is the kinship matrix determined from the correlation between lines based on the marker information. The population structure can be visualized by plotting the first two principal components. By combining the genetic information and the phenotypic data, we can get the p-value of each marker for each trait. Manhattan plots were made for the visualization of the distribution of makers linked to the traits across different chromosomes. The threshold for claiming the significance of the marker was decided by False discovery rate (FDR), which was calculated at 0.2 in the R environment using the function p.adjust() with the method of "BH". The SNPs with a negative log of adjusted p value smaller than 0.2 were claimed as significant markers associated with the traits of interest.

3.3 Results

3.3.1 Plant Agronomic data and correlation between epicuticular wax load and glaucousness score

The range of epicuticular wax load on the AMPSY population was large, from 0.004 mg/dm^2 to 9.479 mg/dm^2 after removing the outliers (Table 7). Both extreme values were from the samples collected in the College Station environment at the 10 DAP stage. Based on the mean, the largest value appeared in Chillicothe at the 10DAP stage. The smallest population mean was taken from the Bushland dry and College Station environments at the flowering stage. Among the environments from which glaucousness data was collected, Bushland irrigated in the year of 2015-2016 has the smallest glaucousness score and Bushland dry in the year of 2016-2017 has the largest mean of the score. We also conducted a correlation analysis to characterize the association between epicuticular wax load and glaucousness score (Table 8). It has been found that in most of the conditions with different combinations of environments and stages we studied, the correlation between EWL and glaucousness were highly significant. However, the correlation coefficients were low, which meant that the expression pattern of glaucousness can explain the variation about EWL in the population to some extent. Only in the Bushland irrigated environment was the correlation between EWL and glaucousness score negative, which was contrary to the results from the stressed environments. The correlation between EWL and glaucousness was largely environment dependent. In non-optimal environments, the association could

be positive or neutral, while the correlation was negative in optimal environment. The glaucousness score at the different stages were positively correlated and this correlation was much higher in drought stressed environment than that in the irrigated environment.

Table 7 Wax-related traits on the AMPSY population in different conditions.

			EWL (mg/dm^2)			Glaucousness		
Year	Location	Stage	Mean	Min	Max	Mean	Min	Max
2015-2016	BD	Heading	NA	NA	NA	2.173	1	3
	BI	Heading	NA	NA	NA	2.003	1	3
	BD	Flower	1.34	0.91	3.06	2.17	1	3
	BI	Flower	4.08	0.544	8.346	1.947	1	3
	CH	10DAP	5.021	0.254	9.67	2.052	1	3
	CS	Flower	1.34	0.024	3.061	NA	NA	NA
	CS	10DAP	3.865	0.004	9.479	NA	NA	NA
2016-2017	BD	Flower	3.23	1.08	5.38	2.247	1	3
	BI	Flower	1.95	0.99	3.15	NA	NA	NA
	CL	Flower	2.919	0.389	5.446	NA	NA	NA
	PR	Flower	NA	NA	NA	2.002	1	3

Table 8 Pearson correlation analysis of epicuticular wax load and glaucousness visual score in different conditions.

	EWL (BD/2016/Flower)	Glau (BD/2016/heading)
Glau (BD/2016/heading)	0.16***	
Glau (BD/2016/Flower)	0.15***	0.63***

	EWL (BI/2016/Flower)	Glau (BI/2016/heading)
Glau (BI/2016/heading)	-0.36***	
Glau (BI/2016/Flower)	0.07ns	0.25***

	EWL (CH/2016/10DAP)
Glau (CH/2016/10DAP)	0.02ns

	EWL (BD/2017/Flower)
Glau(BD/2017/Flower)	0.16***

3.3.2 SNP statistics and population structure

After the bioinformatics analysis of the ddRAD-seq data, 137,856 polymorphic SNPs have been selected for further analysis. The distribution of SNPs on different chromosomes was uneven, with 7D having the largest amount of SNPs and 3D having the lowest number of markers (Figure 4). There are 31.33%, 37.04% and 29.98% of SNPs located on the A, B and D genomes, respectively. This set of SNPs was used for the characterization of population structure of the 300 wheat lines using the principal component analysis (PCA) output from TASSEL 5.0. By plotting the first two principal components explaining the 4.5% and 1% of the genetic variance in the AMPSY population, respectively, we can clearly see that this set of SNPs can separate the wheat lines into two clusters (Figure 5). Based on the pedigree information, the maternal parent of all the lines in red in Figure 5 is TAM111, and that of the lines in green is TAM112. The population structure is largely dependent on the maternal parents of the hybrid cross.

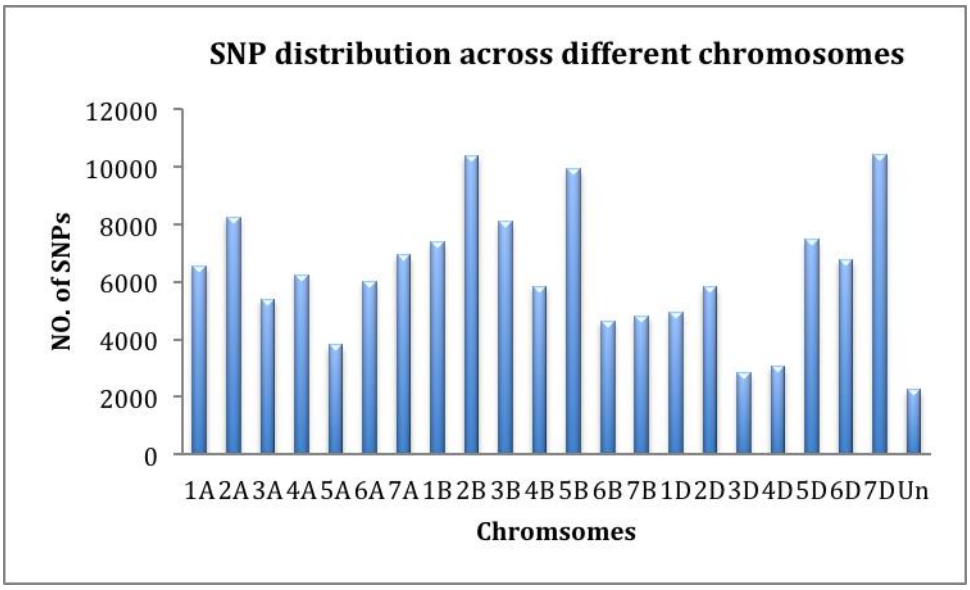

Figure 4 The distribution of polymorphic SNPs identified from ddRAD-seq across different chromosomes.

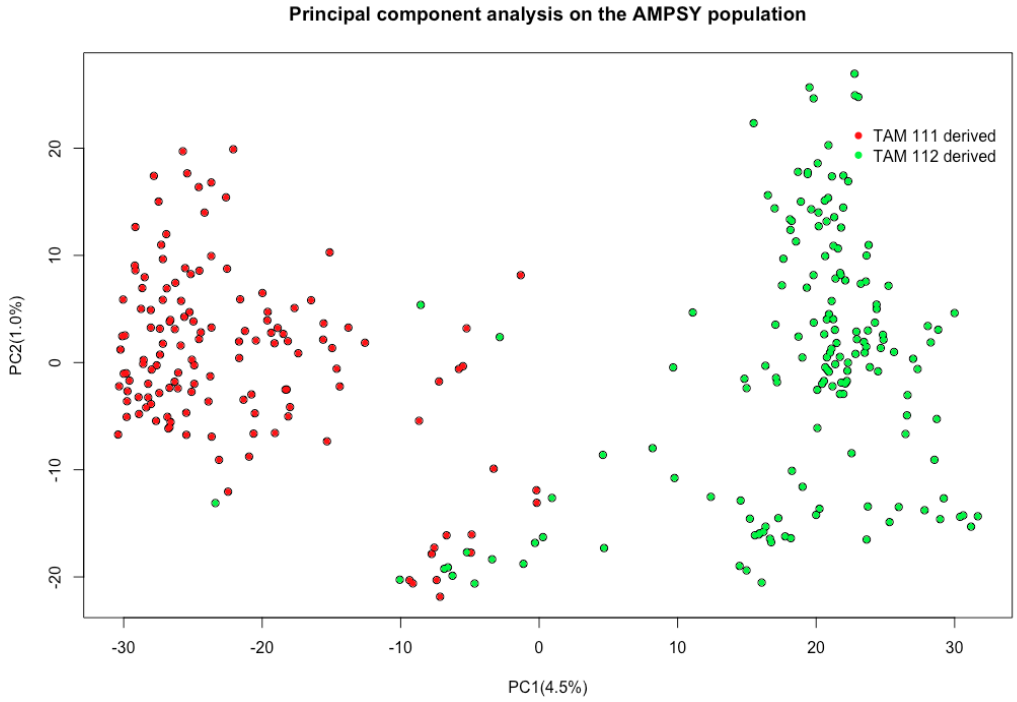

Figure 5 Principal component analysis of the population structure of the AMPSY population.

3.3.3 Association mapping analysis

The association mapping analysis was performed using TASSEL 5.0 to identify the significant marker trait associations. The p value for every marker for each trait was adjusted using the "BH" method in the R function p.adjust(). The BH method, developed by Benjamini and Hochberg, controls the expected proportion of false discoveries amongst the rejected hypotheses, which is a powerful method in detecting significance (Benjamini and Hochberg, 1995). It is less stringent than the Bonferroni correction. FDR values were calculated at 0.2, and those SNPs with FDR values smaller than 0.2 were declared as significant SNPs associated with the traits. With these criteria, a total of 199 significant SNPs covering 54 wheat Chromosome Survey Sequence (CSS) contigs have been identified across different conditions.

Among the identified significant markers, only 2 SNPs were significantly associated with EWL and 197 were significantly linked to glaucousness. The SNP *10813777_5bl_503* was identified in the College Station environment in 2016 and *6918051_3dl_1555* in the Bushland dry environment in 2017, which accounted for about 12% and 9% of the EWL variation in the population in these two environments, respectively. These two markers are uniquely linked to EWL, because we couldn't find significant associations with glaucousness. In the Bushland dry environment in 2017, 95 significant markers associated with wax-related traits at the flowering stage have been identified, which was the highest amount of the identified SNPs. The top two highest amounts of the significant marker trait associations (44) have been characterized in the same Bushland dry environment in 2016. And 23 and 28 markers were identified in

Chillicothe 2016 at the 10DAP stage and Prosper 2017 at the flowering stage. At the heading stage, we recorded glaucousness score in Bushland dry and Bushland irrigated environments in 2016. Only seven SNPs have been found significantly linked to glaucousness in the Bushland dry environment. Among all the identified SNPs, *5388952_2ds_6337* and *5337369_2ds_2020* were the most significant ones, as well as having the lowest adjusted p-value.

Glaucousness was recorded in seven conditions of different combinations of environments and stages, with five out of them have significant marker-trait associations identified. That is, Bushland dry environment in 2016 at the heading stage (BD16HD), Bushland dry environment in 2016 at the flowering stage (BD16FL), Chillicothe in 2016 at the 10DAP stage (CH16TD), Bushland dry environment in 2017 at the flowering stage (BD17FL) and Prosper in 2017 at the flowering stage (PR17FL). Based on the Manhattan plot (Figure 6), we can clearly see that the significant SNPs were aggregated on chromosome 2D and consistently existed in the five conditions mentioned before. For every condition, the genetic regions covered by the significant SNPs were defined as QTLs (Table 9), and the common region detected across the five different conditions on 2D was viewed as stable QTL. The SNPs with the highest negative log p value was defined as peak marker. A pseudo physical map based on the Chromosome Survey Sequence (CSS) for *Triticum aestivum* cv. Chinese Spring (IWGSC RefSeq v1.0, https://wheat-urgi.versailles.inra.fr/Seq-Repository/Assemblies) was provided by the Genomics and Bioinformatics Center, Texas A&M Agrilife Research at College Station.

And this map also has the corresponding alignment on the CSS consensus map and W7984 map. As table 9 showed, the peak makers for glaucousness QTLs in different conditions were different. *5293194_2ds_2515*, *5388952_2ds_6337*, *5340435_2ds_8207*, *5324961_2ds_11010* and *5337369_2ds_2020* were the peak SNP in the condition of BD16HD, BD16FL, CH16TD, BD17FL and PR17FL, respectively, explaining the variation in the population ranged from 8.4% - 13.5%. All the peak SNPs were frequently identified across four different conditions except for 5388952_2ds_6337 detected in the conditions of BD16FL, CH16TD and BD17FL. Based on the physical position of flanking SNPs on the pseudomolecule, a common genetic region detected consistently across five non-optimal conditions was identified (Table 10). This region was delimited by the SNP *5293194_2ds_2515* and *5348611_2ds_1248* within a 5434347bp-interval, which should be viewed as a stable QTL.

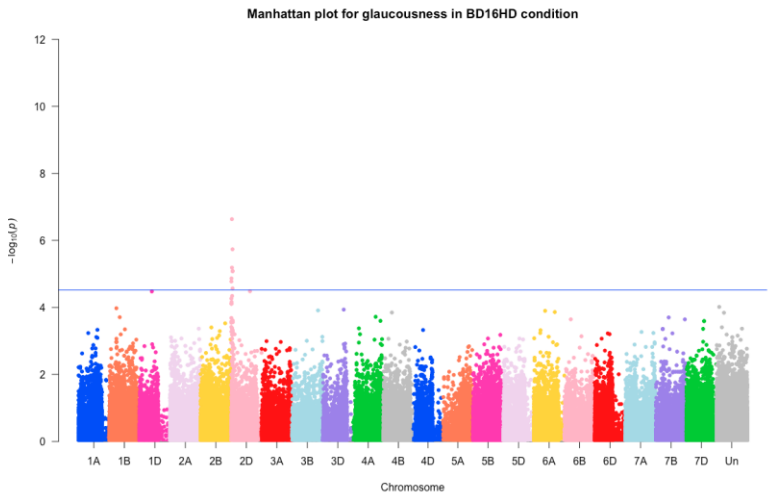

Figure 6 Manhattan plot for significant SNPs associated with glaucousness in different conditions.

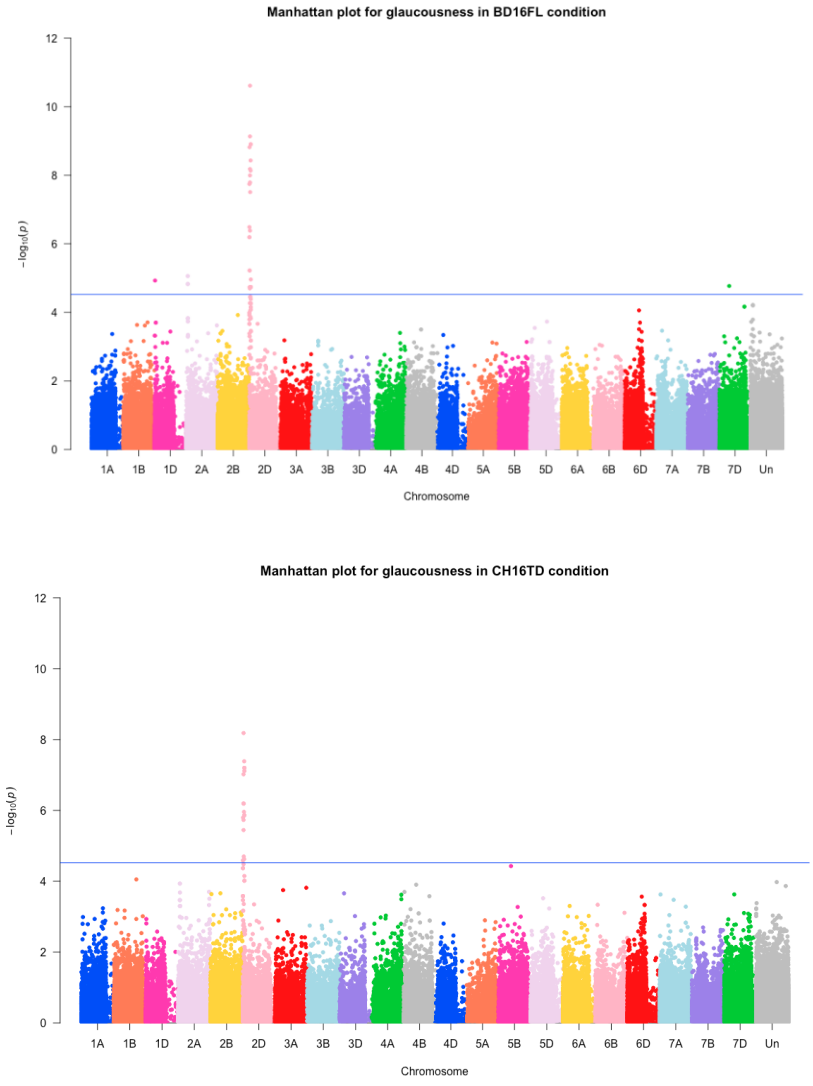

Figure 6 Continued

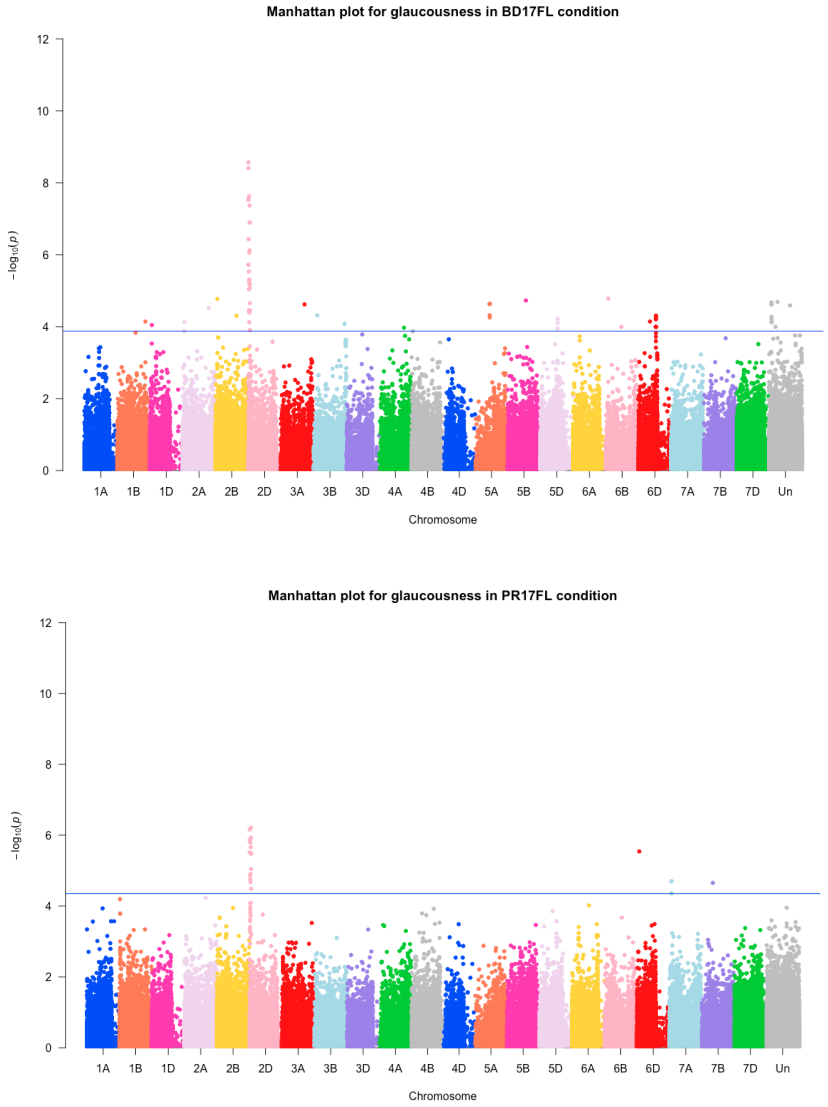

Figure 6 Continued

Table 9 The QTLs for glaucousness on 2DS identified in different conditions.

Condition	Property	SNP	Pseudo chr	Pseudo physical position (bp)	CSS Chr	CSS map (cM)	W7984 Contig	W7984 Chr	W7984 map (cM)
BD16HD	Peak	5293194_2ds_2515	chr2D	7089473	2ds	0	Scaffold3121468	2D	2.273
	Flanking	5348611_2ds_1248	chr2D	12523820	2ds	9.2	Scaffold658258	2D	7.957
BD16FL	Flanking	5329977_2ds_1265	chr2D	2113524	2ds	0	Scaffold835137	2D	0
	Peak	5388952_2ds_6337	chr2D	7098489	2ds	0	Scaffold1154612	2D	2.273
	Flanking	5347768_2ds_2912	chr2D	13853647	2ds	12.03	Scaffold5518806	2D	9.094
CH16TD	Flanking	5324961_2ds_11010	chr2D	2344410	2ds	0	Scaffold811880	2D	0
	Peak	5340435_2ds_8207	chr2D	7297826	2ds	0	Scaffold3609743	2D	3.41
	Flanking	5334799_2ds_1966	chr2D	13586612	2ds	9.2	Scaffold190068	2B	15.931
BD17FL	flanking	5329977_2ds_1265	chr2D	2113524	2ds	0	Scaffold835137	2D	0
	Peak	5324961_2ds_11010	chr2D	2344410	2ds	0	Scaffold811880	2D	0
	Flanking	5347768_2ds_2912	chr2D	13853647	2ds	12.03	Scaffold5518806	2D	9.094
PR17FL	Flanking	5329977_2ds_1265	chr2D	2113524	2ds	0	Scaffold835137	2D	0
	Peak	5337369_2ds_2020	chr2D	11988277	3b	78.75	Scaffold3079099	2D	7.957
	Flanking	5342586_2ds_3665	chr2D	13845859	2ds	12.03	Scaffold5518806	2D	9.094

Table 10 Stable glaucousness QTL on 2D detected across different non-optimal conditions.

SNP	Pseudo physical position (bp)	BD16HD	BD16FL	CH16TD	BD17FL	PR17FL	W7984 scalffold	CSS map (cM)	W7984 map (cM)
5329977_2ds_1265	2113524						Scaffold835137	0	0
5324961_2ds_11010	2344410						Scaffold811880	0	0
5293194_2ds_2515	7089473						Scaffold3121468	0	2.273
5388952_2ds_6337	7098489						Scaffold1154612	0	2.273
5340435_2ds_8207	7297826						Scaffold3609743	0	3.41
5337369_2ds_2020	11988277						Scaffold3079099	78.75	7.957
5348611_2ds_1248	12523820						Scaffold658258	9.2	7.957
5334799_2ds_1966	13586612						Scaffold190068	9.2	15.931
5342586_2ds_3665	13845859						Scaffold5518806	12.03	9.094
5347768_2ds_2912	13853647						Scaffold5518806	12.03	9.094

Based on the repeatability of the makers identified across different conditions, all the significant markers were categorized into four sets: the SNPs identified stably in four conditions (Table 11), three conditions (Table 12), two conditions (Table 13) and unique condition (Table 14). Fifteen of the significant SNP-glaucousness associations were consistently identified in four conditions (Table 11), and a total of 42 SNPs were found in more than one condition (Table 12, Table 13). Seventy three SNPs were identified uniquely for one condition (Table 14). All the significant SNPs consistently identified in four conditions were located on chromosome 2D, covering 8 CSS contigs. The SNP *5337369_2ds_2020* has the lowest adjusted p value. It can explain 11.7% of the genetic variation in the population in the condition of BD16FL, which was the third highest maker R^2 among all the SNPs. The marker *5340435_2ds_8207* covered the highest variation (13.5%) in the condition CH16TD, which explained as high as 11.5% variation in BD17FL and also accounted for 7.6% and 9.1% of the variation in the AMPSY population in the conditions of BD16HD and PR17FL, respectively. This SNP was consistently found in three different locations and three important reproductive stages we studied.

Table 11 Summary of significantly associated SNPs with glaucousness consistently identified in four conditions.

SNP	Chr	Pseudo physical position (bp)	Condition	P value	FDR	R^2
5293194_2ds_2515	2D	7089473	BD16HD	2.32E-07	3.20E-02	0.0990
			CH16TD	1.86E-06	1.40E-02	0.0930
			BD17FL	9.16E-06	4.20E-02	0.0740
			PR17FL	1.75E-05	1.11E-01	0.0740
5325544_2ds_1091	2D	11818822	BD16HD	1.84E-06	1.27E-01	0.0730
			CH16TD	4.10E-08	1.00E-03	0.1070
			BD17FL	7.59E-07	7.00E-03	0.0780
			PR17FL	2.18E-06	2.90E-02	0.0760
5340435_2ds_8207	2D	7297826	BD16HD	6.50E-06	1.63E-01	0.0760
			CH16TD	6.55E-09	1.00E-03	0.1350
			BD17FL	2.35E-08	1.00E-03	0.1150
			PR17FL	1.62E-06	2.50E-02	0.0910
5348611_2ds_1202	2D	12523774	BD16HD	8.27E-06	1.63E-01	0.0630
			CH16TD	1.38E-06	1.20E-02	0.0820
			BD17FL	1.27E-07	1.00E-03	0.0900
			PR17FL	1.19E-06	2.40E-02	0.0800
5348611_2ds_1230	2D	12523802	BD16HD	8.27E-06	1.63E-01	0.0630
			CH16TD	1.38E-06	1.20E-02	0.0820
			BD17FL	1.27E-07	1.00E-03	0.0900
			PR17FL	1.19E-06	2.40E-02	0.0800
5348611_2ds_1248	2D	12523820	BD16HD	8.27E-06	1.63E-01	0.0630
			CH16TD	1.38E-06	1.20E-02	0.0820
			BD17FL	1.27E-07	1.00E-03	0.0900
			PR17FL	1.19E-06	2.40E-02	0.0800
5348611_2ds_944	2D	12523516	BD16HD	8.27E-06	1.63E-01	0.0630
			CH16TD	1.38E-06	1.20E-02	0.0820
			BD17FL	1.27E-07	1.00E-03	0.0900
			PR17FL	1.19E-06	2.40E-02	0.0800
5324961_2ds_11010	2D	2344410	BD16FL	1.81E-08	1.78E-04	0.1120
			CH16TD	2.58E-05	1.61E-01	0.0620
			BD17FL	2.68E-09	2.71E-04	0.1160
			PR17FL	6.97E-07	2.40E-02	0.0840
5334799_2ds_1966	2D	13586612	BD16FL	4.13E-05	1.42E-01	0.0570
			CH16TD	7.71E-08	2.00E-03	0.1020
			BD17FL	2.23E-05	7.50E-02	0.0570
			PR17FL	9.02E-06	7.30E-02	0.0660
5334799_2ds_2065	2D	13586513	BD16FL	1.83E-05	7.50E-02	0.0620
			CH16TD	6.32E-08	1.00E-03	0.1040
			BD17FL	6.65E-06	3.30E-02	0.0650
			PR17FL	3.32E-06	2.90E-02	0.0730
5334799_2ds_2110	2D	13586468	BD16FL	1.83E-05	7.50E-02	0.0620

Table 11 Continued

SNP	Chr	Pseudo physical position (bp)	Condition	P value	FDR	R^2
5334799_2ds_2110	2D	13586468	CH16TD	6.32E-08	1.00E-03	0.1040
			BD17FL	6.65E-06	3.30E-02	0.0650
			PR17FL	3.32E-06	2.90E-02	0.0730
5334799_2ds_2131	2D	13586447	BD16FL	1.83E-05	7.50E-02	0.0620
			CH16TD	6.32E-08	1.00E-03	0.1040
			BD17FL	6.65E-06	3.30E-02	0.0650
			PR17FL	3.32E-06	2.90E-02	0.0730
5334799_2ds_2152	2D	13586426	BD16FL	1.83E-05	7.50E-02	0.0620
			CH16TD	6.32E-08	1.00E-03	0.1040
			BD17FL	6.65E-06	3.30E-02	0.0650
			PR17FL	3.32E-06	2.90E-02	0.0730
5337369_2ds_2020	2D	11988277	BD16FL	7.31E-09	1.00E-04	0.1170
			CH16TD	2.37E-05	1.56E-01	0.0620
			BD17FL	4.28E-08	1.00E-03	0.0970
			PR17FL	6.18E-07	2.40E-02	0.0840
5361743_2ds_6694	2D	8501050	BD16FL	3.10E-08	2.80E-04	0.1060
			CH16TD	6.44E-07	8.00E-03	0.0870
			BD17FL	8.82E-07	8.00E-03	0.0770
			PR17FL	2.13E-05	1.13E-01	0.0610

Table 12 Summary of significantly associated SNPs with glaucousness consistently identified in three conditions.

SNP	Chr	Pseudo physical position (bp)	Condition	P value	FDR	R^2
3661444_2ds_385	2D	7202036	BD16FL	4.14E-07	3.00E-03	0.0880
			CH16TD	3.31E-05	1.99E-01	0.0600
			BD17FL	3.47E-05	1.00E-01	0.0540
5388952_2ds_6337	2D	7098489	BD16FL	6.60E-09	1.00E-04	0.1190
			CH16TD	9.56E-08	2.00E-03	0.1020
			BD17FL	6.15E-06	3.30E-02	0.0660
5388952_2ds_6352	2D	7098504	BD16FL	1.63E-08	1.00E-04	0.1120
			CH16TD	6.38E-07	8.00E-03	0.0880
			BD17FL	3.76E-05	1.02E-01	0.0550
5388952_2ds_6375	2D	7098527	BD16FL	1.01E-08	1.23E-04	0.1150
			CH16TD	3.59E-06	2.60E-02	0.0760
			BD17FL	2.92E-06	2.10E-02	0.0710
5388952_2ds_6383	2D	7098535	BD16FL	1.63E-08	1.73E-04	0.1120
			CH16TD	6.38E-07	8.00E-03	0.0880

Table 12 Continued

SNP	Chr	Pseudo physical position (bp)	Condition	P value	FDR	R^2
5388952_2ds_6383	2D	7098535	BD17FL	3.76E-05	1.02E-01	0.0550
5324961_2ds_10720	2D	2344700	BD16FL	6.41E-07	5.00E-03	0.0860
			BD17FL	1.90E-06	1.50E-02	0.0730
			PR17FL	1.37E-06	2.40E-02	0.0800
5324961_2ds_11008	2D	2344412	BD16FL	6.41E-07	5.00E-03	0.0860
			BD17FL	1.90E-06	1.50E-02	0.0730
			PR17FL	1.37E-06	2.40E-02	0.0800
5329977_2ds_1265	2D	2113524	BD16FL	3.25E-07	3.00E-03	0.0910
			BD17FL	3.93E-09	2.70E-04	0.1130
			PR17FL	3.07E-06	2.90E-02	0.0740
5353487_2ds_18304	2D	8671026	BD16FL	3.61E-05	1.28E-01	0.0700
			BD17FL	7.49E-05	1.43E-01	0.0600
			PR17FL	1.25E-05	9.60E-02	0.0760
5389992_2ds_20313	2D	3033186	CH16TD	1.59E-06	1.30E-02	0.0810
			BD17FL	3.68E-07	4.00E-03	0.0830
			PR17FL	1.38E-05	1.00E-01	0.0640

Table 13 Summary of significantly associated SNPs with glaucousness consistently identified in two conditions.

SNP	Chr	Pseudo physical position (bp)	Condition	P value	FDR	R^2
1889160_1ds_603	1D	20658499	BD16FL	6.27E-05	1.80E-01	0.0590
			BD17FL	2.41E-05	7.50E-02	0.0610
1889160_1ds_604	1D	20658498	BD16FL	6.10E-05	1.80E-01	0.0590
			BD17FL	2.10E-05	7.50E-02	0.0640
1889160_1ds_616	1D	20658486	BD16FL	6.16E-05	1.80E-01	0.0590
			BD17FL	2.27E-05	7.50E-02	0.0610
1889160_1ds_828	1D	20658274	BD16FL	6.27E-05	1.80E-01	0.0590
			BD17FL	2.41E-05	7.50E-02	0.0610
5206312_2as_7033	2A	14067411	BD16FL	1.49E-05	7.30E-02	0.0760
			BD17FL	1.33E-04	1.95E-01	0.0560
5206312_2as_7041	2A	14067403	BD16FL	1.49E-05	7.30E-02	0.0760
			BD17FL	1.33E-04	1.95E-01	0.0560
5206312_2as_7078	2A	14067366	BD16FL	1.49E-05	7.30E-02	0.0760
			BD17FL	1.33E-04	1.95E-01	0.0560
4845479_2ds_1137	2D	9346417	BD16FL	3.53E-05	1.28E-01	0.0700

Table 13 Continued

SNP	Chr	Pseudo physical position (bp)	Condition	P value	FDR	R^2
4845479_2ds_1137	2D	9346417	BD17FL	4.95E-06	3.10E-02	0.0780
4845479_2ds_1139	2D	9346415	BD16FL	3.53E-05	1.28E-01	0.0700
			BD17FL	4.95E-06	3.10E-02	0.0780
4845479_2ds_1145	2D	9346409	BD16FL	3.53E-05	1.28E-01	0.0700
			BD17FL	4.95E-06	3.10E-02	0.0780
5347768_2ds_2750	2D	13853485	BD16FL	5.50E-05	1.72E-01	0.0550
			BD17FL	1.25E-04	1.89E-01	0.0460
5347768_2ds_2768	2D	13853503	BD16FL	5.50E-05	1.72E-01	0.0550
			BD17FL	1.25E-04	1.89E-01	0.0460
5347768_2ds_2912	2D	13853647	BD16FL	5.50E-05	1.72E-01	0.0550
			BD17FL	1.25E-04	1.89E-01	0.0460
5370731_2ds_1511	2D	13775950	BD16FL	7.07E-05	1.87E-01	0.0530
			BD17FL	3.55E-05	1.00E-01	0.0550
5370731_2ds_1536	2D	13775975	BD16FL	7.07E-05	1.87E-01	0.0530
			BD17FL	3.55E-05	1.00E-01	0.0550
5334947_2ds_849	2D	10094481	CH16FL	1.10E-06	1.20E-02	0.0830
			BD17FL	4.08E-05	1.08E-01	0.0530
5353487_2ds_7426	2D	8660148	CH16FL	2.00E-05	1.38E-01	0.0630
			BD17FL	5.16E-06	3.10E-02	0.0660

Table 14 Summary of significantly associated SNPs with glaucousness uniquely identified in one condition.

SNP	Chr	Pseudo physical position (bp)	Condition	P value	FDR	R^2
1890447_1ds_1298	1D	3864245	BD16FL	1.18E-05	6.51E-02	0.0653
5206312_2as_6751	2A	14067693	BD16FL	8.74E-06	5.24E-02	0.0673
5206312_2as_6755	2A	14067689	BD16FL	8.74E-06	5.24E-02	0.0673
5359296_2ds_7310	2D	3754652	BD16FL	6.01E-06	3.94E-02	0.0824
5359296_2ds_7473	2D	3754489	BD16FL	5.99E-06	3.94E-02	0.0824
5359296_2ds_7535	2D	3754427	BD16FL	1.84E-05	7.45E-02	0.0744
5369310_2ds_6319	2D	13640756	BD16FL	1.10E-05	6.31E-02	0.0658
5380866_2ds_6118	2D	5468650	BD16FL	2.00E-05	7.87E-02	0.0618
5380866_2ds_6315	2D	5468847	BD16FL	5.39E-05	1.72E-01	0.0552
3325013_7dl_7745	7D	610242237	BD16FL	6.83E-05	1.87E-01	0.0536

Table 14 Continued

SNP	Chr	Pseudo physical position (bp)	Condition	P value	FDR	R^2
3325013_7dl_7780	7D	610242272	BD16FL	6.83E-05	1.87E-01	0.0536
3966785_7ds_682	7D	167058018	BD16FL	1.70E-05	7.45E-02	0.0628
3885661_1bl_2800	1B	655588443	BD17FL	7.21E-05	1.43E-01	0.0497
1889160_1ds_799	1D	20658303	BD17FL	6.00E-05	1.33E-01	0.0553
1889160_1ds_831	1D	20658271	BD17FL	5.30E-05	1.26E-01	0.0672
1913632_1ds_3156	1D	15322278	BD17FL	9.01E-05	1.64E-01	0.0484
5206312_2as_6759	2A	14067685	BD17FL	7.49E-05	1.43E-01	0.0602
6438836_2al_23093	2A	611951357	BD17FL	3.07E-05	9.19E-02	0.0550
5244845_2bs_2994	2B	22021259	BD17FL	7.44E-05	1.43E-01	0.0638
5244845_2bs_3001	2B	22021266	BD17FL	7.44E-05	1.43E-01	0.0638
5244845_2bs_3002	2B	22021267	BD17FL	7.44E-05	1.43E-01	0.0638
5244845_2bs_3013	2B	22021278	BD17FL	7.34E-05	1.43E-01	0.0644
8091715_2bl_18723	2B	525521894	BD17FL	4.94E-05	1.20E-01	0.0629
5331486_2ds_6265	2D	2257093	BD17FL	2.94E-08	5.07E-04	0.1130
5331486_2ds_6288	2D	2257070	BD17FL	2.94E-08	5.07E-04	0.1130
5331486_2ds_6301	2D	2257057	BD17FL	2.94E-08	5.07E-04	0.1130
5331486_2ds_6311	2D	2257047	BD17FL	2.94E-08	5.07E-04	0.1130
5331486_2ds_6313	2D	2257045	BD17FL	2.94E-08	5.07E-04	0.1130
5348611_2ds_1205	2D	12523777	BD17FL	8.38E-06	3.99E-02	0.0634
4453192_3al_312	3A	573480170	BD17FL	2.40E-05	7.55E-02	0.0565
10494000_3b_4095	3B	112280060	BD17FL	2.05E-05	7.55E-02	0.0615
10594888_3b_1945	3B	715787839	BD17FL	8.30E-05	1.55E-01	0.0489
3243507_6dl_8125	3D	217989720	BD17FL	7.16E-05	1.43E-01	0.0605
7150884_4al_12755	4A	595292750	BD17FL	1.07E-04	1.71E-01	0.0473
7171117_4al_4600	4A	521610821	BD17FL	2.56E-05	7.85E-02	0.0695
4878199_4bs_5510	4B	10563289	BD17FL	1.34E-04	1.95E-01	0.0459
2695026_5al_510	5A	364167085	BD17FL	2.28E-05	7.55E-02	0.0684
2695026_5al_517	5A	364167078	BD17FL	2.34E-05	7.55E-02	0.0683
2695026_5al_533	5A	364167062	BD17FL	2.34E-05	7.55E-02	0.0683
2695026_5al_547	5A	364167048	BD17FL	5.52E-05	1.28E-01	0.0626
2695026_5al_582	5A	364167013	BD17FL	2.34E-05	7.55E-02	0.0683
2695026_5al_598	5A	364166997	BD17FL	4.82E-05	1.20E-01	0.0635
10803407_5bl_7264	5B	462121589	BD17FL	1.88E-05	7.55E-02	0.0580

Table 14 Continued

SNP	Chr	Pseudo physical position (bp)	Condition	P value	FDR	R^2
2290635_5bs_4113	5B	70705753	BD17FL	1.01E-04	1.64E-01	0.0649
4516260_5dl_2632	5D	439774946	BD17FL	7.83E-05	1.48E-01	0.0492
4608040_5dl_14077	5D	438551346	BD17FL	1.14E-04	1.78E-01	0.0469
4608040_5dl_14259	5D	438551164	BD17FL	6.13E-05	1.34E-01	0.0507
4608040_5dl_14267	5D	438551156	BD17FL	1.14E-04	1.78E-01	0.0469
2967159_6bs_1484	6B	21489080	BD17FL	1.66E-05	7.27E-02	0.0588
4295804_6bl_1512	6B	394670290	BD17FL	1.01E-04	1.64E-01	0.0477
3278379_6dl_4487	6D	440488549	BD17FL	1.01E-04	1.64E-01	0.0582
3278379_6dl_4499	6D	440488537	BD17FL	6.24E-05	1.34E-01	0.0614
3278379_6dl_4516	6D	440488520	BD17FL	5.66E-05	1.28E-01	0.0620
3278379_6dl_4522	6D	440488514	BD17FL	1.01E-04	1.64E-01	0.0582
3278379_6dl_4692	6D	440488344	BD17FL	1.01E-04	1.64E-01	0.0582
3278379_6dl_4697	6D	440488339	BD17FL	5.66E-05	1.28E-01	0.0620
3278379_6dl_4706	6D	440488330	BD17FL	1.01E-04	1.64E-01	0.0582
3278379_6dl_4712	6D	440488324	BD17FL	1.01E-04	1.64E-01	0.0582
3278379_6dl_4714	6D	440488322	BD17FL	1.01E-04	1.64E-01	0.0582
3278379_6dl_4723	6D	440488313	BD17FL	4.95E-05	1.20E-01	0.0629
3278379_6dl_4729	6D	440488307	BD17FL	4.95E-05	1.20E-01	0.0629
3278379_6dl_4738	6D	440488298	BD17FL	1.01E-04	1.64E-01	0.0582
3278379_6dl_4768	6D	440488268	BD17FL	1.01E-04	1.64E-01	0.0582
10703124_3b_5849	Un	34499473	BD17FL	4.82E-05	1.20E-01	0.0524
5244177_2bs_337	Un	15953139	BD17FL	1.69E-05	7.27E-02	0.0730
5342586_2ds_3665	2D	13845859	PR17FL	3.26E-05	1.61E-01	0.0696
382116_6ds_1422	6D	18984507	PR17FL	2.88E-06	2.86E-02	0.0740
4253875_7as_3728	7A	17202971	PR17FL	2.00E-05	1.11E-01	0.0730
4253875_7as_3734	7A	17202977	PR17FL	2.00E-05	1.11E-01	0.0730
4253875_7as_3738	7A	17202981	PR17FL	2.00E-05	1.11E-01	0.0730
4253875_7as_3802	7A	17203045	PR17FL	2.00E-05	1.11E-01	0.0730
4253875_7as_3929	7A	17203172	PR17FL	2.00E-05	1.11E-01	0.0730
3148450_7bs_11203	7B	195220913	PR17FL	2.23E-05	1.14E-01	0.0605

Ten significant SNP-glaucousness associations were consistently found in three conditions (Table 11), among which four SNPs were mapped on the contig of *CSS_5388952*. The SNPs *5324961_2ds_10720* and *5324961_2ds_11008* identified in the conditions of BD16FL, BD17FL and PR17FL were located on the same contig *CSS_5324961*. Additionally, *5329977_2ds_1265* and *5353487_2ds_18304*, located on different contigs of the 2D chromosome, were found in the same three conditions with SNPs *5324961_2ds_10720* and *5324961_2ds_11008*. The four SNPs mentioned were characterized at the flowering stage, with all the markers stably appearing in three conditions located on the chromosome 2D (Table 11).

Seventeen SNPs were consistently identified in two conditions (all of them found at the flowering stage), which were distributed on chromosomes 1D, 2A and 2D. Fifteen out of 17 significant SNPs were identified in Bushland dry environment at the flowering stage for two consecutive years. Four SNPs were mapped on the contig *CSS_1889160* on chromosome 1D. Three significant SNPs were mapped on each of the contigs *CSS_5206312* on the chromosome 2A, *CSS_4845479* and *CSS_5347768* on 2D, respectively. The significant markers detected more that one condition should be viewed as stable marker trait associations (Table 11 - 13).

Twelve, 8 and 53 marker trait associations were uniquely found in the conditions of BD16FL, PR17FL and BD17FL, respectively (Table 14). The distributions of SNPs on the wheat genome were different across different conditions. In the BD16FL condition, the significant SNPs were distributed on the chromosome 1D, 2A, 2D and 7D. In the PR17FL condition, significant markers were located on 2D, 6D, 7A and 7B.

Almost all the chromosomes have significant marker-glaucousness associations identified except for 1A, 4D, 6A, 7A, 7B and 7D in the condition of BD17FL.

3.4 Discussion

In wheat, the major glaucousness genes are mainly located on the B and D subgenome. Studies (Tsunewaki and Ebana 1999; Wu et al. 2013) have shown that *WAX1* (*W1*) and *INHIBITOR OF WAX1* (*Iw1*) were mapped on the distal regions of 2B, while another set consisting of a wax production and wax inhibitor gene, *W2* and *Iw2*, were located far apart on the short arm of 2D. An evolutionary study (Tsunewaki 1966) on wheat suggested that *W1* and *W2*, along with *Iw1* and *Iw2*, are duplicated genes. Both *Iw1* and *Iw2* were mapped on the distal region of 2BS and 2DS, indicating that *Iw1* and *Iw2* may be homologs (Wu et al. 2013). The characterization of the first set of wax genes is going further than *W2* and *Iw2*. A recent study has dissected the *W1* locus in wheat. *W1* locus is a gene-coding region in which three genes are orthologous to the *Cer-C*, *Cer-Q*, *Cer-U* locus in barley (Schneider et al. 2016; Hen-Avivi et al. 2016) encoding a lipase/carboxylesterase, a chalcone synthase-like polyketide synthase and a cytochrome P450-type hydroxylase, respectively. However, *Iw1* is not a protein-coding region. Its transcript is a long noncoding RNA (lncRNA) that can be processed into a miRNA suppressing the expression of *W1-COE*, the *Cer-C* orthologs, through a miRNA-mediated cleavage (Huang et al. 2017). As a homolog to *Iw1*, the *Iw2* locus also can produce a non-protein coding regulatory element.

In this study, we cannot identify many significant SNPs associated with epicuticular wax load, but can identify rich SNPs associated with glaucousness. Lack of phenotypic variation is not the reason for our finding no significant MTAs linked to epicuticular wax load in the association mapping analysis. Based on Table 8, we can see a large variation in terms of EWL existing in the AMPSY population. The probable reason is that the frequency of the alleles controlling epicuticular wax load is low in the AMPSY population, and there is insufficient statistical power to detect the significant marker-trait associations. Besides, wheat genome has large repetitive and non-coding sequence (Bennetzen et al. 2005; IWGSC 2014). Compared with 90K SNP array data, the proportion of gene-based markers identified from ddRAD-seq should be lower than that from 90K wheat SNP array. The non-coding elements controlling the traits should have more probability to be identified in GWAS. The large amount of SNPs linked to glaucousness found in this study might be related to regulatory elements. A recent paper has characterized that the *Iw1* is a long noncoding RNA (lncRNA) that can be transcribed into a miRNA precursor suppressing the expression of *W1-COE* through a miRNA-mediated cleavage (Huang et al. 2017).

Among all the identified SNPs, *5388952_2ds_6337* and *5337369_2ds_2020* were the most significant ones with the lowest adjusted p-value, explaining 11.9% and 9.7% of the variation in AMPSY population in the condition of BD16FL. Both can be consistently identified in more than three conditions. *5324961_2ds_11010* identified in BD17FL had the highest negative log p-value (Figure 6), which also belongs to the set of the SNPs consistently found in 4 conditions (Table 11). If we sort the marker based on

the marker R^2, *5340435_2ds_8207*, as a peak marker in the condition of CH16TD, can explain as high as 13.5% of the genetic variation in the AMPSY population. It can be stably found in BD16HD, CH16TD, BD17FL and PR17FL conditions. All four significant marker-trait associations mentioned above were located on 2DS and can be consistently identified in multiple conditions. The common region shown in table 10 is the stable QTL consistently identified across five conditions that need to be further dissected.

In our study, the majority of stable significant SNPs were mapped on the short arm of 2D. Based on information of reference genome including the SNP sequence alignment on the CSS reference and W7984 reference (Table 9). It has been shown that all the stable SNPs on 2D identified in this study were mapped on the distal region of the short arm of 2D within the interval of 0-12.03 cM, which is in consensus with the previous results. A well-known wax-related gene *Iw2* has been mapped on the distal region of 2DS, which is from the ancestor of the D genome *Aegilops tauschii* (Wu et al. 2013). In that study (Wu et al. 2013), 8 EST markers linked to *Iw2* have been mapped on the 4.1-5.4-cM interval in the chromosome 2DS. This region is also collinear with a 2.3 cM region containing the *Iw1* gene on chromosome 2BS. It has been reported that the non-glaucousness gene *Iw2* was mapped on the 2DS in an F2 segregation population of *Aegilops tauschii* (Watanabe et al. 2005). In hexaploid wheat, the non-glaucousness gene was also mapped on the distal region of 2DS. The mapping populations are derived from the cross between the non-glaucousness genotype, a synthetic hexaploid wheat Line 3672 and the glaucousness common wheat Line 9753. Five SSR markers have been

identified as being linked to the non-glaucousness gene *Iw3872* in the wheat line 3672, and these markers were located on the same distal region of 2DS as *Iw2* (Liu et al. 2007). Chu (2008) has mapped the dominant non-glaucousness gene on the genetic region within a 0-23.2 cM interval on 2DS using a double haploid wheat population. In a recent study *Iw2* was consistently identified in the in the distal region of the 2DS in two F2 populations of *Ae. tauschii* and three F2 populations of the synthetic wheat lines (Nishijima et al. 2014). To date, there exists no study about the identification of wax-related QTL in synthetic wheat using genome-wide association study. Nishijima (2014) used a panel of 210 *Ae. tauschii* accessions to verify the association between the developed high-confidence markers from the comparative analysis and *Iw2* genes. Through linkage mapping and the comparative analysis, the contigs in *Ae. tauschii* around *Iw2* have been identified. They also have collinearity with the genomic regions in *Brachypodium*. Among the annotated regions, 10 of them were the putative cytochrome P450 monooxygenase genes and 8 of them were disease-related genes. The genes encoding laccase, agmatine coumaroyltransferase, receptor kinase, and cell number regulator 2-like were found co-localized with *Iw2* (Nishijima et al. 2014). In our study, 5 out of the SNPs with known annotation have the putative CYP450 function. All of these indicated that the genomic regions located on the short arm of 2D in our study may contain *Iw2* locus, and this locus may regulate the glaucousness at the transcription level.

3.5 Conclusion

This is the first time wax-related genes in hexaploid wheat have been dissected using genome-wide association study. More than 130,000 polymorphic SNPs densely distributed across different chromosomes have been used to genotype the 300 synthetic-derived wheat lines in the AMPSY population. In all, 199 significant marker-trait associations have been identified in different sampling conditions with non-optimal growth environments and 197 of SNPs were related to glaucousness. Most of the significant SNPs were located on 2DS, especially for those SNPs consistently identified in more than one condition. Fifteen, 10 and 17 consistent significant SNPs were found in four, three and two sampling conditions, respectively. Seventy-three markers uniquely identified in the condition of BD16FL, BD17FL and PR17FL were distributed on the all chromosomes except for 1A, 4D and 6A. However, no significant marker-trait associations in the optimal environment were detected, which indicates that wax may be a stress-triggered trait.

A stable glaucousness QTL located on chromosome 2D has been identified. This QTL flanked by *5293194_2ds_2515* and *5348611_2ds_1248* can be detected in all the non-optimal conditions. 4 out of 5 peak SNPs were included in this region showing strong associations with glaucousness like *5388952_2ds_6337*, *5337369_2ds_2020* and *5340435_2ds_8207*, indicating a high negative log p value and the marker R^2 in most cases.

Several evidence may indicate that the regions on 2DS identified in this study may contain *Iw2* locus. Based on the wheat consensus map, the SNPs significantly

associated with glaucousness were mapped on the distal region of the short arm of the chromosome 2D. This was in consensus with the previous studies that *Iw2* locus was located on 2DS (Chu et al. 2008; Nishijima et al. 2014). Using a blast search, the best hits for the majority of the SNPs on 2D were on *Ae. tauschii* scaffolds. The annotated contigs have the functions of putative cytochrome P450 protein (CYP450), which is similar to the comparative analysis of the genomic regions around *Iw2* in *Ae. tauschii*. In Nishijima's (2014) study, most of the syntenic contigs in *Brachypodium* have the putative CYP450 function. *Iw1* sequence in wheat shared high similarity with the homologs in *Ae. tauschii* (Nishijima et al. 2014). Both of *Iw1* and *Iw2* were mapped on the distal region of 2BS and 2DS, respectively (Tsunewaki and Ebana 1999). This indicates that *Iw1* is the homolog of *Iw2*. *Iw1* encodes a long non-coding RNA regulating the genes involved in the β-diketone pathway. *Iw2* has also been proposed as a non-protein coding region encoding a regulatory RNA (Huang et al. 2017). The contig has high similarity with a non-coding RNA in *Ae. tauschii*. The associations between the significant SNPs on 2D and *Iw2* need to be further verified. A large proportion of significant SNPs correlated with glaucousness were mapped on 2DS. The SNPs consistently identified in multiple conditions should be further verified and the stable QTL located on 2D should be further dissected.

CHAPTER IV

SUMMARY

Global warming and water deficiency are the main problems limiting plant growth and development. Plants have developed various mechanisms coping with biotic and abiotic stresses, one of which is the biosynthesis of wax covering on the plant surface. Clarification of the genetic basis underlying the wax biosynthesis would lay a foundation for breeders to develop lines with tolerance to heat or drought stress.

This study marks the first time characterization of the association between the genomic regions in wheat and the wax variations combining the bi-parental QTL analysis and the genome-wide association study has been conducted. The Hal x Len RIL population at the eighth generation has been genotyped using the gene-based wheat SNP array, while a high-density genetic linkage map has been constructed. Two main-effect pleiotropic QTLs controlling multiple traits have been identified from the linkage mapping analysis. One is located on the short arm of 2B, correlated to epicuticular wax load at the late booting stage (S1) and the 5DAP (S3), along with glaucousness at the late booting (S1) and flowering stages (S2). This explains up to 18.6% EWL variation, 18.9% glaucousness variation, 8.9% tiller number variation and 13% head length variation in the RIL population. Together with the significantly positive correlation between wax and head length across all the stages we studied, this may indicate that the genes controlling wax biosynthesis may also be involved in the regulation of yield-contributing traits.

The QTLs mapped on 4B were also the important genomic regions in terms of being detected at the early reproductive stages. This developmental stage-specific QTL was also co-localized with the QTLs for plant height. Additionally, the QTLs with significant effects for plant height, head length, tiller number and awn has been characterized in this study. Compared with previous studies, not only consensus QTLs can be identified. The novel QTLs related to plant height was also detected in this study, which provided a clue for the dissection of the genetic basis underlying complex quantitative traits.

In the genome-wide association study, focus was directed toward the wax-related traits, including epicuticular wax load and glaucousness visual score. No significant marker trait associations for wax-related traits were detected in the optimal environment. Only two out of 199 significant SNPs were identified for the association with epicuticular wax load. One hundred and ninety seven significant marker-trait associations were related to glaucousness, most of them being mapped on the short arm of the chromosome 2D, which is in consensus with the previous study of the localization of wax inhibitors *Iw2*. Since *Iw1* is the homolog of *Iw2*, *Iw2* locus has been demonstrated to encode a long ncRNA like *Iw1*. The stable QTL on 2D and the consistently identified SNPs across different conditions should be further dissected and verified. Comparative analysis should be conducted for the identification of the collinearity of the important genomic region for wax in wheat with the D genome contributor *Ae. Tauschii*, as well as with other model plants in the future.

In this study, QTLs for wax were mapped on the short arm of 2B in the bi-parental mapping population, and 2DS in the AMPSY association panel, which indicated that the expression of wax genes may be dependent on genetic background. Stage-specific QTLs have been identified in the linkage mapping analysis, while unique significant marker trait associations have been found in different conditions in the GWAS. It illustrated that wax biosynthesis relied on the developmental stages and outer environment. Previous studies showed that the *Iw1* and *Iw2* are homologs, with both being located on the distal region of 2B and 2D, respectively (Tsunewaki and Ebana 1999, Wu et al. 2013). In our study, wax genes were mapped on the genomic region positioned from 24.26 to 36.36 cM on the chromosome 2BS in the bi-parental QTL mapping study, as well as on the consensus genomic region of 0-12.3 cM on the chromosome 2DS in the genome-wide association study. By mapping the *Iw1* cds sequence (accession NO. KX823910) and the sequence of flanking markers for wax-related QTL on 2B identified in the bi-parental linkage mapping analysis to 2D reference genome (IWGSC RefSeq v1.0, https://wheat-urgi.versailles.inra.fr/Seq-Repository/Assemblies), the pseudo physical locations of these two regions were far apart from each other, which may indicate that *QGlau.tam-2B* detected in this study may not contain *Iw1* locus. The QTL *QGlau.tam-2B* and the glaucousness QTL on 2D identified in GWAS may not be homeologous regions. The associations of these two regions identified in this research with *Iw1* and *Iw2* need to be further characterized.

In general, wax expression largely depends on genetic background and environment. The major QTLs and significant marker-trait associations identified in this

study will lay a good foundation for the dissection of the genomic regions involved in the regulation of spatiotemporal expression of wax.

REFERENCES

Adamski NM, Bush MS, Simmonds J, et al (2013) The Inhibitor of wax 1 locus (*Iw1*) prevents formation of β- and OH- β- diketones in wheat cuticular waxes and maps to a sub- cM interval on chromosome arm 2BS. The Plant Journal 74:989–1002. doi: 10.1111/tpj.12185

Adhikari TB, Jackson EW, Gurung S, et al (2011) Association mapping of quantitative resistance to Phaeosphaeria nodorum in spring wheat landraces from the USDA National Small Grains Collection. Phytopathology 101:1301–1310. doi: 10.1094/PHYTO-03-11-0076

Al-Abdallat A, Al-Debei H, Ayad J, et al (2014) Over-Expression of SlSHN1 Gene improves drought ttolerance by increasing cuticular wax accumulation in tomato. IJMS 15:19499–19515. doi: 10.3390/ijms151119499

Alghabari F, Lukac M, Jones HE, et al (2014) Effect of Rht alleles on the tolerance of wheat grain set to high temperature and drought stress during booting and anthesis. Journal of Agronomy and Crop Science 200:36–45. doi: 10.1111/jac.12038

Austin MB, Noel JP (2002) The chalcone synthase superfamily of type III polyketide synthases. Nat Prod Rep 20:79–110. doi: 10.1039/b100917f

Bajgain P, Rouse MN, Tsilo TJ, et al (2016) Nested association mapping of stem rust resistance in wheat using genotyping by sequencing. Plos One 11:e0155760. doi: 10.1371/journal.pone.0155760

Baker EA (1974) The influence of environment of leaf wax development in Brassica oleracea var. gemmifera. New Phytologist 73:955–966. doi: 10.1111/j.1469-8137.1974.tb01324.x

Barber HN, Netting AG (1968) Chemical genetics of b-diketone formation in wheat. . Phytochemistry 7:2089–2093.

Bariana HS, Miah H, Brown GN, et al (2007) Molecular mapping of durable rust resistance in wheat and its implication in breeding. In: Wheat Production in Stressed Environments. Springer, Dordrecht,723–728

Barnabas B, Jaeger K, Feher A (2008) The effect of drought and heat stress on reproductive processes in cereals. Plant Cell Environ 31:11–38. doi: 10.1111/j.1365-3040.2007.01727.x

Battenfield SD, Klatt AR, Raun WR (2013) Genetic yield potential improvement of

semidwarf winter wheat in the great plains. Crop Science 53:946–955. doi: 10.2135/cropsci2012.03.0158

Bianchi A, Bianchi G, Avato P, et al (1985) Biosynthetic pathways of epicuticular wax of maize as assessed by mutation, light, plant age and inhibitor studies. Maydica 30:179–98

Benjamini Y, and Hochberg Y (1995) Controlling the false discovery rate: a practical and powerful approach to multiple testing. Journal of the Royal Statistical Society. Series B (Methodological) 57(1): 289-300.

Bennett D, Izanloo A, Edwards J, et al (2012) Identification of novel quantitative trait loci for days to ear emergence and flag leaf glaucousness in a bread wheat (*Triticum aestivum* L.) population adapted to southern Australian conditions. Theor Appl Genet 124:697–711. doi: 10.1007/s00122-011-1740-3

Bennetzen JL, Ma JX, Devos KM (2005) Mechanisms of recent genome size variation in flowering plants. Ann Bot 95:127–132. doi: 10.1093/aob/mci008

Bernard A, Domergue F, Pascal S, et al (2012) Reconstitution of plant alkane biosynthesis in yeast demonstrates that arabidopsis ECERIFERUM1 and ECERIFERUM3 are core components of a very-long-chain alkane synthesis complex. The Plant Cell 24:3106–3118. doi: 10.1105/tpc.112.099796

Bernard A, Joubès J (2013) Arabidopsis cuticular waxes: Advances in synthesis, export and regulation. Progress in Lipid Research 52:110–129. doi: 10.1016/j.plipres.2012.10.002

Berridge MJ (1993) Inositol trisphosphate and calcium signaling. Nature 361:315–325.

Bessire M, Borel S, Fabre G, et al (2011) A member of the PLEIOTROPIC DRUG RESISTANCE family of atp binding cassette transporters is required for the formation of a functional cuticle in arabidopsis. The Plant Cell 23:1958–1970. doi: 10.1105/tpc.111.083121

Bianchi G, Figini ML (1986) Epicuticular Waxes of Glaucous and Nonglaucous Durum Wheat Lines. JAgricFood Chem 429–433.

Bird D, Beisson F, Brigham A, et al (2007) Characterization of Arabidopsis ABCG11/WBC11, an ATP binding cassette (ABC) transporter that is required for cuticular lipid secretion. The Plant Journal 52:485–498. doi: 10.1111/j.1365-313X.2007.03252.x

Borisjuk N, Hrmova M, Lopato S (2014) Transcriptional regulation of cuticle biosynthesis. Biotechnology Advances 32:526–540. doi:

10.1016/j.biotechadv.2014.01.005

Börner A, Schumann E, Fürste A, et al (2002) Mapping of quantitative trait loci determining agronomic important characters in hexaploid wheat (Triticum aestivum L.). Theor Appl Genet 105:921–936. doi: 10.1007/s00122-002-0994-1

Breseghello F, Sorrells ME (2006) Association mapping of kernel size and milling quality in wheat (*Triticum aestivum* L.) cultivars. Genetics 172:1165–1177. doi: 10.1534/genetics.105.044586

Broman KW, Wu H, Sen Ś, et al (2003) R/qtl: QTL mapping in experimental crosses. Bioinformatics 19:889–890. doi: 10.1093/bioinformatics/btg112

Burow GB, Franks CD, Acosta-Martinez V, et al (2008) Molecular mapping and characterization of BLMC, a locus for profuse wax (bloom) and enhanced cuticular features of Sorghum (Sorghum bicolor (L.) Moench.). Theor Appl Genet 118:423–431. doi: 10.1007/s00122-008-0908-y

Buschhaus C, Jetter R (2011) Composition differences between epicuticular and intracuticular wax substructures: How do plants seal their epidermal surfaces? Journal of Experimental Botany 62:841–853. doi: 10.1093/jxb/erq366

Cameron KD, Teece MA, Smart LB (2006) Increased Accumulation of Cuticular Wax and Expression of Lipid Transfer Protein in Response to Periodic Drying Events in Leaves of Tree Tobacco. Plant physiol 140:176–183. doi: 10.2307/4282042?ref=search-gateway:70ba8ebdd5c6aeda4ebcfd6dd01ac65d

Chatterton NJ, LEE DR, Powell JB (1975) Photosynthesis and transpiration of bloom and bloomless sorghum.

Cheesbrough TM, Kolattukudy PE (1984) Alkane biosynthesis by decarbonylation of aldehydes catalyzed by a particulate preparation from Pisum sativum. Proc Natl Acad Sci USA 81:6613–6617.

Chu CG, Xu SS, Friesen TL, et al (2008) Whole genome mapping in a wheat doubled haploid population using SSRs and TRAPs and the identification of QTL for agronomic traits. Molecular Breeding 22:251–266. doi: 10.1007/s11032-008-9171-9

Cossani CM, Reynolds MP (2012) Physiological traits for improving heat tolerance in wheat. Plant physiol 160:1710–1718. doi: 10.1104/pp.112.207753

Craufurd PQ, Vadez V, Jagadish SVK, et al (2013) Crop science experiments designed to inform crop modeling. Agricultural and Forest Meteorology 170:8–18. doi: 10.1016/j.agrformet.2011.09.003

Crossa J, Burgueño J, Dreisigacker S, et al (2007) Association analysis of historical bread wheat germplasm using additive genetic covariance of relatives and population structure. Genetics 177:1889–1913. doi: 10.1534/genetics.107.078659

Cui F, Ding A, Li J, et al (2012) QTL detection of seven spike-related traits and their genetic correlations in wheat using two related RIL populations. Euphytica 186:177–192. doi: 10.1007/s10681-011-0550-7

Cullings KW (1992) Design and testing of a plant- specific PCR primer for ecological and evolutionary studies. Molecular Ecology 1:233–240. doi: 10.1111/j.1365-294X.1992.tb00182.x

Damon SJ, Havey MJ (2014) Quantitative trait loci controlling amounts and types of epicuticular waxes in onion. Journal of the American Society for Horticultural Science 139:597–602.

Dhakal S, Tan C, Paezold L, et al (2017) Wheat curl mite resistance in hard winter wheat in the us great plains. Crop Sci. 57:53-61. doi:10.2135/cropsci2016.02.0121

Debono A, Yeats TH, Rose JKC, et al (2009) Arabidopsis LTPG is a glycosylphosphatidylinositol-anchored lipid transfer protein required for export of lipids to the plant surface. The Plant Cell 21:1230–1238. doi: 10.1105/tpc.108.064451

Dennis MW, Kolattukudy PE (1991) Alkane biosynthesis by decarbonylation of aldehyde catalyzed by a microsomal preparation from *Botryococcus braunii*. Archives of Biochemistry and Biophysics 287:268–275. doi: 10.1016/0003-9861(91)90478-2

Dhakal S (2014) Resistance sources of hard red winter wheat against wheat curl mite. West Texas A&M Univ, Canyon, TX.

Doyle JJ (1987) A rapid DNA isolation procedure for small quantities of fresh leaf tissue. Phytochem Bull 19: 11–15.

Dubcovsky J, Echaide M, Giancola S, et al (1997) Seed-storage-protein loci in RFLP maps of diploid, tetraploid, and hexaploid wheat. Theoretical and Applied Genetics 95:1169–1180.

Ebercon A, Blum A, Jordan WR (1977) A rapid colorimetric method for epicuticular wax contest of sorghum leaves. Crop Science 17:179–180. doi: 10.2135/cropsci1977.0011183X001700010047x

Eigenbrode SD, Espelie KE (1995) Effects of plant epicuticular lipids on insect herbivores. Annual review of entomology 171–194.

Eigenbrode SD, Rayor L, Chow J, et al (2000) Effects of wax bloom variation in Brassica oleracea on foraging by a vespid wasp. Entomologia Experimentalis et Applicata 97:161–166. doi: 10.1046/j.1570-7458.2000.00726.x

Elham F, Khavari-Nejad RA, Salekdeh GH, et al (2012) Evaluation of cuticular wax deposition, stomata and carbohydrate of wheat leaves for screening drought tolerance.

Ellis MH, Rebetzke GJ, Chandler P, et al (2004) The effect of different height reducing genes on the early growth of wheat. Functional Plant Biology 31:583–7. doi: 10.1071/FP03207

Esten Mason R, Mondal S, Beecher FW, et al (2010) QTL associated with heat susceptibility index in wheat (*Triticum aestivum* L.) under short-term reproductive stage heat stress. Euphytica 174:423–436. doi: 10.1007/s10681-010-0151-x

Esten Mason R, Mondal S, Beecher FW, et al (2011) Genetic loci linking improved heat tolerance in wheat (*Triticum aestivum* L.) to lower leaf and spike temperatures under controlled conditions. Euphytica 180:181–194. doi: 10.1007/s10681-011-0349-6

FAO (2009) How to feed the world in 2050 http://www.fao.org/fileadmin/templates/wsfs/docs/expert_paper/How_to_Feed_the_World_in_2050.pdf)

FAO (2016) Food Outlook. http://www.fao.org/worldfoodsituation/csdb/en/

Febrero A, ndez SF, Molina-Cano JL, et al (1998) Yield, carbon isotope discrimination, canopy reflectance and cuticular conductance of barley isolines of differing glaucousness. Journal of Experimental Botany 1575–1581. doi:https://doi.org/10.1093/jxb/49.326.1575

Fiebig A, Mayfield JA, Miley NL, et al (2000) Alterations in CER6, a gene identical to CUT1, differentially affect long-chain lipid content on the surface of pollen and stems. The Plant Cell 12:2001–2008. doi: 10.1105/tpc.12.10.2001

Frizell-Armitage A (2016) The effect of non-glaucousness, as conferred by *Inhibitor of Wax 1*, on physiology and yield of UK wheat.

Gadaleta A, Giancaspro A, Giove SL, et al (2009) Genetic and physical mapping of new EST-derived SSRs on the A and B genome chromosomes of wheat. Theor Appl Genet 118:1015–1025. doi: 10.1007/s00122-008-0958-1

Gao F, Wen W, Liu J, et al (2015) Genome-wide linkage mapping of qtl for yield components, plant height and yield-related physiological traits in the chinese wheat cross Zhou 8425b/Chinese Spring. Front Plant Sci 6:507–17. doi:

10.3389/fpls.2015.01099

Giese BN (1975) Effects of light and temperature on the composition of epicuticular wax of barley leaves. Phytochemistry 14:921–929. doi: 10.1016/0031-9422(75)85160-0

Gonzalez A, Ayerbe L (2010) Effect of terminal water stress on leaf epicuticular wax load, residual transpiration and grain yield in barley. Euphytica 172:341–349. doi: 10.1007/s10681-009-0027-0

Gooding MJ, Ellis RH, Shewry PR, et al (2003) Effects of restricted water availability and increased temperature on the grain filling, drying and quality of winter wheat. Journal of Cereal Science 37:295–309. doi: 10.1006/jcrs.2002.0501

Gosney BJ, Potts BM, O'Reilly-Wapstra JM, et al (2016) Genetic control of cuticular wax compounds in Eucalyptus globulus. New Phytologist 209:202–215. doi: 10.1111/nph.13600

Greer S, Wen M, Bird D, et al (2007) The cytochrome P450 enzyme CYP96A15 is the midchain alkane hydroxylase responsible for formation of secondary alcohols and ketones in stem cuticular wax of Arabidopsis. Plant physiol 145:653–667. doi: 10.1104/pp.107.107300

Grncarevic M, Radler F (1967) The effect of wax components on cuticular transpiration-model experiments. Planta 75:23–27. doi: 10.1007/BF00380835

Grover A, Sharma PC (2016) Development and use of molecular markers: past and present. Critical Reviews in Biotechnology 36:290–302. doi: 10.3109/07388551.2014.959891

Gupta PK, Kulwal PL, Jaiswal V (2014) Chapter Two – Association Mapping in Crop Plants: Opportunities and Challenges. Elsevier

Hen-Avivi S, Savin O, Racovita RC, et al (2016) A metabolic gene cluster in the wheat *w1* and the barley *cer-cqu* loci determines β-diketone biosynthesis and glaucousness. Plant Cell 28:1440–1460. doi: 10.1105/tpc.16.00197

Holmes MG, Keiller DR (2002) Effects of pubescence and waxes on the reflectance of leaves in the ultraviolet and photosynthetic wavebands: a comparison of a range of species. Plant, Cell & Environment 25:85–93. doi: 10.1046/j.1365-3040.2002.00779.x

Hooker TS, Millar AA, Kunst L (2002) Significance of the expression of the CER6 condensing enzyme for cuticular wax production in Arabidopsis. Plant physiol 129:1568–1580. doi: 10.1104/pp.003707

Hua L, Wang DR, Tan L, et al (2015) LABA1, a domestication gene associated with long, barbed awns in wild rice. The Plant Cell 27:1875–1888. doi: 10.1105/tpc.15.00260

Huang D, Feurtado JA, Smith MA, et al (2017) Long noncoding miRNA gene represses wheat β-diketone waxes. Proc Natl Acad Sci USA 114:E3149–E3158. doi: 10.1073/pnas.1617483114

Huang X, Wei X, Sang T, et al (2010) Genome-wide association studies of 14 agronomic traits in rice landraces. Nat Genet 42:961–967. doi: 10.1038/ng.695

Huang X, Zhao Y, Wei X, et al (2012) Genome-wide association study of flowering time and grain yield traits in a worldwide collection of rice germplasm. Nat Genet 44:32–39. doi: 10.1038/ng.1018

Huang XQ, Cöster H, Ganal MW, et al (2003) Advanced backcross QTL analysis for the identification of quantitative trait loci alleles from wild relatives of wheat (*Triticum aestivum* L.). Theor Appl Genet 106:1379–1389. doi: 10.1007/s00122-002-1179-7

Huggins T (2014) Understanding the genetic interactions that regulate heat and drought tolerance in relation to wax deposition and yield stability in wheat (*Triticum Aestivum* L.).

Huijser P, Schmid M (2011) The control of developmental phase transitions in plants. Development 138:4117–4129. doi: 10.1242/dev.063511

Hund A, Ruta N, Liedgens M (2009) Rooting depth and water use efficiency of tropical maize inbred lines, differing in drought tolerance. Plant Soil 318:311–325. doi: 10.1007/s11104-008-9843-6

IWGSC (2014) A chromosome-based draft sequence of the hexaploid bread wheat (Triticum aestivum) genome. Science 345:1251788. doi: 10.1126/science.1251788

Jackson LL (1971) Beta-Diketone, Alcohol and Hydrocarbons of Barley Surface Lipids. Phytochemistry 10:487–490. doi: 10.1016/S0031-9422(00)94091-3

Jaleel CA, Manivannan P, Lakshmanan GMA, et al (2008) Alterations in morphological parameters and photosynthetic pigment responses of Catharanthus roseus under soil water deficits. Colloids and Surfaces B: Biointerfaces 61:298–303. doi: 10.1016/j.colsurfb.2007.09.008

Jantasuriyarat C, Vales MI, Watson CJW, et al (2004) Identification and mapping of genetic loci affecting the free-threshing habit and spike compactness in wheat (*Triticum aestivum* L.). Theor Appl Genet 108:261–273. doi: 10.1007/s00122-003-1432-8

Javelle M, Vernoud V, Rogowsky PM, et al (2010) Epidermis: the formation and functions of a fundamental plant tissue. New Phytologist 189:17–39. doi: 10.1111/j.1469-8137.2010.03514.x

Jefferson PG, Johnson DA, Rumbaugh MD, et al (2016) Water stress and genotypic effects on epicuticular wax production of alfalfa and crested wheatgrass in relation to yield and excised leaf water loss. Canadian Journal of Plant Science 1989, 69(2):481–490.

Jenks MA, Joly RJ, Peters PJ, et al (1994) Chemically Induced cuticle mutation affecting epidermal conductance to water vapor and disease susceptibility in Sorghum bicolor (L.) Moench. Plant physiol 105:1239–1245. doi: 10.1104/pp.105.4.1239

Jenks MA, Tuttle HA, Eigenbrode SD, et al (1995) Leaf epicuticular waxes of the *Eceriferum* mutants in *Arabidopsis*. Plant physiol 369–377.

Jenks MA, Wood AJ (2002) Critical issues with the plant cuticle's function in drought tolerance. Biochemical Molecular Responses of Plants to the Environment 97–127.

Jighly A, Oyiga BC, Makdis F, et al (2015) Genome-wide DArT and SNP scan for QTL associated with resistance to stripe rust (*Puccinia striiformis f. sp. tritici*) in elite ICARDA wheat (*Triticum aestivum* L.) germplasm. Theoretical and Applied Genetics 128:1277–1295. doi: 10.1007/s00122-015-2504-2

Johnson PE, Smith MO, Taylor George S, et al (1983) A semiempirical method for analysis of the reflectance spectra of binary mineral mixtures. Journal of Geophysical Research: Solid Earth 88:3557–3561. doi: 10.1029/JB088iB04p03557

Jordan KW (2016) A haplotype map of allohexaploid wheat reveals distinct patterns of selection on homoeologous genomes. 1–18. doi: 10.1186/s13059-015-0606-4

Jordan WR, Shouse PJ, Blum A, et al (1984) Environmental physiology of sorghum. II. epicuticular wax load and cuticular transpiration. Crop Science 24:1168–1173. doi: 10.2135/cropsci1984.0011183X002400060038x

Kalinowski ST (2011) The computer program STRUCTURE does not reliably identify the main genetic clusters within species: simulations and implications for human population structure. Heredity 106:625–632. doi: 10.1038/hdy.2010.95

Kang HM, Sul JH, Service SK, et al (2010) Variance component model to account for sample structure in genome-wide association studies. Nature Publishing Group 42:348–354. doi: 10.1038/ng.548

Kato K, Miura H, Sawada S (2000) Mapping QTLs controlling grain yield and its components on chromosome 5A of wheat. Theor Appl Genet 101:1114–1121. doi:

10.1007/s001220051587

Kebrom TH, Chandler PM, Swain SM, et al (2012) Inhibition of tiller bud outgrowth in the tin mutant of wheat is associated with precocious internode development. Plant physiol 160:308–318. doi: 10.1104/pp.112.197954

Kerstiens G (1996a) Cuticular water permeability and its physiological significance. Journal of Experimental Botany 47:1813–1832. doi: 10.1093/jxb/47.12.1813

Kerstiens G (1996b) Signalling across the divide: a wider perspective of cuticular structure—function relationships. Trends in Plant Science 1:125–129. doi: 10.1016/S1360-1385(96)90007-2

Kertho A, Mamidi S, Bonman JM, et al (2015) Genome-wide association mapping for resistance to leaf and stripe rust in winter-habit hexaploid wheat landraces. Plos One 10:e0129580. doi: 10.1371/journal.pone.0129580

KiliÇ H, YaĞbasanlar T (2010) The effect of drought stress on grain yield, yield components and some quality traits of durum wheat (*Triticum turgidum ssp. durum*) cultivars. Notulae Botanicae Horti Agrobotanici Cluj-Napoca 164–170.

Kim H, Lee SB, Kim HJ, et al (2012) Characterization of glycosylphosphatidylinositol-anchored lipid transfer protein 2 (LTPG2) and overlapping function between LTPG/LTPG1 and LTPG2 in cuticular wax export or accumulation in *Arabidopsis thaliana*. Plant Cell Physiol 53:1391–1403. doi: 10.1093/pcp/pcs083

Kim KS, Park SH, Jenks MA (2007) Changes in leaf cuticular waxes of sesame (Sesamum indicum L.) plants exposed to water deficit. J Plant Physiol 164:1134–1143. doi: 10.1016/j.jplph.2006.07.004

Kissinger M, Tuvia-Alkalai S, Shalom Y, et al (2005) Characterization of physiological and biochemical factors associated with postharvest water loss in ripe pepper fruit during storage. Journal of the American Society for Horticultural Science 130:735–741.

Koch K, Barthlott W, Koch S, et al (2006) Structural analysis of wheat wax (*Triticum aestivum, c.v. "Naturastar"* L.): from the molecular level to three dimensional crystals. Planta 223:258–270. doi: 10.1007/s00425-005-0081-3

Kolmer JA, Garvin DF, Jin Y (2011) Expression of a thatcher wheat adult plant stem rust resistance qtl on chromosome arm 2bl is enhanced by *Lr34*. Crop Science 51:526–533. doi: 10.2135/cropsci2010.06.0381

Kosma DK, Bourdenx B, Bernard A, et al (2009) The impact of water deficiency on leaf cuticle lipids of arabidopsis. Plant physiol 151:1918–1929. doi:

10.1104/pp.109.141911

Kosma DK, Jenks MA (2007) Eco-physiological and molecular-genetic determinants of plant cuticle function in drought and salt stress tolerance. In: Advances in Molecular Breeding Toward Drought and Salt Tolerant Crops. Springer Netherlands, Dordrecht, pp 91–120

Kosma DK, Rowland O (2016) Answering a four decade-old question on epicuticular wax biosynthesis. Journal of Experimental Botany 67:2538–2540. doi: 10.1093/jxb/erw144

Kover PX, Valdar W, Trakalo J, et al (2009) A multiparent advanced generation inter-cross to fine-map quantitative traits in *Arabidopsis thaliana.* PLoS Genet 5:e1000551–15. doi: 10.1371/journal.pgen.1000551

Kumar N, Kulwal PL, Balyan HS, et al (2007) QTL mapping for yield and yield contributing traits in two mapping populations of bread wheat. Molecular Breeding 19:163–177. doi: 10.1007/s11032-006-9056-8

Kumar S, Banks TW, Cloutier S (2012) SNP discovery through next-generation sequencing and its applications. International Journal of Plant Genomics 2012:1–15. doi: 10.1155/2012/831460

Kumar V, Singh A, Mithra S (2015) Genome-wide association mapping of salinity tolerance in rice (*Oryza sativa*) | DNA Research | Oxford Academic.

Kunst L, Samuels AL (2003) Biosynthesis and secretion of plant cuticular wax. Progress in Lipid Research 42:51–80. doi: 10.1016/S0163-7827(02)00045-0

Kunst L, Samuels L (2009) Plant cuticles shine: advances in wax biosynthesis and export. Current Opinion in Plant Biology 12:721–727. doi: 10.1016/j.pbi.2009.09.009

Kuraparthy V, Sood S, Dhaliwal HS, et al (2007) Identification and mapping of a tiller inhibition gene (tin3) in wheat. Theor Appl Genet 114:285–294. doi: 10.1007/s00122-006-0431-y

Lai C, Kunst L, Jetter R (2007) Composition of alkyl esters in the cuticular wax on inflorescence stems of Arabidopsis thaliana cer mutants. Plant Journal 50:189–196. doi: 10.1111/j.1365-313X.2007.03054.x

Law CN (1967) The location of genetic factors controlling a number of quantitative characters in wheat. Genetics 56:445–461.

Lazar MD, Worrall WD, Peterson GL, et al (2004) Registration of 'TAM 111'. Crop Sci.

44:355–356 10.2135/cropsci2004.3550.

Lee SB, Suh MC (2016) Recent Advances in Cuticular Wax Biosynthesis and Its Regulation in Arabidopsis. Molecular Plant 6:246–249. doi: 10.1093/mp/sss159

Li C, Bai G, Carver BF, et al (2016) Mapping quantitative trait loci for plant adaptation and morphology traits in wheat using single nucleotide polymorphisms. Euphytica 208:299–312. doi: 10.1007/s10681-015-1594-x

Li F, Wu X, Lam P, et al (2008) Identification of the wax ester synthase/acyl-coenzyme A: diacylglycerol acyltransferase WSD1 required for stem wax ester biosynthesis in Arabidopsis. Plant physiol 148:97–107. doi: 10.1104/pp.108.123471

Li WL, Nelson JC, Chu CY, et al (2002) Chromosomal locations and genetic relationships of tiller and spike characters in wheat. Euphytica 125:357–366. doi: 10.1023/A:1016069809977

Li-Beisson Y, Shorrosh B, Beisson F, et al (2010) Acyl-Lipid Metabolism. The Arabidopsis Book 8:1–65. doi: 10.1199/tab.0133

Liu Q, Ni Z, Peng H, et al (2007) Molecular mapping of a dominant non-glaucousness gene from synthetic hexaploid wheat (*Triticum aestivum* L.). Euphytica 155:71–78. doi: 10.1007/s10681-006-9302-5

Liu S, Assanga SO, Dhakal S, et al (2015) Validation of Chromosomal Locations of 90K Array Single Nucleotide Polymorphisms in US Wheat. Crop Science 56:364–373. doi: 10.2135/cropsci2015.03.0194

Liu SY, Rudd JC, Bai G, (2014) Validation of Chromosomal Locations of 90K Array Single Nucleotide Polymorphisms in US Wheat : Molecular markers linked to important genes in hard winter wheat. Crop Sci. 54:1304–1321. doi:10.2135/ cropsci2013.08.0564

Liu S, Yeh C-T, Tang HM, et al (2012) Gene Mapping via Bulked Segregant RNA-Seq (BSR-Seq). Plos One 7:1–8. doi: 10.1371/journal.pone.0036406

Lu S, Zhao H, Marais Des DL, et al (2012) *Arabidopsis* ECERIFERUM9 involvement in cuticle formation and maintenance of plant water status. Plant physiol 159:930–944. doi: 10.1104/pp.112.198697

Lu P, Qin J, Wang G, et al (2017) Comparative fine mapping of the Wax 1 (*W1*) locus in hexaploid wheat. Theoretical and Applied Genetics 128:1595–1603. doi: 10.1007/s00122-015-2534-9

Lobell DB, Hammer GL, McLean G, et al (2013) The critical role of extreme heat for

maize production in the United States. Nature Climate Change 3:497–501. doi: 10.1038/NCLIMATE1832

Lobell DB, Schlenker W, Costa-Roberts J (2011) Climate trends and global crop production since 1980. Science 333:616–620. doi: 10.1126/science.1204531

Lovelock CE, Robinson SA (2002) Surface reflectance properties of Antarctic moss and their relationship to plant species, pigment composition and photosynthetic function. Plant Cell Environ 25:1239–1250.

Lu P, Qin J, Wang G, et al (2015) Comparative fine mapping of the Wax 1 (W1) locus in hexaploid wheat. Theoretical and Applied Genetics 128:1595–1603. doi: 10.1007/s00122-015-2534-9

Lu S, Zhao H, Marais Des DL, et al (2012) *Arabidopsis* ECERIFERUM9 involvement in cuticle formation and maintenance of plant water status. Plant physiol 159:930–944. doi: 10.1104/pp.112.198697

Maccaferri M, El-Feki W, Nazemi G, et al (2016) Prioritizing quantitative trait loci for root system architecture in tetraploid wheat. Journal of Experimental Botany 67:1161–1178. doi: 10.1093/jxb/erw039

Mackay IJ, Bansept-Basler P, Barber T, et al (2014) An eight-parent multiparent advanced generation inter-cross population for winter-sown wheat: creation, properties, and validation. G3 (Bethesda) 4:1603–1610. doi: 10.1534/g3.114.012963

Margarido GRA, Souza AP, Garcia AAF (2007) OneMap: software for genetic mapping in outcrossing species. Hereditas 144:78–79. doi: 10.1111/j.2007.0018-0661.02000.x

Massman J, Cooper B, Horsley R, et al (2011) Genome-wide association mapping of Fusarium head blight resistance in contemporary barley breeding germplasm. Molecular Breeding 27:439–454. doi: 10.1007/s11032-010-9442-0

McIntosh RA, Hart GE, Devos KM, et al (1998) Catalogue of gene symbols for wheat. Proc 9th Int Wheat Genet Symp. Saskatoon 5: 235.

McMullen MD, Kresovich S, Villeda HS, et al (2009) Genetic properties of the maize Nested Association Mapping Population. Science 325:737–740. doi: 10.1126/science.1174320

Merah O, Deleens E, Souyris I, et al (2000) Effect of glaucousness on carbon isotope discrimination and grain yield in durum wheat. Journal of Agronomy and Crop Science 185:259–265. doi: 10.1046/j.1439-037x.2000.00434.x

Mikkelsen J (1978) The effects of inhibitors on the biosynthesis of the long chain lipids with even carbon numbers in barley spike epicuticular wax. Carlsberg Res Commun 15–35.

Millar AA, Clemens S, Zachgo S, et al (1999) CUT1, an *Arabidopsis* gene required for cuticular wax biosynthesis and pollen fertility, encodes a very-long-chain fatty acid condensing enzyme. The Plant Cell 11:825–838. doi: 10.1105/tpc.11.5.825

Mohammed S (2014) The role of epicuticular wax an improved adaptation to moisture deficit environments in wheat.

Mondal S (2011) Defining the molecular and ohysiological role of leaf cuticular waxes in reproductive stage heat tolerance wheat.

Mondal S, Mason RE, Huggins T, Hays DB (2014) QTL on wheat (*Triticum aestivum* L.) chromosomes 1B, 3D and 5A are associated with constitutive production of leaf cuticular wax and may contribute to lower leaf temperatures under heat stress. Euphytica 201:123–130. doi: 10.1007/s10681-014-1193-2

Monneveux P, Reynolds MP, González Santoyo H, et al (2004) Relationships between Grain Yield, Flag Leaf Morphology, Carbon Isotope Discrimination and Ash Content in Irrigated Wheat. Journal of Agronomy and Crop Science 190:395–401. doi: 10.1111/j.1439-037X.2004.00116.x

Naruoka Y, Talbert LE, Lanning SP, et al (2011) Identification of quantitative trait loci for productive tiller number and its relationship to agronomic traits in spring wheat. Theor Appl Genet 123:1043. doi: 10.1007/s00122-011-1646-0

Nesbitt M, Samuel D (1996) From staple crop to extinction? The archaeology and history of the hulled wheats. Hulled wheats 4:41-100.

Nishijima R, Iehisa JCM, Matsuoka Y, et al (2014) The cuticular wax inhibitor locus Iw2 in wild diploid wheat Aegilops tauschii: phenotypic survey, genetic analysis, and implications for the evolution of common wheat. BMC Plant Biology 14:1138–14. doi: 10.1186/s12870-014-0246-y

Nordborg M, Tavaré S (2002) Linkage disequilibrium: what history has to tell us. Trends in Genetics 18:83–90. doi: 10.1016/S0168-9525(02)02557-X

Oliveira AFM, Meirelles ST, Salatino A (2003) Epicuticular waxes from caatinga and cerrado species and their efficiency against water loss. Anais da Academia Brasileira de Ciências 75:431–439. doi: 10.1590/S0001-37652003000400003

Oshima Y, Shikata M, Koyama T, et al (2013) MIXTA-like transcription factors and WAX INDUCER1/ SHINE1 coordinately regulate cuticle development in

Arabidopsis and Torenia fournieri. Plant Cell 25, 1609–1624. doi:10.1105/tpc.113.110783

Panikashvili D, Savaldi-Goldstein S, Mandel T, et al (2007) The Arabidopsis DESPERADO/AtWBC11 transporter is required for cutin and wax secretion. Plant physiol 145:1345–1360. doi: 10.1104/pp.107.105676

Patel RK, Jain M (2012) NGS QC Toolkit: A Toolkit for Quality Control of Next Generation Sequencing Data. Plos One 7:e30619. doi:10.1371/journal.pone.0030619

Patterson N, Price AL, Reich D (2006) Population structure and eigenanalysis. PLoS Genet 2:e190. doi: 10.1371/journal.pgen.0020190

Paull JG, Chalmers KJ, Karakousis A, et al (1998) Genetic diversity in Australian wheat varieties and breeding material based on RFLP data. Theor Appl Genet 96:435–446. doi: 10.1007/s001220050760

Paull JG, Nable RO, Rathjen AJ (1992) Physiological and genetic control of the tolerance of wheat to high concentrations of boron and implications for plant breeding. Plant Soil 146:251–260. doi: 10.1007/BF00012019

Peleg Z, Saranga Y, Fahima T, et al (2010) Genetic control over silica deposition in wheat awns. Physiologia Plantarum 140:10–20. doi: 10.1111/j.1399-3054.2010.01376.x

Pighin JA, Zheng H, Balakshin LJ, et al (2004) Plant Cuticular Lipid Export Requires an ABC Transporter. Science 306:702–704. doi: 10.1126/science.1102331

Pinto RS, Reynolds MP, Mathews KL, et al (2010) Heat and drought adaptive QTL in a wheat population designed to minimize confounding agronomic effects. Theor Appl Genet 121:1001–1021. doi: 10.1007/s00122-010-1351-4

Pinto S, Chapman S, McIntyre C, et al (2008) QTL for canopy temperature response related to yield in both heat and drought environments. pp 1–3

Porras-Hurtado L, Ruiz Y, Santos C, et al (2013) An overview of STRUCTURE: applications, parameter settings, and supporting software. frontiers in Genetics 4:1–13. doi: 10.3389/fgene.2013.00098/abstract

Porter JR, Semenov MA (2005) Crop responses to climatic variation. Philosophical Transactions of the Royal Society B-Biological Sciences 360:2021–2035. doi: 10.1098/rstb.2005.1752

PostBeittenmiller D (1996) Biochemistry and molecular biology of wax production in plants. Annual Review of Plant Physiology and Plant Molecular Biology 47:405–

430. doi: 10.1146/annurev.arplant.47.1.405

Price AL, Patterson NJ, Plenge RM, et al (2006) Principal components analysis corrects for stratification in genome-wide association studies. Nat Genet 38:904–909. doi: 10.1038/ng1847

Pritchard JK, Stephens M, Rosenberg NA, et al (2000) Association Mapping in Structured Populations. The American Journal of Human Genetics 67:170–181. doi: 10.1086/302959

Qin B-X, Tang D, Huang J, et al (2011) Rice OsGL1-1 Is Involved in leaf cuticular wax and cuticle membrane. Molecular Plant 4:985–995. doi: 10.1093/mp/ssr028

Qiu Y, Tittiger C, Wicker-Thomas C, et al (2012) An insect-specific P450 oxidative decarbonylase for cuticular hydrocarbon biosynthesis. Proc Natl Acad Sci USA 109:14858–14863. doi: 10.1073/pnas.1208650109

R Development Core Team (2014) R: A language and environment for statistical computing. R Foundation for Statistical Computing, Vienna, Austria ISBN: 3-900051-07-0.

Rafalski JA (2010) Association genetics in crop improvement. Current Opinion in Plant Biology 13:174–180. doi: 10.1016/j.pbi.2009.12.004

Reddy SK, Liu S, Rudd JC, et al (2014) Physiology and transcriptomics of water-deficit stress responses in wheat cultivars TAM 111 and TAM 112. J Plant Physiol 171:1289–1298. doi: 10.1016/j.jplph.2014.05.005

Reed JR, Vanderwel D, Choi SW, et al (1994) Unusual mechanism of hydrocarbon formation in the housefly - Cytochrome-P450 converts aldehyde to the sex-pheromone component (z)-9-tricosene and CO2. Proc Natl Acad Sci USA 91:10000–10004. doi: 10.1073/pnas.91.21.10000

Reicosky D, Hanover J (1978) Physiological effects of surface water, I, Light retleclance lor glaucous and nonglaucous Picca pungetis. Plant physiol 101–104.

Remy E, Cabrito TR, Baster P, et al (2013) A major facilitator superfamily transporter plays a dual role in polar auxin transport and drought stress Tolerance in Arabidopsis. Plant Cell 25:901–926. doi: 10.1105/tpc.113.110353

Reynolds MP, Balota M, Delgado M, et al (1994) Physiological and morphological traits associated with spring wheat yield under hot, irrigated conditions. Functional Plant Biology 21:717–730. doi: 10.1071/pp9940717

Reynolds MP, Singh RP, Ibrahim A, et al (1998) Evaluating physiological traits to

complement empirical selection for wheat in warm environments. Euphytica 100:85–94. doi: 10.1023/A:1018355906553

Reynolds M P, Manes Y, Izanloo A, et al (2009) Phenotyping for physiological breeding and gene discovery in wheat. Ann. Appl. Biol. 155: 309–320. 10.1111/j.1744-7348.2009.00351.x

Rhee SG (2001) Regulation of phosphoinositide-specific phospholipase C. Annual review of biochemistry 70:281–312.

Richard RA (1988) A tiller inhibitor gene in wheat and its effect on plant growth. Aust J Agric Res 39:749–757. doi: 10.1071/ar9880749

Richard RA, Rawson HM, Johnson DA (1986) Glaucousness in wheat: its development and effect on water-use efficiency, gas exchange and photosynthetic tissue temperatures. Functional Plant Biology 13:465–473. doi: 10.1071/PP9860465

Richard RA, Romagosa I, Jana S, et al (1983) Relationship of excised-leaf water loss rate and yield of durum wheat in diverse environments. Canadian Journal of Plant Science 1075–1081.

Richardson A, Franke R, Kerstiens G, et al (2005) Cuticular wax deposition in growing barley (Hordeum vulgare) leaves commences in relation to the point of emergence of epidermal cells from the sheaths of older leaves. Planta 222:472–483. doi: 10.1007/s00425-005-1552-2

Riederer M, Schreiber L (1995) Waxes—the transport barriers of plant cuticles. In: Waxes chemistry, molecular biology and functions, 6 edn. pp 131–156

Risch N, Merikangas AK (1996) The future of genetic studies of complex human diseases.

Risk JM, Selter LL, Chauhan H, et al (2013) The wheat *Lr34* gene provides resistance against multiple fungal pathogens in barley. Plant Biotechnol J 11:847–854. doi: 10.1111/pbi.12077

Rowland O, Zheng H, Hepworth SR, et al (2006) CER4 encodes an alcohol-forming fatty acyl-coenzyme a reductase involved in cuticular wax production in Arabidopsis. Plant physiol 142:866–877. doi: 10.1104/pp.106.086785

Rudd JC, Devkota RN, Baker JA, et al (2014) 'TAM 112' wheat: A greenbug and wheat curl mite resistant cultivar adapted to the dryland production system in the Southern High Plains. J. Plant Reg. 8:291–297. doi:10.3198/jpr2014.03.0016crc

Rupwate SD, Rajasekharan R (2012) Plant phosphoinositide-specific phospholipase C.

Plant Signaling & Behavior 7:1281–1283. doi: 10.4161/psb.21436

Saintenac C, Jiang D, Wang S, et al (2013a) Sequence-Based mapping of the polyploid wheat genome. 3:1105–1114. doi: 10.1534/g3.113.005819/-/DC1

Saintenac C, Zhang W, Salcedo A, et al (2013b) Identification of wheat gene *Sr35* that confers resistance to Ug99 stem rust race group. Science 341:783–786. doi: 10.1126/science.1239022

Samuels L, Kunst L, Jetter R (2008) Sealing Plant Surfaces: Cuticular wax formation by epidermal cells. Annu Rev Plant Biol 59:683–707. doi: 10.1146/annurev.arplant.59.103006.093219

Scarcelli N, Cheverud JM, Schaal BA, et al (2007) Antagonistic pleiotropic effects reduce the potential adaptive value of the FRIGIDA locus. Proc Natl Acad Sci USA 104:16986–16991. doi: 10.1073/pnas.0708209104

Schneider LM, Adamski NM, Christensen CE, et al (2016) The *Cer*-cqugene cluster determines three key players in a β-diketone synthase polyketide pathway synthesizing aliphatics in epicuticular waxes. Journal of Experimental Botany 67:2715–2730. doi: 10.1093/jxb/erw105

Sears E.R. (1954)The Aneuploids of Common Wheat. Missouri Agr Exp Stn Res Bull 572

Seo PJ, Park C-M (2011) Cuticular wax biosynthesis as a way of inducing drought resistance. Plant Signaling & Behavior 6:1043–1045. doi: 10.4161/psb.6.7.15606

Serrano M, Coluccia F, Torres M, et al (2014) The cuticle and plant defense to pathogens. Front Plant Sci 5:1–8. doi: 10.3389/fpls.2014.00274

Shepherd T, Griffiths DW (2006) The effects of stress on plant cuticular waxes. The New Phytologist 171:469–499. doi: 10.2307/4091470?ref=search-gateway:9a35e35aa6c459fbd2cb01e85bc9c0aa

Shepherd T, Wynne Griffiths D (2006) The effects of stress on plant cuticular waxes. New Phytologist 171:469–499. doi: 10.1111/j.1469-8137.2006.01826.x

Shinozaki K, Yamaguchi-Shinozaki K (2007) Gene networks involved in drought stress response and tolerance. Journal of Experimental Botany 58:221–227. doi: 10.1093/jxb/erl164

Silverman M (1991) Structure and function of hexose transporters.

Simmonds JR, Fish LJ, Leverington-Waite MA, et al (2008) Mapping of a gene (*Vir*) for a non-glaucous, viridescent phenotype in bread wheat derived from Triticum

dicoccoides, and its association with yield variation. Euphytica 159:333–341. doi: 10.1007/s10681-007-9514-3

Sonah H, ODonoughue L, Cober E, et al (2014) Combining genome-wide association and qtl analysis: Opportunities and challenges. ISB news report 1–4.

Sorensen AE (1986) Seed dispersal by adhesion.

Sourdille P, Cadalen T, Guyomarc'h H, et al (2003) An update of the Courtot × Chinese Spring intervarietal molecular marker linkage map for the QTL detection of agronomic traits in wheat. Theor Appl Genet 106:530–538. doi: 10.1007/s00122-002-1044-8

Spielmeyer W, Richard RA (2004) Comparative mapping of wheat chromosome 1AS which contains the tiller inhibition gene (tin) with rice chromosome 5S. Theor Appl Genet 109:1303–1310. doi: 10.1007/s00122-004-1745-2

Srinivasan S, Gomez SM, Kumar SS, et al (2008) QTLs linked to leaf epicuticular wax, physio-morphological and plant production traits under drought stress in rice (Oryza sativa L.). Plant Growth Regulation 56:245–256. doi: 10.1007/s10725-008-9304-5

Stein N, Herren G, Keller B (2001) A new DNA extraction method for high- throughput marker analysis in a large- genome species such as Triticum aestivum. Plant Breed 120:354–356. doi: 10.1046/j.1439-0523.2001.00615.x

Stoveken T, Kalscheuer R, Malkus U, et al (2005) The wax ester synthase/acyl coenzyme A : diacylglycerol acyltransferase from Acinetobacter sp strain ADP1: Characterization of a novel type of acyltransferase. Journal of Bacteriology 187:1369–1376. doi: 10.1128/JB.187.4.1369-1376.2005

Sukumaran S, Dreisigacker S, Lopes M, et al (2015) Genome-wide association study for grain yield and related traits in an elite spring wheat population grown in temperate irrigated environments. Theor Appl Genet 128:353–363. doi: 10.1007/s00122-014-2435-3

Tadesse W, Ogbonnaya FC, Jighly A, et al (2014) Association Mapping of Resistance to Yellow Rust in Winter Wheat Cultivars and Elite Genotypes. Crop Science 54:607–616. doi: 10.2135/cropsci2013.05.0289

Tadesse W, Ogbonnaya FC, Jighly A, et al (2015) Genome-wide association mapping of yield and grain quality traits in winter wheat genotypes. Plos One 10:e0141339–18. doi: 10.1371/journal.pone.0141339

Taylor J, Butler D (2014) ASMap: Linkage map construction using the MSTMap algorithm. R package version 0.3–2. Available: http://CRAN.R-

project.org/package=ASMap.

The Wheat Initiative (2011) Breakout session P1.1 national food security- the Wheat Initiative - an international research initiative for wheat improvement

Todd J, Post Beittenmiller D, Jaworski JG (1999) KCS1encodes a fatty acid elongase 3- ketoacyl- CoA synthase affecting wax biosynthesis inArabidopsis thaliana. The Plant Journal 17:119–130. doi: 10.1046/j.1365-313X.1999.00352.x

Torada A, Koike M, Mochida K, et al (2006) SSR-based linkage map with new markers using an intraspecific population of common wheat. Theor Appl Genet 112:1042–1051. doi: 10.1007/s00122-006-0206-5

Tsunewaki K (1966) Comparative gene analysis of common wheat and its ancestral species. III. Glume Hairiness. Genetics 53:303.

Tsunewaki K, Ebana K (1999) Production of near-isogenic lines of common wheat for glaucousness and genetic basis of this trait clarified by their use. Genes Genet Syst 74:33–41. doi: 10.1266/ggs.74.33

Tulloch AP (1973) Composition of leaf surface waxes of Triticum species: Variation with age and tissue. Phytochemistry 12:2225–2232. doi: 10.1016/00319422(73)85124-6

Urano K, Kurihara Y, Seki M, et al (2010) "Omics" analyses of regulatory networks in plant abiotic stress responses. Current Opinion in Plant Biology 13:132–138. doi: 10.1016/j.pbi.2009.12.006

Van Ooijen JW (2011) MapQTL 6: Software for the mapping of quantitative trait loci in experimental populations of diploid species. Kyazma BV, Wageningen, Netherlands.

Van Ooijen JW (2006) JoinMap 4. Software for the calculation of genetic linkage maps in experimental populations. Kyazma BV, Wageningen, Netherlands

Verbruggen N, Hermans C (2008) Proline accumulation in plants: a review. Amino Acids 35:753–759. doi: 10.1007/s00726-008-0061-6

Vioque J, Kolattukudy PE (1997) Resolution and purification of an aldehyde-generating and an alcohol-generating fatty acyl-coa reductase from pea leaves (*Pisum sativum* L.). Archives of Biochemistry and Biophysics 340:64–72. doi: 10.1006/abbi.1997.9932

Voorrips RE (2002) MapChart: Software for the graphical presentation of linkage maps and QTLs. J Hered 93:77–78. doi: 10.1093/jhered/93.1.77

Wallace JG, Bradbury PJ, Zhang N, et al (2014) Association mapping across numerous traits reveals patterns of functional variation in maize. PLoS Genet 10:e1004845–10. doi: 10.1371/journal.pgen.1004845

Wang C, Yang Y, Yuan X, et al (2014a) Genome-wide association study of blast resistance in indica rice. BMC Plant Biology 14:311. doi: 10.1186/s12870-014-0311-6

Wang J, Li W, Wang W (2014b) Fine mapping and metabolic and physiological characterization of the glume glaucousness inhibitor locus Iw3 derived from wild wheat. Theor Appl Genet 127:831–841. doi: 10.1007/s00122-014-2260-8

Wang J, Li W, Wang W (2014c) Fine mapping and metabolic and physiological characterization of the glume glaucousness inhibitor locus Iw3. Theor Appl Genet 127:831–841. doi: 10.1007/s00122-014-2260-8

Wang Q, Xie W, Xing H, et al (2015a) Genetic architecture of natural variation in rice chlorophyll content revealed by a genome-wide association study. Molecular Plant 8:946–957. doi: 10.1016/j.molp.2015.02.014

Wang S, Wong D, Forrest K, et al (2014d) Characterization of polyploid wheat genomic diversity using a high-density 90 000 single nucleotide polymorphism array. Plant Biotechnol J 12:787–796. doi: 10.1111/pbi.12183

Wang Y, Wan L, Zhang L, et al (2012) An ethylene response factor OsWR1 responsive to drought stress transcriptionally activates wax synthesis related genes and increases wax production in rice. Plant Mol Biol 78:275–288. doi: 10.1007/s11103-011-9861-2

Wang Y, Wang J, Chai G, et al (2015b) Developmental changes in composition and morphology of cuticular waxes on leaves and spikes of glossy and glaucous wheat (*Triticum aestivum* L.). Plos One 10:e0141239–17. doi: 10.1371/journal.pone.0141239

Wang Y, Wang M, Sun Y, et al (2015) FAR5, a fatty acyl-coenzyme A reductase, is involved in primary alcohol biosynthesis of the leaf blade cuticular wax in wheat (Triticum aestivum L.). Journal of Experimental Botany 66:1165–1178. doi: 10.1093/jxb/eru457

Wang Z, Liu Y, Shi H, et al (2016) Identification and validation of novel low-tiller number QTL in common wheat. Theoretical and Applied Genetics 1–11. doi: 10.1007/s00122-015-2652-4

Watanabe N, Takesada N, Shibata Y, et al (2005) Genetic mapping of the genes for glaucous leaf and tough rachis in *Aegilops tauschii*, the D-genome progenitor of

wheat. Euphytica 144:119–123. doi: 10.1007/s10681-005-5193-0

Watkins AE, Ellerton S (1940) Variation and genetics of the awn in Triticum. J Genet 40: 243–270.

Wettstein-Knowles von P (1982) Elongases and epicuticular wax biosynthesis. Physiologie Vegetale 4:797–809.

Wettstein-Knowles von P (2012) Plant Waxes. John Wiley & Sons, Ltd, Chichester, UK

Williams MH, Rosenqvist E, Buchhave M (1999) Response of potted miniature roses (Rosa x hybrida) to reduced water availability during production. The Journal of Horticultural Science and Biotechnology 74:301–308. doi: 10.1080/14620316.1999.11511113

Williams MH, Rosenqvist E, Buchhave M (2000) The effect of reducing production water availability on the post-production quality of potted miniature roses (Rosa×hybrida). Postharvest Biology and Technology 18:143–150. doi: 10.1016/S0925-5214(99)00076-9

Wu H, Qin J, Han J, et al (2013) Comparative high-resolution mapping of the wax inhibitors *iw1* and *iw2* in hexaploid wheat. Plos One 8:e84691–7. doi: 10.1371/journal.pone.0084691

Wu Y, Bhat P, Close TJ, Lonardi S (2007) Efficient and accurate construction of genetic linkage maps from noisy and missing genotyping data. In: Algorithms in Bioinformatics. Springer, Berlin, Heidelberg, pp 395–406

Xu Y, Wang R, Tong Y, et al (2013) Mapping QTLs for yield and nitrogen-related traits in wheat: influence of nitrogen and phosphorus fertilization on QTL expression. Theor Appl Genet 127:59–72. doi: 10.1007/s00122-013-2201-y

Yan JQ, Zhu J, He CX, et al (1998) Quantitative trait loci analysis for the developmental behavior of tiller number in rice (Oryza sativa L.). Theor Appl Genet 97:267–274. doi: 10.1007/s001220050895

Yazaki J, Shimatani Z, Hashimoto A, et al (2004) Transcriptional profiling of genes responsive to abscisic acid and gibberellin in rice: phenotyping and comparative analysis between rice and Arabidopsis. Physiological Genomics 17:87–100. doi: 10.1152/physiolgenomics.00201.2003

Yeats TH, Rose JKC (2013) The Formation and Function of Plant Cuticles. Plant physiol 163:5–20. doi: 10.1104/pp.113.222737

Yu J, Pressoir G, Briggs WH, et al (2006) A unified mixed-model method for

association mapping that accounts for multiple levels of relatedness. Nat Genet 38:203–208. doi: 10.1038/ng1702

Zhai H, Feng Z, Li J, et al (2016) QTL analysis of spike morphological traits and plant height in winter wheat (*Triticum aestivum* L.) Using a High-Density SNP and SSR-Based Linkage Map. Front Plant Sci 7:8057–13. doi: 10.3389/fpls.2016.01617

Zhang K, Jin C, Wu L, et al (2014) Expression analysis of a stress-related phosphoinositide-specific phospholipase c gene in wheat (*Triticum aestivum* L.). Plos One 9:e105061–10. doi: 10.1371/journal.pone.0105061

Zhang Z, Wang W, Li W (2013) Genetic interactions underlying the biosynthesis and inhibition of β-diketones in wheat and their impact on glaucousness and cuticle permeability. Plos One 8:e54129. doi: 10.1371/journal.pone.0054129

Zhang Z, Wei W, Zhu H, et al (2015) *W3* is a new wax locus that is essential for biosynthesis of beta-diketone, development of glaucousness, and reduction of cuticle permeability in common wheat. Plos One. doi: 10.1371/journal.pone.0140524

Zhao K, Tung C-W, Eizenga GC, et al (2011) Genome-wide association mapping reveals a rich genetic architecture of complex traits in Oryza sativa. Nature Communications 2:467. doi: 10.1038/ncomms1467

Zheng H, Rowland O, Kunst L (2005) Disruptions of the *Arabidopsis* Enoyl-CoA reductase gene reveal an essential role for very-long-chain fatty acid synthesis in cell expansion during plant morphogenesis. The Plant Cell 17:1467–1481. doi: 10.1105/tpc.104.030155

Zhou X, Jenks MA, Liu J, et al (2013) Overexpression of transcription factor OsWR2 regulates wax and cutin biosynthesis in rice and enhances its tolerance to water deficit. Plant Mol Biol Rep 32:719–731. doi: 10.1007/s11105-013-0687-8